7-2024

Characterizing the Quorum Sensing (QS) System in the Model Eukaryote Chlamydomonas reinhardtii

Kirstin Donnette Cutshaw
Florida Institute of Technology, kcutshaw2016@my.fit.edu

Characterizing the Quorum Sensing (QS) System in the Model Eukaryote *Chlamydomonas reinhardtii*

by

Kirstin Donnette Cutshaw

B.S. Biochemistry, Florida Institute of Technology

A dissertation
submitted to the College of Engineering and Sciences
at Florida Institute of Technology
in partial fulfillment of the requirements
for the degree of

Doctor of Philosophy
in
Biological Sciences

Melbourne, Florida
July, 2024

We the undersigned committee hereby approve the attached dissertation,
"Characterizing the Quorum Sensing (QS) System in the Model Eukaryote *Chlamydomonas reinhardtii*"
by
Kirstin Donnette Cutshaw

_____
Andrew G. Palmer, Ph.D.
Assistant Professor
Department of Ocean Engineering and Marine Sciences
Major Advisor

_____
David Carroll, Ph.D.
Assistant Professor
Department of Biochemistry and Molecular Genetics
Midwestern University

_____
Eric Guisbert, Ph.D.
Associate Professor
Department of Biomedical Engineering and Sciences

_____
Christopher Chouinard, Ph.D.
Assistant Professor
Department of Chemistry
Clemson University

_____
Brooke Wheeler, Ph.D.
Associate Professor
College of Aeronautics

_____
Richard Aronson, Ph.D.
Professor and Department Head
Department of Ocean Engineering and Marine Sciences

Abstract

Title: Characterizing the Quorum Sensing (QS) System in the Model Eukaryote *Chlamydomonas reinhardtii*

Author: Kirstin Donnette Cutshaw

Advisor: Andrew G. Palmer, Ph.D.

Group behaviors in microorganisms are often regulated by low-molecular weight molecules that enable them to sense population density, a signaling system known as quorum sensing (QS). QS in prokaryotes has provided insight into the role 'social' behaviors play in the bacterial world and refined our models of virulence, bacterial motility, and more. While less common, similar behaviors are observed in certain fungi, primarily yeasts, in which QS controls cell morphology, biofilm production, and other phenotypes. We have recently pursued the potential for QS to be more broadly distributed among unicellular eukaryotes, which could significantly alter our understanding of social behaviors in the microscopic world. Specifically, I have investigated the potential for QS in the globally distributed green algae, *Chlamydomonas reinhardtii*.

C. reinhardtii is a model for studying motility in unicellular organisms and is used in the biomanufacturing of biofuels and pharmaceuticals. Since motility is an integral response to changing environments, understanding the systems regulating motility is crucial. However, manually tracking a statistically significant number of cells is

impractical. Therefore, we developed an automated method to observe *C. reinhardtii* motility, enabling us to identify individual cells and gather global data on their direction, speed, and size.

Our findings include a population-dependent increase in the swimming speed of *C. reinhardtii*. Through a series of experiments, we confirmed that this increase in swimming speed is due to cell density rather than age or nutrient availability. This phenomenon relies on the synthesis and detection of a low-molecular-weight compound, dubbed the *Chlamydomonas* swim speed factor (CSSF). Extracts containing CSSF increased swimming speeds in the closely related *Chlamydomonas moewusii*, and vice versa, indicating that this signaling system is conserved within the genus.

We next developed a refined procedure for preparing CSSF-containing extracts using solid-phase extraction (SPE), accelerating the discovery process for identification of this signal. By iteratively applying high-performance liquid chromatography (HPLC) to the extracts, coupled to image analysis with subsequent fractions, we identified extract fractions containing one or more CSSFs. Further analysis using liquid chromatography-tandem mass spectrometry (LC-MS/MS) and nuclear magnetic resonance (NMR) helped us identify terpenes/sesquiterpenes, fatty acids, sterols/phytohormones, and an as of yet unnamed molecule with a mass-to-charge ratio of ~171.12 as potential candidates for this signaling molecule.

The works collected herein establish new tools for evaluating and modeling motility in this model organism as well as a methodology for similar studies in other unicellular microorganisms. Understanding and controlling QS can have broad impacts on

food production and safety, human health, biofuel production, waste management, and other important fields. Expanding our understanding of QS to include these unicellular eukaryotes offers valuable insights into the evolution and regulation of microbial "social" behaviors. Discovery of QS in *C. reinhardtii* and the closely related species, *C. moewusii*, impacts our understanding of microbial ecology and broadens the potential for discovery of QS among other unicellular eukaryotic species.

Table of Contents

List of Figures

List of Tables

Acknowledgement

As many before me have already stated, the acknowledgement section of any thesis or dissertation is by far the most difficult portion to write. How are you supposed to fit in all of the gratitude you feel for every person that has helped you or supported you along your journey? It is a nearly impossible task, truly. And yet, we endeavor to do so. Before I start this herculean effort, allow me to just say that even though you may not be mentioned in this acknowledgement by name, if you have been a part of my journey at any point and have provided me with words of encouragement, kindness, or even just caffeine, I truly do remember and appreciate it (especially the caffeine).

First and foremost, I need to thank my partner and husband, Randall Garland. Without him having wandered into my life when he did, 12 years ago, I would not have even started this journey in pursuit of a doctorate. He encouraged me to start college and helped me see the worth in myself. He has been there, pushing me to continue from before day one, and continues to bolster my belief in myself and my own abilities. He was with me during my darkest days, when all thoughts of continuing were mere memories, begging, pleading, bending over backwards, to help me see the light and continue pursuing my goals. From the bottom of my heart, the deepest, most heartfelt thank you.

Secondly, and just as importantly as my husband, I need to thank my daughter, Threnody Cutshaw. This amazing human has helped inspire me every day to be the best iteration of myself possible. I know she does not realize this, but she is an amazing person—

intelligent, funny, talented—and without her I would have been lost years ago. I am so glad you are my child; you make me proud every day. I work extra hard to make you proud to call me your mother.

Next, to my family, my grandfather, Francis Kucheravy, my mother, Brenda Coe, and my aunt and uncle, Beth and Greg Hookstra, a deep and profound thank you. You helped support me not only in words but in actions. I appreciate all the coffee sent, the phone calls made, and the quiet but profound strength radiating off you, trying to keep me focused and upbeat. You are the best family a woman could ask for and I appreciate all that you have done, and continue to do, for me.

To David Schmeiske, Chrystina Strickland, and Andrew Riffe, thank you for being my friends through all this insanity! You have helped make every day of this struggle more manageable. Even though I know most of my work is still mysterious to you, you have helped me stay focused and provided me with endless hours of comfort and distraction. Thank you for being in my life and sticking with me. I know I have been insufferable at times, but that's what friends are for, right?

Before I go on, listing all the generous, amazing, talented humans I have had the absolute pleasure of working with, I need to say that I have had the most incredible experience while in college with the most remarkable people as my professors and mentors! Every teacher, staff member, and advisor I have had from day one at Eastern Florida State College (though it was called Brevard Community College when I first started there) to my last day in my PhD program at Florida Institute of Technology, has been incredible. The faculty and staff have been so supportive, kind, and compassionate that they all deserve

every kind word imaginable. Special thanks go to Dr. Ramona Smith-Burrell, Dr. Jessica Schraeder, Mark McBride, and Patrick Richards. I appreciate all the mentorship, deep talks, and laughs we have shared over the years!

Now, perhaps most deserving of thanks for being there for me—both professionally and personally—throughout my doctorate is Dr. Andrew Palmer. He is, without a doubt, the best principal investigator one could possibly have. The amount of guidance, reassurance, and compassion that comes from him is almost unbelievable. His ability to maintain such an upbeat, energetic attitude after setbacks and failures is beyond words. He is always there to provide insight and energy when you hit a wall and cannot seem to progress. Thank you so much for all that you do for us! The world is a brighter, more wonderful place to be because of you.

My committee members, Dr. Eric Guisbert, Dr. David Carroll, Dr. Christopher Chouinard, and Dr. Brooke Wheeler, all deserve special praise. They have been infinitely patient with me while I navigate the intricacies of academia. Their knowledge and expertise have been instrumental in helping to shape the scientist that I am today, and for that I am eternally grateful.

While in the Palmer Lab at FL Tech, I have had the immense pleasure of working with some of the most intelligent and talented people I have ever met. A special thanks goes out to Dr. Tatiana Karpova and Aurora Burkus-Matesevac for their never-ending supply of patience and instrument expertise. Without these two phenomenal women, both the biology and chemistry programs at FL Tech would cease to operate. Their skill, ability, and kindness go a long way.

I also want to highlight just few others who have helped me more than most throughout this crazy odyssey:

Dr. Thiara Bento, thank you so much for your time and patience with me! I truly enjoyed the time we spent in the lab together, talking about everything from kin recognition to best analytical techniques to political turmoil and everything in between. You deserve the world and I wish you the best in everything you do. (And Dr. Mark Moffett, your partner in crime and life, who is without a doubt the most amazing engineer I have ever met!)

Dr. David Handy, my Ph.D. partner in misery. Thank you for being there and both commiserating and celebrating with me over everything from failed experiments to passing classes. I am always happy to be the "rubber ducky" for your thought experiments. You and your partner, Indigo Blackwell, are truly amazing, kind people who deserve all the wonderful things coming in your future. Good luck to you both in all your endeavors!

McKenna Taylor, Lucy Turner, Adam Bach, and Trevor Mello, you are some of the best undergraduate students that I have ever had the pleasure with which to work. You are all amazing people. I greatly appreciate Trevor's inexhaustible enthusiasm for science and the pursuit of knowledge, Lucy's ability to take a rational look at every piece of the research puzzle, making connections that would otherwise go unnoticed, Adam's stoic personality and incredible chemistry knowledge, and McKenna's down-to-Earth nature with dry, witty humor. My time working with you, short as it may have been, has helped keep me both grounded and excited. I look forward to the future you each create for yourselves and the world. I know you'll make us all proud!

To everyone that I have not mentioned by name: I promise I appreciate you and all your kind words, thoughtfulness, and compassion! Words cannot truly express how much I appreciate each and every one of you that has been there with me and/or for me. Your kindness is what we need most in this world, so go out there and make it amazing! I know I will be right there with you, working hard to make the world a kinder, better place.

Dedication

This dissertation is dedicated to all the women who came before me. May my efforts make you proud and help to inspire the generations to come.

Chapter 1
Insights and Implications of Quorum Sensing Mechanisms in Unicellular Eukaryotes

Introduction

Once thought to function autonomously, it is now clear that many unicellular organisms can coordinate a variety of phenotypes to improve the overall fitness of a population. Such group behaviors are associated with the perception of, and response to, biotic and abiotic signals and cues within the environment. Examples of these cues include shifts in temperature, depletion of food sources, proximity of predators, etc. (Bowers and Parke, 1993; Hibbing et al., 2010; Tans-Kersten et al., 2001; Xie and Wu, 2014). Group behaviors that emerge from these phenotypes are of particular importance to understanding microbial evolution as well as the molecular regulation of behavior in the microbial world.

Dictyostelium discodium, a single-celled amoeba, forms aggregate structures that undergo multicellular stages such as 'slug' and 'fruiting body' when under nutrient starvation (Wingreen and Lavin, 2006) (Fig 1B). *Myxobacteria spp.* also coordinate individual cells into large, complex structures to produce cooperative groups, called 'swarms' or 'wolf packs', that move and feed, utilizing different signaling systems coupled with polysaccharide production to achieve this level of cooperation (Chimileski and Kolter, 2017; Islam, et al., 2020; Kaiser, 2013; Muñoz-Dorado, et al., 2016) (Fig 1C). Unicellular eukaryotes also utilize group behaviors. The propensity for these group behaviors to evolve was recently illustrated by an intriguing study of the unicellular algae, *Chlamydomonas reinhardtii,* which was shown to evolve multicellular structures to escape predation by the

filter-feeder, *Paramecium tetraurelia* (Herron, et al., 2019) (Fig 1A). These findings suggest that the selection of specific phenotypes, which may only be beneficial in larger populations, is an evolutionarily viable strategy and a convergent solution across unicellular organisms regardless of their taxonomic domain.

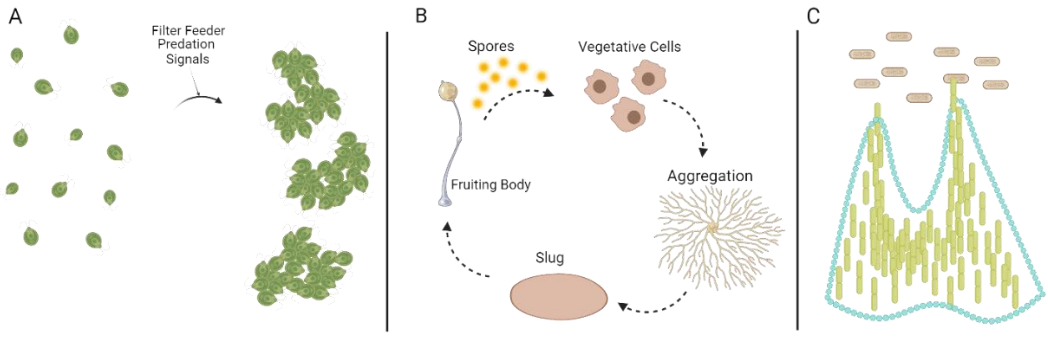

Figure 1.1 Examples of non-quorum sensing group behaviors by microorganisms.

(A) When exposed to filter feeding predators, *C. reinhardtii* adapts by evolving multicellular structures to escape. (B) *Dictostelium discodium* forms aggregate structures that allow this organism to spread out and find nutrient sources. (C) *Myxobacterium spp*. form "hunting" groups to infiltrate and lyse food sources. Teal hexagons denote polysaccharide formation. (Image created using Biorender, www.biorender.com)

Among prokaryotes, one of the most common group behaviors is the phenomenon known as quorum sensing (QS), which couples phenotypic switching to population density via low-molecular weight chemical signals. QS ensures that specific behaviors occur at times that will be the most productive, and therefore beneficial, to the community. QS-related phenotypes are diverse and include behaviors such as motility, conjugation, biofilm production, bioluminescence, virulence factor production, and more (Papenfort and Bassler, 2016; Welsh and Blackwell, 2016). The discovery of QS has provided new insight into microbial behavior and evolution, as well as potential anti-virulence strategies and opportunities to improve, or de novo engineer, beneficial behaviors.

QS regulates the synthesis, diffusion, and perception of low-molecular-weight organic compounds that vary from system to system and are generically referred to as auto-inducers (AIs) in prokaryotes and quorum sensing molecules (QSMs) in eukaryotes. This difference in nomenclature is due to the fact that prokaryotic AI perception upregulates their production, while there is currently little evidence of this occurring with most eukaryotic QSMs. However, for consistency and simplicity, we will refer to all these signals as QSMs in this text. At low cell densities, QSMs are constitutively produced and then diffuse, or are actively transported, out of the cell into the environment. The constant production, diffusion, and sometimes degradation of the QSM as it interacts with the environment allows these compounds to effectively serve as a proxy for cell density. QSMs are then perceived by specific receptors either at the cell surface or intracellularly once they have reached a sufficient concentration for binding. Receptor binding leads to changes in gene expression either: (i) directly, by the QSM:receptor complex acting as a

transcriptional regulator, or (ii) indirectly, by triggering a phosphorylation cascade (Figure 2) (Folcik, et al., 2020).

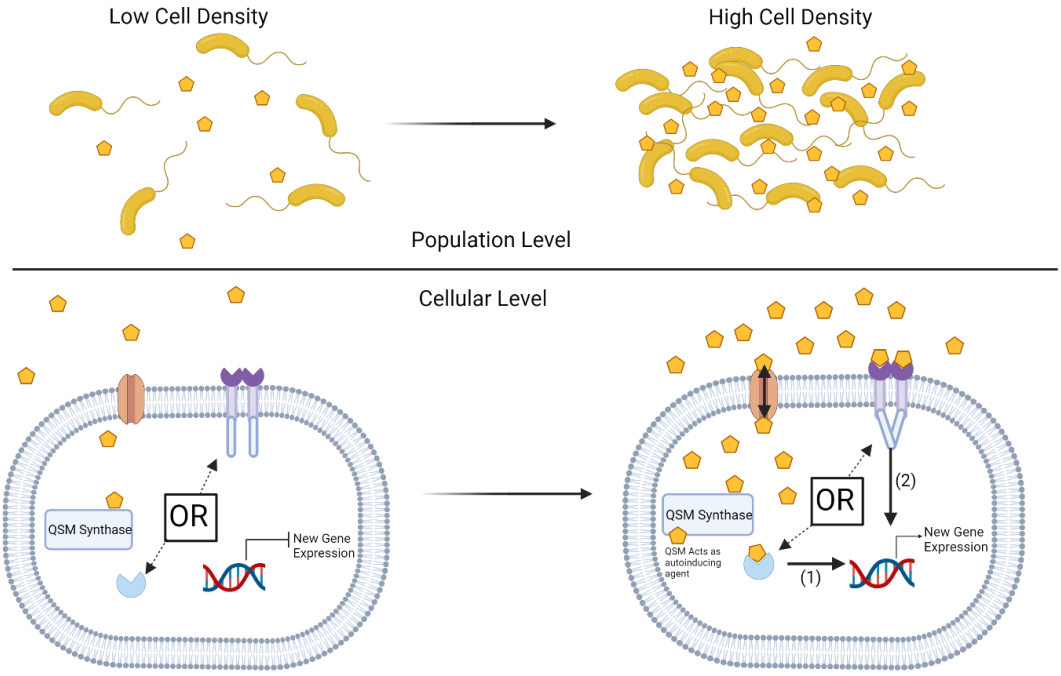

Figure 1.2 General QS Mechanism

As the QSM accumulates, more is available for receptor binding, either intracellularly (1) or to membrane-associated receptors (2). In (1), the QSM:receptor often dimerizes and acts as a transcription factor itself, and in (2) the binding causes a phosphorylation cascade, triggering transcription factor activation. Both types allow transcription factor activation, which causes new gene expression, and a new phenotype emerges. (Image created using Biorender, www.biorender.com)

The most common and best characterized quorum sensing systems are found among Gram-negative bacteria and are an example of the first model, i.e., intracellular binding of a QSM to its cognate receptor which then serves as a transcriptional regulator. These systems utilize N-acyl-L-homoserine lactones, or AHLs, which are composed of an L-homoserine lactone ring and a carbon tail, which varies in length as well as the oxidation of the third carbon (-H, -OH, =O) depending on species (Ahlgren et al. 2011). AHLs are subject to pH-sensitive hydrolysis of the lactone ring, which is inactive as a QS signal in bacteria but can still provide insight into microbial density to plants (Palmer, et al., 2014). At pH>9.0, complete hydrolysis of an AHL can be observed in less than one hour (Fig. 3) (Ziegler, et al., 2019). Yet at pH: 7.0, many AHLs have a half-life >3 days. This pH-sensitive degradation of an active signal couples AHL-mediated QS tightly to the conditions in which they occur either in the environment, at the surface or even inside a prospective host.

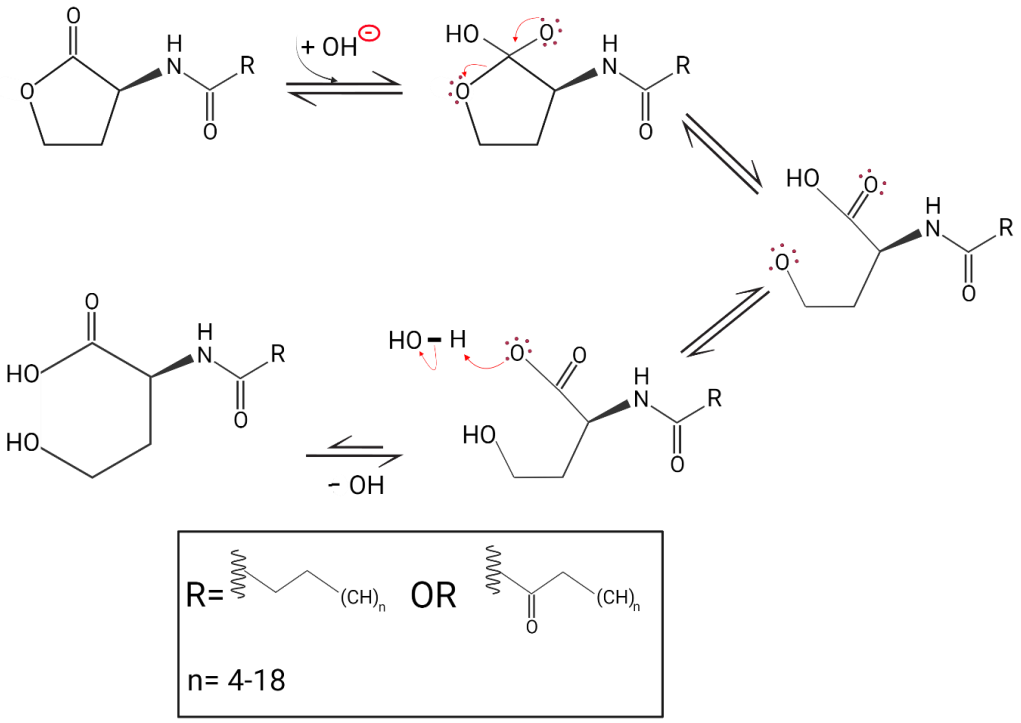

Figure 1.3 Scheme of N-acyl-homoserine lactone hydrolysis.

This reaction has a half-life of >3 days at pH 7 but is pH sensitive. At pH>9.0, this reaction has a half-life of less than an hour.

The marine mutualistic bacteria *Vibrio fischerii* was the first organism in which QS was observed and characterized and remains a model system for understanding AHL-mediated QS. *V. fischerii* resides in the light organ of the Hawaiian Bobtail Squid (*Euprymna scolopes*) which uses the bioluminescence of this bacteria as a type of camouflage, known as counterillumination, protecting itself from predators. *V. fischerii* utilizes the LuxI/LuxR-type QS system, a molecular circuit comprised of an AHL synthase (LuxI) and its cognate AHL receptor (LuxR). In the case of *V. fischerii*, LuxI produces 3-oxo-C6 (an AHL) as a signaling molecule that is secreted in the cytoplasm and can diffuse out of the cell into the extracellular space, where it can interact with other cells. As concentration of 3-oxo-C6 increases within the cytosol of the cell, the interaction potential of the LuxR receptor and 3-oxo-C6 increases. LuxR binds to the 3-oxo-C6 to form LuxR-3-oxo-C6 which then causes dimerization. The AHL:LuxR homodimer then binds to the LuxI operator sequence. This LuxR-3-oxo-C6 homodimer acts as a promoter for the transcription of the LuxI gene. This positive feedback loop results in higher expression of the LuxI gene, raising the concentration of 3-oxo-C6 in the cytosol and extracellular space by diffusion. This causes a forward feeding loop of increased LuxR expression and 3-oxo-C6 biosynthesis, followed by increased operator binding. Homologues of LuxI and LuxR found in many Gram-negative bacteria are responsible for the synthesis and perception of specific AHLs.

Interestingly, the LuxI/R system is not the only QS system at play within *V. fischerii*. At least two other QS systems also play a role in the bioluminescence of this species: AinS-AinR and LuxS-LuxP/Q. In these systems, AinS produces N-octanoyl-

homoserine lactone (C8 AHL), and auto-inducer-2 (AI-2) is produced by LuxS (see figure 4 for signal molecule structures). The C8 AHL is then detected by AinR and LuxR and AI-2 is detected by a periplasmic receptor, LuxP, which also interacts with LuxQ, a histidine-kinase sensor (Lupp, et al., 2003; Neiditch, et al., 2006). Studies of *V. fischeri* mutants reveal that the AinS-signal predominantly induces luminescence in culture, while the LuxI-signal's impact is significant only at high cell densities while in symbiosis. Additionally, AinS regulates essential activities for colonizing *E. scolopes*. AinS regulates gene expression by inactivating LuxO. The *ain* and *lux* QS systems in *V. fischerii* sequentially induce luminescence genes and other colonization factors (Lupp, et al., 2003). These other systems highlight how a “simple” signaling system, like QS, can lead to increasingly complex and dynamic behaviors by linking multiple such circuits together.

Other prokaryotic QSMs include cyclic peptides, AI-2 (**11**), ComX (**12**), quinolones (PQs) and 4-hydroxy-2- alkylquinolines (HQs) (see Fig 1.4 for structures). The majority of autoinducers, such as AHLs (**10**) and oligopeptides (**12**), are used by Gram-negative and Gram-positive bacteria, respectively, for intraspecies communication (Neiditch, et al., 2005; Whiteley, et al., 2017). In contrast, autoinducer-2 (AI-2) is a widely conserved quorum sensing signal produced by both Gram-negative and Gram-positive bacteria, capable of mediating communication both within and between species (Xavier, et al., 2005; Pereira, et al., 2013). AI-2 consists of derivatives of 4,5-dihydroxy-2,3-pentanedione (DPD), which can quickly convert into each other (Chen, et al., 2002; Miller, et al., 2004). DPD is typically synthesized by the enzyme LuxS, though some bacteria without the luxS gene may use alternative synthesis pathways (Neiditch, et al., 2005;

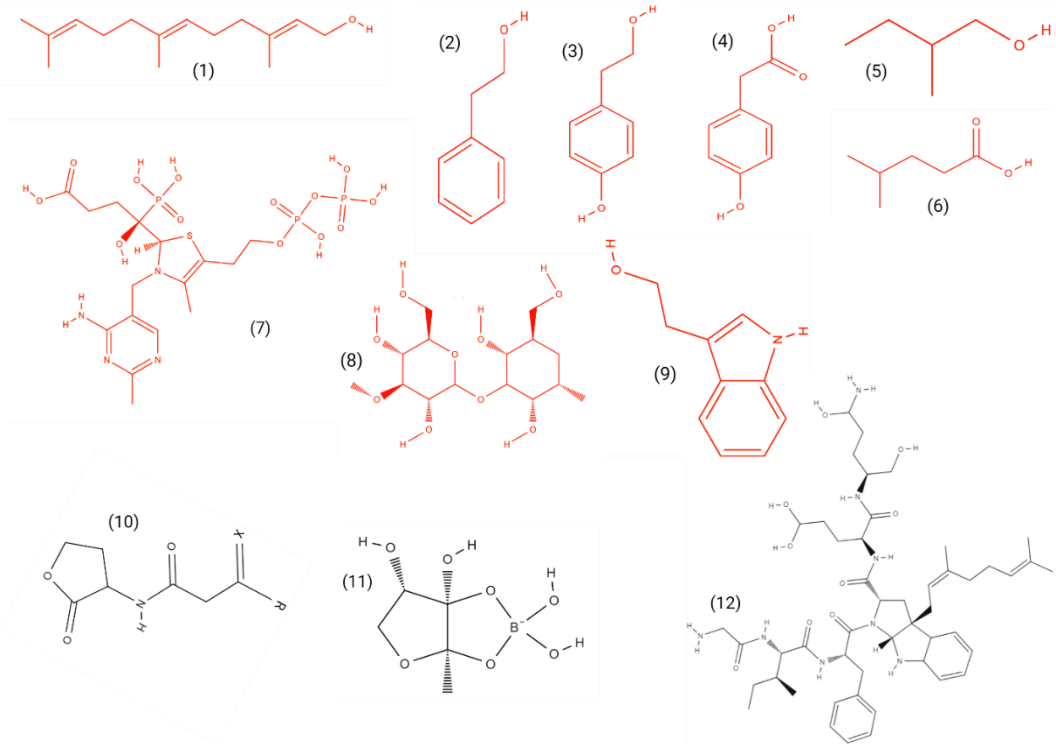

Figure 1.4 Common QSMs for prokaryotes and eukaryotes.

(1) Farnesol, (2) Phenylethanol, (3) Tyrosol, (4) 4-hydroxyphenylacetic acid, (5) 2-methyl-1-butanol, (6) Methylvaleric acid, (7) Qsp1, (8) α-(1,3)-glucan, (9) Tryptophol (10) AHLs (x= -H, -OH, =O; R= 4-18), (11) AI2, (12) ComX. Structures in red denote eukaryotic QSMs, and structures in black denote prokaryotic QSMs (Autoinducers).

Pereira, et al., 2013; Miranda, et al., 2019). Two forms of AI-2 have been identified: the boron-containing S-THMF-borate recognized by LuxP in *Vibrio* species, and the non-borated R-THMF recognized by LsrB in enteric bacteria and some other families (Chen, et al., 2002; Miller, et al., 2004; Rezzonico, et al., 2008; Pereira, et al., 2008; Pereira, et al., 2009; Kavanaugh, et al., 2011; Torcato, et al., 2019; Miranda, et al., 2019). Bacteria with different AI-2 receptors can still communicate because the two active AI-2 forms can rapidly interconvert (Chen, et al., 2002; Whiteley, et al., 2017). ComX, a common QSM in Gram-positive bacteria, encodes a sigma factor that regulates the transcription of multiple genes essential for the uptake of foreign DNA. The ComE protein is activated by autophosphorylation when the competence stimulating peptide (CSP) binds to the ComD histidine kinase receptor. Once phosphorylated, ComE activates target genes, including comCDE, comAB, and comX, creating a positive feedback loop in the QS system (Syvitski, et al., 2007; Verbeke, et al., 2017).

QS in Fungal Species

While significant progress has been made in understanding QS among prokaryotes and some archaea, many of which also use AHLs, only a few examples of QS among unicellular eukaryotes have been observed and characterized. Yet other group behaviors are not foreign to this domain of life, and these preliminary discoveries suggest the QS phenomenon may also be well distributed among eukaryotes. In this review, we will address well-established fungal QS systems as well as recent discoveries in eukaryotic QS.

Prokaryotic QSMs have considerable structural variability, whereas fungi appear to rely predominantly on aromatic alcohols as QSMs (see Figure 4 for structures). Tyrosol (**3**), tryptophol (**9**), and 1-phenylethanol (**2**), as well as the sesquiterpene, farnesol (**1**) and the small peptide, Qsp1 (**7**), have been reported to act as QSMs in *Candida albicans*, *C. parapsilosis, C. tropicalis*, and *Saccharomyces cerevisiae*, among others to control activities such as germ tube formation, virulence, biofilm regulation, iron transport, and phosphatidylglycerophosphate phosphatase (PGPA) production (Hornby et al., 2004; Roca et al., 2005; Albuquerque and Casadevall, 2012).

Candida albicans

Candida albicans—a pathogenic fungus and a common cause of fungal infections in humans—was one of the first fungi discovered to have quorum sensing (Padder et al., 2018). *C. albicans* can change its morphology from a yeast to hyphal growth, a critical ability for *C. albicans* pathogenesis. Research has shown that *C. albicans* strains restricted to either yeast or filamentous forms were significantly less virulent than those able to transition to filaments at different times during systemic infection (Chen and Fink, 2006). Farnesol, a quorum sensing molecule for *C. albicans*, inhibits this morphological change as its concentration increases. Farnesol is produced by *Candida* blastoconidia in suspension, reaching up to 10-50 μM during the stationary phase (Sebaa, et al., 2019). The activation of the cAMP-PKA pathway, and subsequent down-regulation of the hyphal repressor NRG1, is the driving mechanism for the change to the hyphal stage. Farnesol prevents the degradation of the NRG1 protein by preventing *Sok1* expression. SOK1, identified as the kinase for NRG1 degradation, is inhibited by CUP9, a transcription repressor in response

to farnesol. Farnesol inhibits the CUP9 degradation mediated by UBR1, an N-end rule E3 ubiquitin ligase. Both the cAMP-PKA down-regulation of *Sok1* and the SOK1 mediated degradation of NRG1 are needed for *C. albicans* to initiate hyphal growth. Both pathways are inhibited by farnesol's inhibition of CUP9 degradation and promotion of *Sok1* (Lu et al., 2014).

Tyrosol, a tyrosine derivative, was later identified as a second QSM in *C. albicans*. This compound is continuously released into the environment during growth. Tyrosol eliminates the lag phase typically observed when overnight cultures are diluted with fresh medium and accelerates germ tube formation. Tyrosol accelerates germ tube formation but does not counteract farnesol's inhibition of germination. Tyrosol stimulates early-stage hyphal production in micromolar concentrations and inhibits biofilm formation at millimolar concentrations. Thus, the morphological shift between budding yeast and filamentous growth in *C. albicans* is regulated by the interplay of the positive and negative controls exerted by tyrosol and farnesol, respectively (Chen, 2004; Alem, et al., 2006; Sebaa, et al., 2019).

Additionally, farnesol is key for inter-species interactions with *C. albicans*, such as the bacterium *Staphylococcus aureus*. Both *C. albicans* and *S. aureus* are opportunistic microbial pathogens, often found together on hospital patients. In the presence of farnesol, *S. aureus* can exhibit extreme loss of its typical pigment and virulence factor, staphyloxanthin. The exposure to farnesol also resulted in oxidative-stress responses in *S. aureus* while enhancing its tolerance to H_2O_2 and phagocytic killing. Mixed growth of *C.*

albicans and *S. aureus* induced pigment loss, but when *S. aureus* was grown with farnesol-deficient *C. albicans*, this loss was not observed (Vila et al., 2019).

C. albicans, while the first to have QSMs and mechanisms identified in eukaryotes, is not the only fungi to exhibit quorum sensing. *Candida tropicalis* acts similarly to *C. albicans* utilizing both farnesol and tyrosol as QSMs for biofilm formation and hyphae creation (Rodriguez and Černáková 2020). It is believed that the mechanism of farnesol and tyrosol is conserved between *C. tropicalis* and *C. albicans* and may well be conserved across *Candida* species. Farnesol has other properties including biofilm production inhibition and increased cell permeability (Kovács and Majoros 2020). The discovery of farnesol's inhibitory effect on biofilm production has had profound implications in the medical field, where it could be used in conjunction with other antibiotic or antimicrobial strategies to improve health outcomes in patients with implants, cancer, or persistent infections (Cao, et al., 2005; Rossingol, et al., 2007; Sharma, 2011; Webber, et al, 2010; Wang, et al., 2014; Fernández-Rivero, et al., 2017; Dižová and Bujdáková, 2020; Kovács and Majoros 2020).

Saccharomyces cerevisiae

Saccharomyces cerevisiae is a fungal organism that has had a long association with human uses. Known commonly as Brewer's or Baker's yeast, *S. cerevisiae* is a favored model organism among researchers due to its prolific commercial use. Studies have proposed that *S. cerevisiae* utilizes QS to regulate filamentous growth and flocculation (Winters, et al. 2019). *S. cerevisiae* has been found to utilize three possible QSMs: phenylethanol, tryptophol, and tyrosol. These aromatic alcohols are synthesized from their

corresponding amino acids: phenylalanine, tryptophan, and tyrosine. In low nitrogen environments, when only aromatic amino acids are present as nitrogen sources, GAP1 expression is induced, restarting the amino acid permease Gap1p, while the sensor Ssy1p detects these extracellular amino acids (Tan and Prather, 2017; Li, et al. 2023). Gap1p transports the aromatic amino acids into the cell where they are synthesized into their aromatic alcohol counterparts via transamination, decarboxylation, and reduction in the Ehrlich pathway (Li, et al. 2023).

S. cerevisiae's production of QSMs is regulated by cell density, availability of nitrogen, ethanol, and anaerobic/aerobic growth conditions (Li, et al. 2023). *S. cerevisiae* cells release aromatic alcohols as QSMs that induce a morphogenetic switch in response to nitrogen starvation. These alcohols stimulate morphogenesis by increasing the levels of Flo11p, a cell surface protein, and require Tpk2p, part of the PKA signaling pathway. The levels of cAMP within the cell are a critical determining factor in filamentous growth activity, due to its role in regulating PKA activity (Mosch and Fink 1997; Li, et al. 2023). Mutants unable to produce these alcohols exhibit reduced filamentous growth, which can be restored by adding exogenous aromatic alcohols. This filamentous growth is thought to be a response mechanism to nutrient starvation of the organism because filamentation increases the effective surface area of the cell and allows it to actively forage for available nutrients (Jagtap, 2020; Li, et al. 2023). The secretion of these alcohols is regulated by cell density and auto-stimulation, forming a feedback autoregulatory circuit similar to bacterial QS. This pathway enables *Saccharomyces* to respond to both cell density and environmental nutritional conditions.

Cell density regulates the biosynthesis of aromatic alcohols by controlling the levels of ARO9 and ARO10 transcripts, which are higher at high cell densities. The production of these alcohols is also stimulated by tryptophol, which up-regulates ARO9 and ARO10 expression. This regulation requires the transcription factor Aro80p, which directly controls these genes. Thus, there is a cell density-dependent autoinduction loop for producing QSMs in this species, leading to an exponential increase in signaling molecule biosynthesis when activated (Chen and Fink, 2006). Ethanol produced during *S. cerevisiae* fermentation appears to inhibit QSM production, but it is unclear whether this is specifically QSM production inhibition or simply ethanol inhibiting the cells from reaching the density needed for QS (Avbelj, et al. 2015).

A novel mechanism was discovered by which *S. cerevisiae* represses rRNA synthesis in anticipation of nutrient depletion. A study revealed that rRNA synthesis decreases during the log phase. Notably, replenishing nutrients to levels found in fresh media did not restore rRNA synthesis. Moreover, adding spent media quickly inhibits rRNA synthesis in log phase cells, suggesting that QS is responsible for this repression. It was also observed that there was a steady decrease in RNA polymerase I subunits during the log phase, but this does not explain the rapid inhibition caused by spent media. Interestingly, effective rRNA degradation is essential for this repression mechanism, indicating that rRNA degradation is a regulatory point in this QS process. Through standard fractionation, it was found that a small molecule or molecules trigger this repression, though the exact identities remain unknown. Overall, this data indicates that budding yeast utilizes QS to repress rRNA synthesis before reaching the stationary phase,

and that this inhibition is independent of RNA polymerase I availability (Najmi and Schneider, 2021).

Ceratocystis ulmi

Ceratocystis ulmi is a fungus that causes Dutch Elm disease, one of the world's most widespread forestry diseases. This fungus utilizes QS to regulate dimorphic growth using 2-methyl-1-butanol (Fig 4 **5**), methylvaleric acid (Fig4 **6**) and 4-hydroxyphenylacetic acid (Fig 4 **4**). This morphological change serves to enhance the virulence of the fungus. *C. ulmi* secretes these QSMs in order to change from mycelial growth to yeast growth and to mediate inoculum size effect. Its dimorphism is dependent on population-density, as yeasts were found to only form when the inoculum size was $\geq 10^6$ spores/ml. Without this behavior, *C. ulmi* would not be as lethal and would no longer be a threat to the forestry industry.

Cryptococcus neoformans

Cryptococcus neoformans is a fungus that is most known for causing meningoencephalitis and is an opportunistic pathogen that, when at higher cell densities, undergoes a change in autoregulatory signaling that regulates secreted protease activity. One study found that of 11 amino acid peptides that were isolated and tested, the peptide Qsp1 showed quorum sensing-like effects in *C. neoformans* (Lee, et al., 2007). Qsp1 has been shown to mediate protease activity at high cell densities and promote cell wall function (Mehmood, et al. 2019). This peptide is formed from a precursor peptide, known as proQsp1 in *C. neoformans*. ProQsp1 is secreted out of the cell and matures extracellularly into Qsp1. It is hypothesized that CNAG_00150 encodes for Pqp1 and that

cells lacking Pqp1 are defective in processing synthetic proQsp1 into Qsp1 but also respond to Qsp1 itself (Homer et al. 2016).

Qsp1 detection is intracellular and depends on the activity of an oligopeptide transporter (Opt1) that can enable this molecule to cross the cell membrane. Once Qsp1 is inside of the cell, it functions intracellularly to moderate and regulate virulence (Homer, et al. 2016). This peptide, when matured outside the cell and processed inside the cell, plays an important role in the asexual and sexual reproduction of *C. neoformans* (Tian et al. 2018). As the cell density of *C. neoformans* increases, so does the concentration of proQsp1, where it matures extracellularly at a certain concentration threshold, and is transported back into the cells. It then creates a positive feedback loop by increasing the sexual and asexual reproduction of the fungus, which then raises the cell density, consequently raising the concentration of the secreted peptide. Considering the investigation of this process and the impact that cell density has on the concentration and aftereffects of Qsp1, it is more than reasonable to characterize the response of Qsp1 in *C. neoformans* as QS.

Mechanisms for probing and exploiting QS in eukaryotes

Some of these fungal species hold key roles in biomanufacturing (e.g., *Saccharomyces cerevisiae*), human health (e.g., *Candida albicans*, *Cryptococcus neoformans*, and *Histoplasma capsulatum*), and environmental disease events (e.g., *Ceratocystis ulmi*), thus it is especially important to identify and understand these microorganisms' perception and response to their environments. While much work has

been done to identify more about the molecular underpinnings of *S. cerevisiae* and *C. albicans*, not much has been done to identify the workings of QS in *C. ulmi* and *H. capsulatum*. Better understanding of the mechanisms at work in these species would help to devise effective strategies to control disease outbreaks in forests and mammals, respectively, from these organisms.

Candida biofilms exhibit resistance to conventional antifungal treatments and the host immune system. The transition from yeast cells to hyphae is crucial in *C. albicans* biofilm development, and this process is inhibited by the QSM farnesol. A study published in 2020 similar to the structure-activity studies previously done on AHL-producing bacteria (Palmer, et al., 2011a & 2011b) evaluated how the structure of farnesol was related to this activity to find potential analogues for disruption of biofilm formation and filamentous growth without cytotoxicity to a host. Out of 31 tested saturated and unsaturated fatty acids similar in structure to farnesol, six medium-chain saturated fatty acids—heptanoic acid (**1**), octanoic acid (**2**), nonanoic acid (**3**), decanoic acid (**4**), undecanoic acid (**5**), and lauric acid (**6**)—significantly inhibited *C. albicans* biofilm formation by more than 75% at a concentration of 2 μg/ml, with minimum inhibitory concentrations (MICs) ranging from 100 to 200 μg/ml. These six fatty acids, at 2 μg/ml, along with farnesol (**7**) at 100 μg/ml, suppressed hyphal growth and cell aggregation (see figure 6 for structures). Additionally, the accumulation of fatty acids in *C. albicans* cultures reduced the production of farnesol and other sterols. The downregulation of several hyphal and biofilm-related genes by heptanoic or nonanoic acid mirrored the effects induced by farnesol. Moreover, nonanoic acid, the most potent compound,

decreased *C. albicans* virulence in a *Caenorhabditis elegans* model without inducing cytotoxic effects. These findings suggest that medium-chain fatty acids are more effective than farnesol in inhibiting hyphal growth and biofilm formation, which could have a profound impact on pharmaceutical developments for treating infections by this opportunistic pathogen (Lee, et al., 2020).

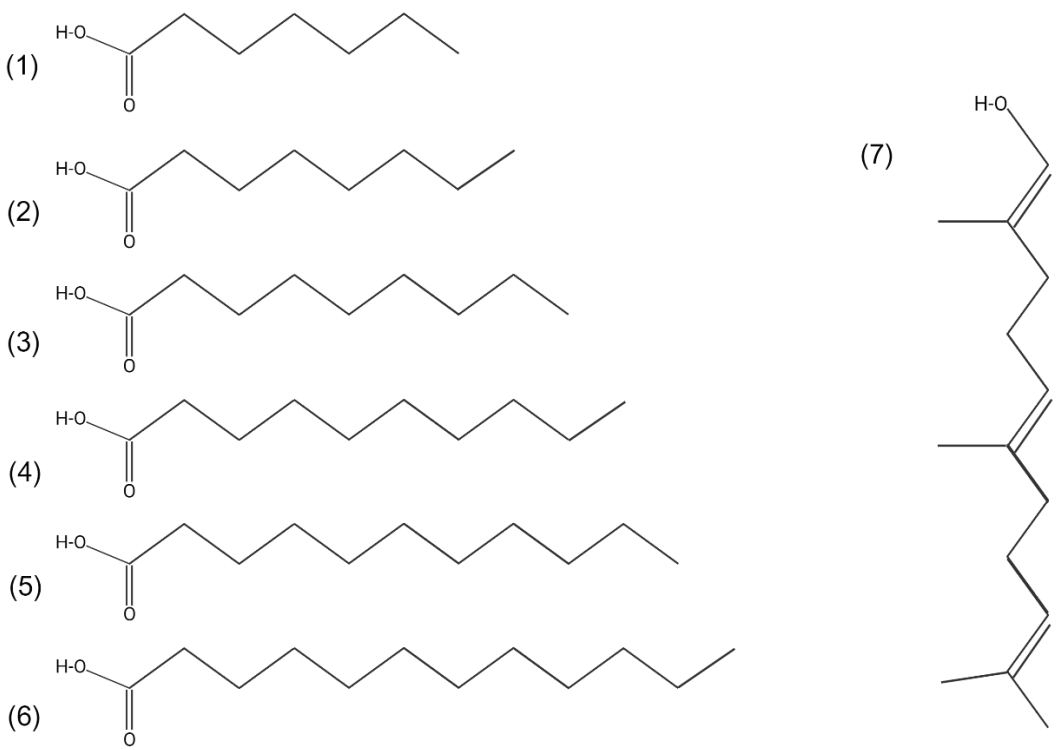

Figure 1.5 2-D structures of (1) heptanoic acid, (2) octanoic acid, (3) nonanoic acid, (4) decanoic acid, (5) undecanoic acid, and (6) lauric acid as compared to (7) farnesol.

These medium chain saturated fatty acids were shown to inhibit biofilm formation by *C. albicans*. (Image was created using Biorender, www.biorender.com).

Histoplasma Capsulatum

Histoplasma capsulatum is a fungal pathogen that can take on two different forms: one being a mold-like fungus found in soil, and the other being yeast, which can be found as an airborne pathogen that affects mammals. The yeast form of *H. capsulatum* can survive in specific phagocytes within the human body called macrophages. Macrophages carry out phagocytosis, yet the yeast cells can withstand the intracellular environment. This suggests that genes expressed solely in the yeast form can contribute to this survival. The yeast has β-glucan components in the cell wall that can be detected as pathogenic by the host cell; the host cell will initiate functions to get rid of the yeast if detection occurs. However, *H. capsulatum* cells release a factor that, as it accumulates, assists in the accumulation of α-(1,3)-glucan in the cell wall. α-(1,3)-glucan was found to be linked to strain-specific pathogenicity or virulence and can mask the β-glucan so the yeast cells go undetected by the host. The density-related switch in yeast cells, due to the accumulation of α-(1,3)-glucan, is an indicator that this species has a QS pathway.

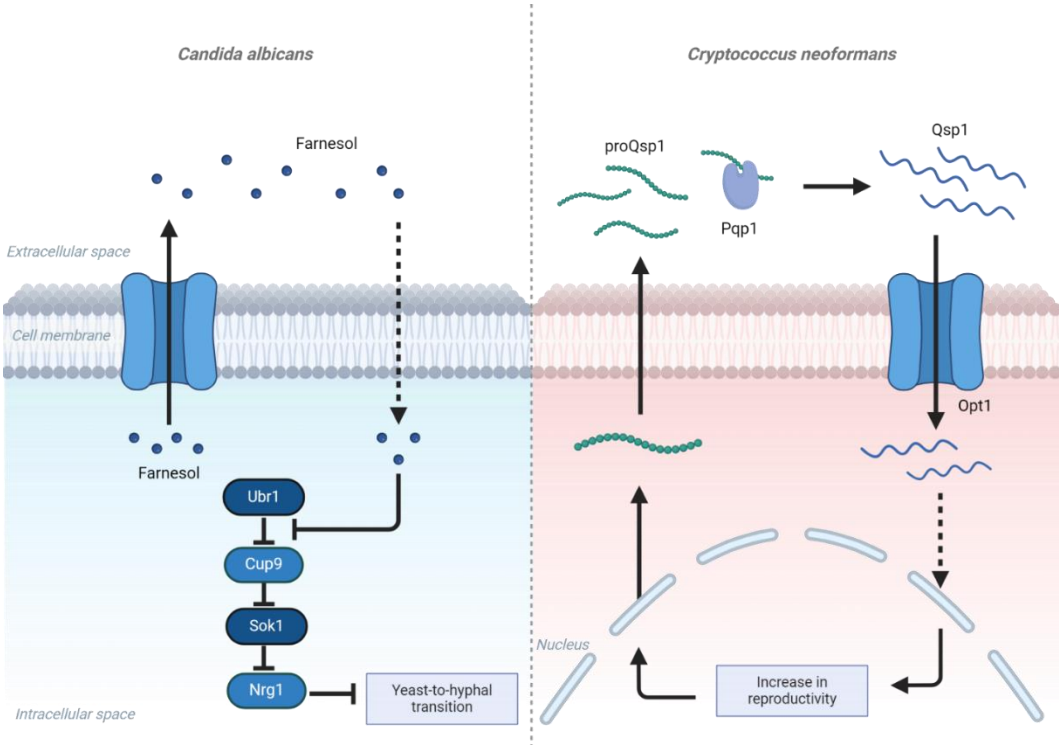

Figure 1.6 QS mechanisms in *Candida albicans* (Left) and *Cryptococcus neoformans* (Right).

C. albicans produces farnesol, which inhibits the yeast-to-hyphal transition, delaying pathogenicity in this species (Left). *C. neoformans* produces a peptide, proQsp1, which is secreted out of the cell, where an extracellular, surface-associated protein, Pqp1, modifies the precursor into the signaling peptide, qsp1. Dashed lines indicate currently unreported transportation and signaling steps. Figure made using Biorender (www.biorender.com).

Novel Eukaryotic QS System Discovery:

The discovery of QS systems in fungal species prompted us to pursue the possibility that this phenomenon may be conserved in other unicellular eukaryotes. The model unicellular eukaryote *Chlamydomonas reinhardtii* is a model organism to study photosynthesis biochemistry, motility, and cellular reproduction, and has previously displayed the capacity to evolve group behaviors (Harris, 2001; Herron, et al., 2019). Specifically, the formation of aggregated cells in response to multi-generational predation. Motility is a major feature of *Chlamydomonas spp.* and is frequently regulated by QS among prokaryotes. This organism is also ideal for the search for new QS phenotypes as it is genetically tractable and there are numerous mutants and wild-type variants available for discovery.

Significance

QS in this species could prove useful for industries such as biofuel production and pharmaceuticals. *C. reinhardtii* is a ubiquitous microorganism and has much genetic variation within its species (Jang and Ehrenreich, 2012; Flowers, et al., 2015), many of which are already used in the biofuel industry (Jones and Mayfield, 2012; Oncel, 2013; Scranton, 2015) and as a biomanufacturing host for producing therapeutics and vaccines (Almaraz-Delgado, et al., 2014; Rasala and Mayfield, 2015; Scranton, 2015). Utilizing a QS pathway to increase and improve the production of these ecologically and economically important outputs would improve the biomanufacturing field and offer a low-cost alternative manufacturing process.

Discovery of QS in *C. reinhardtii* could have many implications for microbial ecology and evolution. The discovery of QS in non-fungal eukaryotes would give evidence that systems to regulate group behaviors allow the population to persist and are a convergent strategy across all domains of life. Indeed, even macro-organisms communicate to control population behaviors, such as kin recognition in plants (Palmer, et al., 2016). This discovery broadens the potential for QS discovery in other unicellular eukaryotes. It is clear that work needs to be done on identifying a QS system in *C. reinhardtii*, as well as other molecular mechanisms that may be at work.

This dissertation addresses the following questions:

> Question 1: How do we measure and characterize the swimming speeds of microorganisms? (Chapter 2)

C. reinhardtii has long been associated with photo-, chemo-, and gravitaxis, which makes it an ideal system for investigating and understanding how stimuli can be integrated to regulate motility in unicellular microorganisms. Motility in this species has previously been done using high-speed photographic evidence and manual tracking, which can be time consuming and error prone (Racey, et al., 1981). Furthermore, cultures can reach densities > 10^5 cells/ml. Manual analysis of <100 tracks are unlikely to accurately reflect a population-wide behavior. Therefore, a computer-automated particle tracking method for characterizing motility, which includes directionality and speeds, was devised to help overcome these limitations.

Question 2: How do we know what behavior to look for in a microorganism when investigating QS? (Chapter 3)

Motility is a common QS strategy in prokaryotes for dealing with nutrient availability, allowing them to spread out in search of new nutrient sources prior to reaching the environment's carrying capacity (Hibbing, et al., 2010). QS strategies related to growth morphology are also found in fungal species, allowing the switch to and from filamentous growth and budding yeast growth (Albuquerque and Cassadevall, 2012). This suggests that strategies dealing with nutrient scarcity are common to all unicellular microorganisms, of which the ability to spread the population out is key.

Question 3: Does *C. reinhardtii* quorum sense? (Chapter 3)

New behaviors emerging as a result of population density is a key feature of QS. In QS systems, the production and perception of a signal molecule is used by the species as a proxy for estimating the population density (Papenfort and Bassler, 2016; Welsh and Blackwell, 2016). We utilize many methods, including the method described in chapter 2, to investigate whether motility is linked to population density in *C. reinhardtii*. We also investigate if this behavior is conserved within this species.

Question 4: What is the identity of the QSM in *C. reinhardtii*? (Chapter 4)

Using what we have learned about QS in *C. reinhardtii*, we investigate what the signal is that causes this behavioral shift. Implementing a new method of QSM extraction that is quicker to produce and better for use on analytical instruments was key in the rapid

turn-around of signal extracts for purification and testing. HPLC, LCMS/MS, and NMR were all used on the signal extract to reduce signal noise in the samples and characterize the QSM in this species.

Chapter 2

Computer-Assisted Tracking of *Chlamydomonas* Species

Published Jan, 2020 in Front. Plant Sci. 10:1616 doi: 10.3389/fpls.2019.01616

Introduction

The unicellular alga *Chlamydomonas reinhardtii* is a model organism for the study of flagellar motility, photosynthesis, and a variety of biotechnology applications among unicellular eukaryotes. This photoautotroph has minimal culture requirements, is genetically tractable, and has an extensive strain repository including numerous motility mutants (Luck et al., 1977; Huang et al., 1981; Huang et al., 1982a; Huang et al., 1982b; Kuchka and Jarvik, 1982; Segal et al., 1984; Kamiya, 1988; Barsel et al., 1988; Bloodgood and Salomonsky, 1989; Kuchka and Jarvik, 1987; Kamiya et al., 1991). Photo-, gravi-, and chemotaxis have all been associated with this organism, making it an ideal system for understanding how multiple inputs can be integrated to regulate motility in unicellular organisms. Prior efforts to quantify *Chlamydomonas* motility have largely focused on high-speed photographic evidence, which was then analyzed by manual tracking (Racey et al., 1981). However, such methods are time-consuming, prone to error, and unlikely to resolve multiple responses within a population. Moreover, algal cultures frequently reach densities ranging from 10^5 to 10^7 cells/ml. The results of a handful of tracks (<30) are unlikely to be an accurate reflection of the behavior of such a population. The ability to observe a larger

sample size would also provide refined insight into the dynamic response range of this model organism rather than just an average.

Automated particle tracking in which individual constituents of a population, biotic or abiotic, are followed over time can yield data on particle speed, directionality, size, and other features of interest for understanding the behavior of the observed population. In the case of *C. reinhardtii*, we hypothesized that such approaches would be able to accommodate significantly more tracks, providing better models of behavior within a population of cells. Here, we report a new method to characterize motility in *C. reinhardtii*, which allows us to identify individual particles (cells) as well as gather population-wide information on speed as well as directionality. The proposed strategy requires only a microscope with a camera to collect images and utilizes a publicly available software package, the TrackMate plugin for ImageJ, for analysis (Schneider et al., 2012; Tinevez et al., 2017).

In the present study, we evaluated the impacts of light and nutrient availability on motility in wild-type *C. reinhardtii*, as well as characterizing a series of motility-deficient mutant lines. The ability to quantify the effects of such mutations provides a refined perspective on the impacts such mutations may have on these organisms. Our work provides a new tool for evaluating and modeling motility in this model organism. Furthermore, we confirm that the established methodology is able to characterize motility in another member of this genus, *Chlamydomonas moewusii*, supporting the broader utility of this approach for observing motility in other unicellular microorganisms which may have important roles in host–microbial associations and/or biotechnology.

Materials and Methods

Materials

Unless stated otherwise, all reagents were purchased from either Fisher Scientific or Sigma Aldrich.

Algae Growth and Media

*C. reinhardtii*wild-type (cc124), *C. reinhardtii* mutants (see Table 2.1), and *C. moewusii* (formerly *Chlamydomonas eugametos*) were acquired from the *Chlamydomonas* Resource Center (http://www.chlamycollection.org/) (Luck et al., 1977; Huang et al., 1981; Huang et al., 1982a; Huang et al., 1982b; Kuchka and Jarvik, 1982; Segal et al., 1984; Kamiya, 1988; Barsel et al., 1988; Bloodgood and Salomonsky, 1989; Kamiya et al., 1991). Individual lines were maintained by streaking cultures on plates of Tris-acetate-phosphate (TAP) media with agar. Liquid cultures were prepared by growing lines individually in 25 ml of TAP media for 72 h under a 16:8-h day/night cycle (~13,800 W/m2) at 23°C on a shaker (~150 rpm) (Haire et al., 2018). Minimal media studies were performed by limiting the amount of available nitrogen by restricting the amount of NH_4Cl, either to low (50%, 400 mg/l) or NH_4-free TAP media.

Video Acquisition

All motility data was acquired under minimal lighting in a darkroom to minimize background phototactic effects. Cell density was determined by fixing 200 µl aliquots of cells in 1.7% formaldehyde and manually counted using a hemocytometer at ×400. The remainder of the culture was incubated at 23°C in the dark for 30 min to reduce the impact of light on cell movement. Algae

cultures were vortexed for ≈30 s to resuspend any settled algae. Aliquots of 30 µl were placed on a slide and viewed under an Olympus CH30 binocular microscope at ×100 magnification. Cells were allowed to settle to avoid artificial movement of the cells caused by convection currents in the liquid on the slide. ToupView software (www.touptek.com) was used to collect videos with an AmScope FMA050 fixed microscope camera. Videos were collected with a frame rate of 7.5 frames/s for approximately 30 s.

Video Analysis

Videos were imported into Fiji for splitting and tracking analysis (Schindelin et al., 2012). Calibration was done using a micrometer ruler slide to determine pixel length. To analyze tracks, the pre-installed Fiji plugin TrackMate was utilized (Tinevez et al., 2017). Cell size was also determined through Fiji. The resulting files were saved in comma-separated values (CSV) format as "Spots in tracks statistics," "Track statistics," and "Links in tracks statistics."

To determine the directionality of each track, the files "Spots in tracks statistics," "Track statistics," and "Links in tracks statistics" were combined using the statistical computing software R using the RStudio interface (www.rstudio.com) (R Development Core Team, 2016). This allowed for the creation of a new file in Tab Delimited Text format containing direction vectors of all cell tracks. From the combined R file, Rose plots were generated by dividing the slide viewing area into eight wedges and plotting the total fraction of cells in each section. Preliminary findings were confirmed using the Chemotaxis and Migration Tool (www.ibidi.com). Histograms of varying speeds within the population were generated by the data analysis package in Excel. Average speeds of tracks

were determined using the “Track statistics” file. Units were converted to micrometers per second by dividing the time of the video by the number of image slices.

Phototaxis Studies

Light intensity studies were completed using a Leica 13410311 Illuminator dissection scope leveled with the microscope platform. This allowed for the light to pass perpendicular to the slide across the sample. Light intensity settings were measured using Digital Luxometer. Cultures of 30 µl were loaded onto slides and exposed to the indicated intensity of light immediately before data collection.

Results

Particle Tracking

The digital equivalent of manual tracking across multiple video frames with hundreds of particles (cells) rapidly becomes computationally restrictive if the spatial coordinates of every possible combination has to be recorded from frame to frame over the period of these videos (30 s). This is an example of what is known as the ‘linear assignment problem’ and is well established in image analysis (Kong et al., 2013; Diem et al., 2015). However, this limit can be overcome by a variety of approaches. We utilized a publicly available software package, the TrackMate plugin for ImageJ, for analysis. In this package, videos are separated into individual frames, and the total number of particles, in this case cells of *C. reinhardtii*, in each frame are counted by identifying the edges using a Laplacian of Gaussian (LoG) detector, a common approach in image analysis (Leal Taixé et al., 2009; Kalaidzidis, 2009). TrackMate then matches particles across multiple frames

using the Munkres–Kuhn (aka Hungarian) algorithm which identifies the most likely matches for the particles between frames and is also a well-established method for tracking multiple particles (Kong et al., 2013; Diem et al., 2015).

Table 1 *Chlamydomonas reinhardtii* motility mutants, their mutation types, and average speeds (±standard error) as compared to wild-type (cc124)

Strain ID	Mutation Type[1]	Avg. Speed[2]	% Wild-type	Reference
cc124	Wild-type	40.0 ± 4.5	100	
cc125	Phototactic aggregation	46.0 ± 2.0	115	Pröschold et al., 2005
cc602 pf1	No radial spoke heads	2.8 ± 0.6	5	Luck et al., 1977
cc1026 pf13	Axonemal protein defects	9.0 ± 5.0	20	Huang et al., 1982b
cc1032 pf14	Lacks radial spokes	3.5 ± 0.1	6	Huang et al., 1981
cc1036 pf18	No central microtubules	1.5 ± 0.7	3	Bloodgood and Salomonsky, 1989
cc1926 uni1	Single flagellum cells	15.0 ± 3.0	38	Huang et al., 1982a
cc2228 oda1	Lacks outer dynein arms	11.0 ± 2.0	23	Kamiya, 1988
cc2288 lf2-4	Long flagella	32.0 ± 1.0	80	Barsel et al., 1988
cc2530 vfl2	0–6 flagella	4.0 ± 2.0	10	Kuchka and Jarvik, 1982
cc2670 ida4	Dynein arms	14.0 ± 2.0	35	Kamiya et al., 1991
cc2679 mbo1	Flagellar axoneme	3.4 ± 0.6	9	Segal et al., 1984
cc3663 shf1	Short flagella	22.0 ± 2.25	50	Kuchka and Jarvik, 1987

[1]Reference, [2]Average speed expressed in terms of micrometers per second with standard error as determined by image analysis in this study.

Visualizing Cells and Quantifying Motility

We selected *C. reinhardtii* cc124, a common lab strain, for our initial experiments as it is the parent line for a number of motility mutants. Cultures were grown for 72 h in standard TAP media at room temperature to a density of 10^7 cells/ml (see Methods). Thirty-second videos of 30 µl aliquots of cultures were acquired and subsequently processed and analyzed in ImageJ with the help of the TrackMate plugin. A representative image slice extracted from one of the videos is shown in Figure 2.1A. Each frame of the video is automatically separated into different slices and the particles (algal cells) counted (Figure 2.1B). *C. reinhardtii* is known to form motile aggregates such as diads and tetrads, which could skew the counting process. However, the software reliably distinguished individual members of this collection of cells (Figure 2.1C). From these videos, we were able to acquire 3,000–6,000 individual tracks for analysis over a 30-s period (see Supplementary Video 1).

Cells were then tracked frame by frame to determine average speeds (Figure 2.1D). The average speed of our cc124 populations at 72 h was 40 ± 4.5 µm/s (Figure 2.1E). These findings are slower than some of those derived from previous studies, which can range from 80 to 200 µm/s (Racey et al., 1981; Marshall, 2009; Engel et al., 2011). However, close inspection of our track speeds confirmed an upper rate of ≈93 µm/s, in the range of these previously reported values. A histogram of speed distributions in this population confirmed that >50% of the total tracks for each sample (3,000–6,000 tracks/video) were within the 31- to 60-µm/s range (Figure 2.1F), consistent with the average speed.

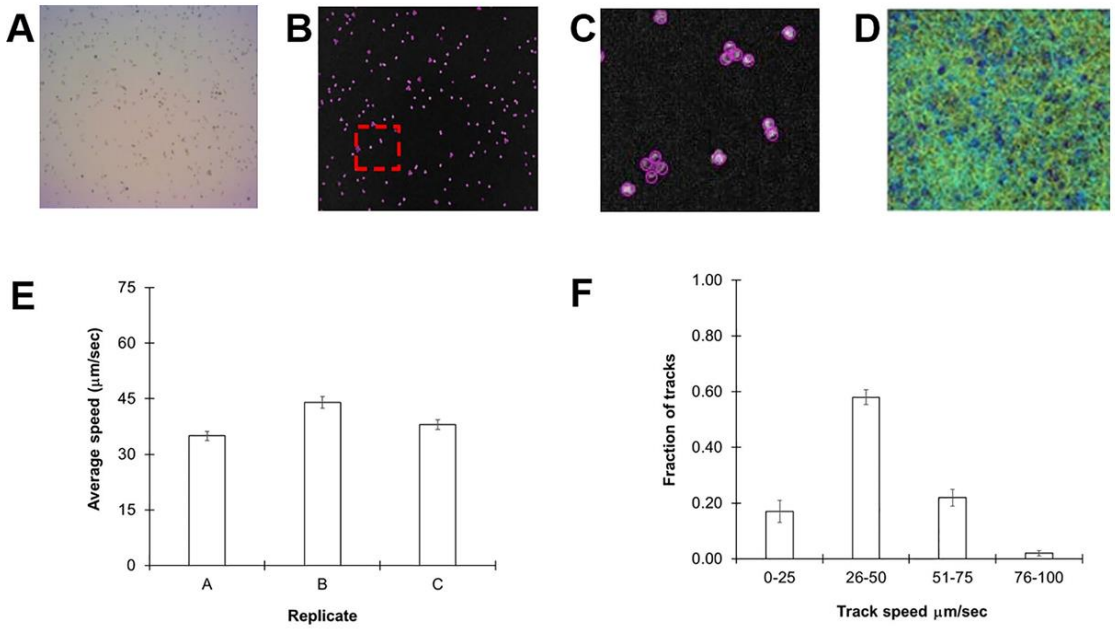

Figure 2.1 Monitoring *Chlamydomonas reinhardtii* motility by automated video tracking.

(A) Image slice from cc124 72-h culture. (B) Isolated video frame/slice from ImageJ. (C) Magnification of image contained within red box of (B), highlights individual spheres around tetrads and diads, underscoring the ability of the software to distinguish individual cells even in aggregates. (D) Heat map showing all tracks over a 30-s video from a 72-h culture. (E) Replicate study of 72-h-old cc-124 cultures. Each replicate was performed on a different day and is expressed as the average of three different samples recorded on that day, with error bars representing standard error. (F) Histogram showing distribution of tracks at different speeds from the same samples, with error bars representing the standard error.

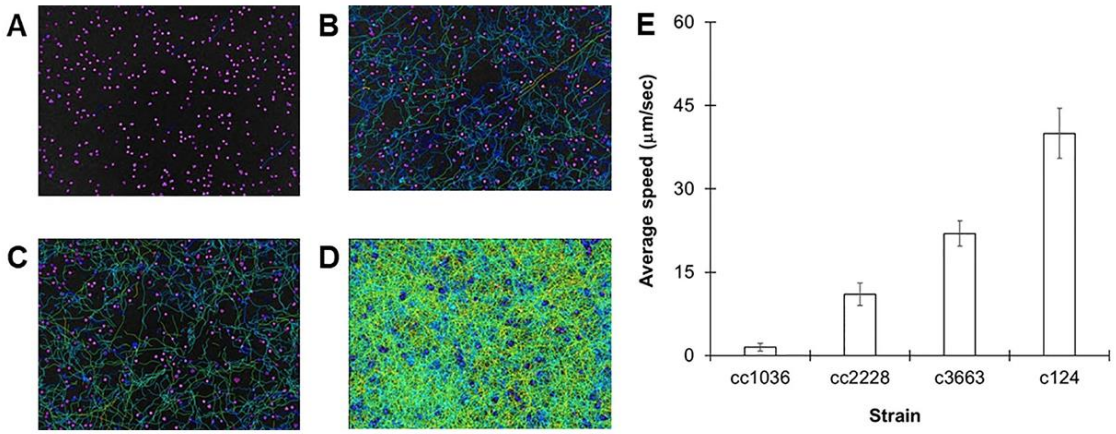

Figure 2.2 Using *C. reinhardtii* motility mutants to observe different populations.

(A–D) Heat maps showing all tracks over 30-s videos from 72-h cultures for cc1036 (A), cc2228 (B), cc3663 (C), and cc124 (D) strains. (e) Average speed in micrometers per second for the indicated strain of *C. reinhardtii*. Results are expressed as the mean of three videos, with error bars representing standard error. Using *Chlamydomonas* Mutants to Observe Changes in Motility.

A large assortment of motility mutants are available for *C. reinhardtii* which have helped elucidate the mechanisms of flagellar motility. Unfortunately, the characterization of such mutants is generally limited to relative statements, i.e., "slower" or "extremely slow," rather than being quantified. In order to confirm the robustness of our tracking approach, we evaluated the swimming speeds of several mutant cell lines of *C. reinhardtii*. We initially investigated three specific mutant strains: cc1036, a non-motile line, as well as cc2228 and cc3663, both motility-deficient lines. Video analysis confirmed that the total number of tracks for each sample increased in the following order: cc1036, cc2228, cc3663, and finally cc124, respectively (Figures 2.2A–D). The average speed of the mutant lines ranged from ≈1 μm/s (cc1036) to 20 μm/s (cc3663) based on a minimum of 1,000 tracks/video for each mutant (Figure 2.2E and Table 2.1).

Our results establish lines cc1036, cc2228, and cc3663 as examples of 0%, 25%, and 50% motility lines, respectively, when compared to the wild-type cc124 strain. A sample video for cc3663 is provided as Supplementary Video 2 (see Supplementary Material). Closer inspection of the 25% mutant (cc2228) showed that a small fraction of these mutants (<0.01%) were actually able to obtain speeds in the 21- to 40-μm/s category, with a maximal speed of 30 μm/s. The ability to obtain this information provides valuable insight into the stochastic nature of cell populations, but may also be used for identifying unique behaviors and compensatory mutations which may arise. Using this method, we obtained the average cell speeds for 12 different *C. reinhardtii* mutant lines (Table 2.1). We note that the cc125 line, which is deficient in phototaxis, actually moves slightly faster than the cc124 strain (115%, $p = 0.05$, as determined by Student's *t* test). In addition to the successful characterization of swimming speeds in mutant lines, this approach appears to

have even broader utility as we were also able to characterize the swimming speed of a closely related species, *C. moewusii* (48 +/– 6 μm/s).

Characterizing Mixed Populations

Our method was able to measure swimming speeds in populations which converged around a single maximum number of tracks. However, it should also be robust enough to handle mixed populations of varying speeds. In order to evaluate this, we combined equal concentrations of 72-h cultures of cc124 and cc2228, a mutant with 25% motility of wild-type. As seen in Figure 2.3, the distribution of track speeds for mixed cultures was distinct from either of the cultures for each line individually, with an average speed of 36 ± 2.5 μm/s. These findings underscore the ability of this approach to observe variations within the population.

Effects of Culture Conditions on Speed

While specific mutations impact swimming speed, it is changing environmental conditions, such as nutrient availability and light, which influence speed and directionality of motility in the wild type. As previously stated, this particular strain of *C. reinhardtii*is known to be

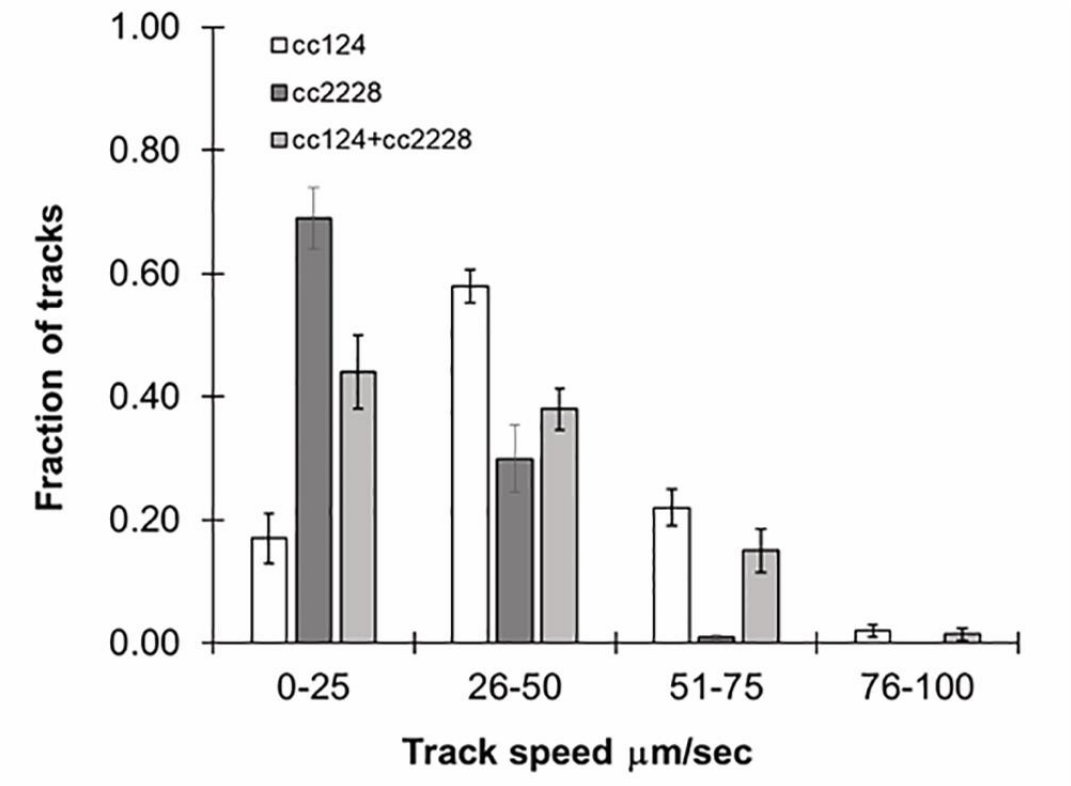

Figure 2.3 Following mixed populations by video tracking.

Histograms showing the distribution of speeds for 72-h cultures of cc124 (wild type), cc2228 (25% motility), and a combined culture of both. Results are the mean of three videos, with error bars representing standard error.

sensitive to nitrogen availability, and we tested the effect of this on swimming speed. We prepared reduced nitrogen TAP by limiting the amount of NH_4Cl added to the media to either 50% or no NH_4Cl. As shown in Figure 2.4, a fraction of the algae cultured in 50% NH_4Cl TAP (≈40%) were observed in the 51- to 75-μm/s range, while in regular TAP only 20% of the cultures reached this range. We propose that this unexpected increase in swimming speed is to support the search for new nitrogen sources in this nutrient-depleted environment. This was in stark contrast to cells cultured in NH_4Cl-free TAP, which significantly reduced motility, not surprising given its importance in flagellar motility and development (Engel et al., 2012). We note that a small fraction of these cultures (<5%) seemed unaffected by the nitrogen availability differences in these media, suggesting some compensatory mechanisms may be at work. Ongoing studies in our lab are further exploring media effects on swimming speeds in this model organism.

Visualizing Phototaxis in cc124

The studies above confirm the utility of this approach to obtain population-level resolution of variations in swimming speed in response to mutation or changing environmental conditions. However, the same method used to determine speed also provides spatial coordinates for each track, allowing us to measure overall changes in the directionality of our samples. In this approach, the coordinates of each track are used to determine where the samples reside within the image. The image space is then divided into eight distinct sectors and populated accordingly. Analysis of our 30-s videos of cc124 in regular TAP media confirmed that the cells were uniformly distributed across the slide, establishing that there is no directionality bias (artifact) in our technique, which might impact our study (Figure 2.5A).

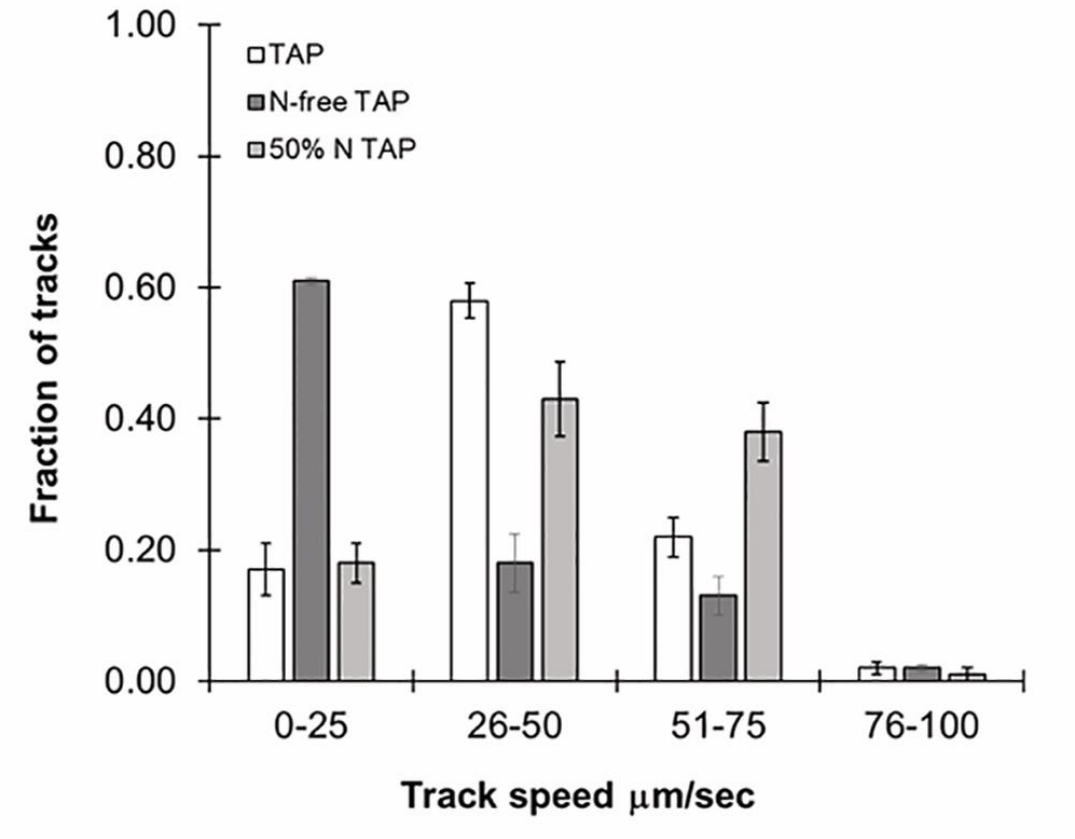

Figure 2.4 Effects of different media types on motility.

Histograms showing distribution of speed across cc124 cultures grown in Tris-acetate-phosphate (TAP), N-free TAP, or 50% N-TAP, respectively. Results are the mean of three videos, with error bars representing standard error.

Phototaxis is a commonly observed phenomenon in the cc124 line. Cells will move into the path of light, but also away from the source, presumably to minimize photosynthetic stress. We next sought to exploit this response to see if we could observe population-wide directionality changes utilizing our approach (Harris et al., 2013). Phototaxis was induced by placing a narrow beam of white light (≈75,000 W/m_2) perpendicular to the focal plane of the slide. As shown in Figure 2.5B, within 5 min of light exposure, the bulk of the cells in the sample oriented into the path of the light but also into the three sectors furthest from the light source. Surprisingly, there was no increase in swimming speeds within the population in response to this stimulus. These findings confirm the ability of our approach to detect changes in directionality across the window provided by the microscope camera (8.19 mm diagonally across the camera window). While preliminary, this experiment confirms the ability of this approach to observe responses to stimuli within the experimental environment (i.e., the microscope slide). Future experiments will explore the potential for chemotaxis across the surface area of the slide.

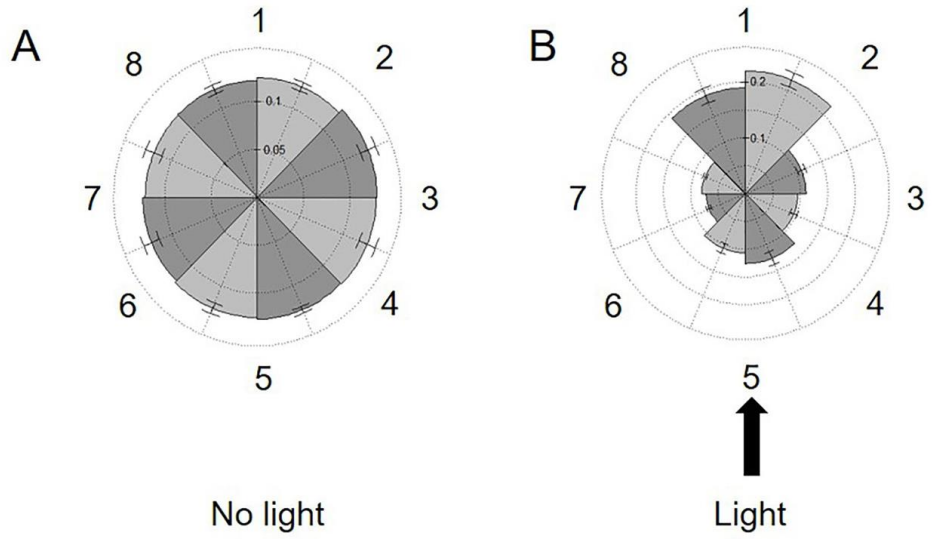

Figure 2.5 Measuring phototaxis across the imaging area.

Rose plots dividing the viewing area into eight sections (numbered left to right 1–8) are populated with the spatial coordinates of all tracks in 30-s videos of 72-h cultures of *C. reinhardtii* cc124 either: (A) without or (B) in the presence of a 75,172-W/m_2 external light source. This light source was placed perpendicular to the slide surface (at section 5). The fraction of tracks in each section is noted on the internal axes/spokes. Results are expressed as the average of three experimental replicates, with error expressed as standard deviation.

Discussion

Automated image analysis provides us with an opportunity to observe and characterize population-level responses, overcoming the limits to statistical resolution and bias associated with manual measurements. In the present study, we have developed a method requiring no custom-designed equipment or software, only a microscope, camera, and the free software package Fiji to analyze the motility of *C. reinhardtii*. Employing this method, we were able to observe differences in swimming speeds between the wild-type strain and several motility mutants, providing quantitative values to these mutants for the first time. In addition to motility mutants, we showed that our approach was sensitive to changes in media composition such as nitrogen availability. As expected, the removal of NH_4Cl from TAP seriously compromised motility, but unexpectedly, a 50% reduction in NH_4Cl resulted in an increase in the swimming speed of a portion (20%) of the cells. We propose that this rate increase facilitates the search for new nitrogen sources under nitrogen-limited conditions.

When coupled to the microplate-based methods we have already developed for investigating the growth and viability of this microorganism, we are now prepared to thoroughly explore and characterize the impacts of changing environmental conditions and/or mutation on multiple aspects of *Chlamydomonas* biology (Haire et al., 2018). Indeed, our ability to measure swimming speeds in *C. moewusii* strongly supports the utility of this approach for understanding motility in this important genus of over 300 species. While focused on this model unicellular eukaryote, the approaches outlined here should be easily exportable to other genera, potentially

providing new insights into microbial ecology, modes of pathogenesis, and other aspects of microbial behavior.

Chapter 3

Quorum Sensing Behavior in the Model Unicellular Eukaryote *Chlamydomonas reinhardtii*

Published Oct 2020 in iScience 23:11 doi: 10.1016/j.isci.2020.101714

Introduction

Once thought to operate as completely independent entities, microorganisms are now understood to engage in behaviors as complex and diverse as any of the large, multicellular organisms, with which they frequently associate. These interactions are crucial to allowing the community to respond to changing environmental conditions such as a decline in nutrients, changes in temperature, the introduction of invasive species, and more (Bowers and Parke, 1993; Hibbing et al., 2010; Tans-Kersten et al., 2001; Xie and Wu, 2014). The phenomenon known as quorum sensing (QS) allows microorganisms to couple phenotypic switching to cell density, ensuring the emergence of specific behaviors when they will be most productive. For example, at low cell densities, the production of exopolysaccharides by bacteria is unlikely to produce a beneficial biofilm. However, at high cell densities, the excretion of these extracellular matrices results in biofilms that provide significant advantages to resource sharing and persistence (Stewart and Franklin, 2008). Other QS-regulated phenotypes include motility, conjugation, antibody production, bioluminescence, virulence factor production, and more (for recent reviews, see (Papenfort and Bassler, 2016; Welsh and Blackwell, 2016)). QS has provided new targets for the

regulation of specific microbial behaviors and revolutionized the field of synthetic biology (Palmer et al., 2011a; Tamsir et al., 2011). QS is regulated by the diffusion of a broad assortment of low-molecular-weight organic compounds, generically referred to as autoinducers (AIs). At low cell densities, these signals are synthesized at a constitutive level and then diffuse or are actively transported out of the cell into the surrounding environment. AIs are perceived by dedicated receptors either at the cell surface or intracellularly once a sufficient concentration has been reached. Formation of the AI:receptor complex directs changes in the gene expression either directly by receptor binding to specific promoter sites on DNA or indirectly through a phosphorylation cascade. Regardless of the exact mechanism, these relatively simple biological circuits allow AI concentration to serve as a proxy for cell density.

While originally discovered in bacteria, QS has also been observed in the other two major domains (super kingdoms) of life: Archaea and Eukarya. For example, *Methanothrix harundinacea*, a methanogenic archaeon, forms filaments due to the accumulation of carboxylated N-acyl-L-homoserine lactones, a class of AIs commonly used by Gram-negative bacteria (Montgomeryetal.,2013). Similarly, *Candida albicans*, a fungus found primarily in human microbiota, exhibits a filamentous phenotype at low cell densities but grows instead as budding yeast at high cell densities. In this example, the isoprenoid farnesol serves as the AI which regulates QS (Albuquerque and Casadevall, 2012). Additional studies have established the presence of other QS-regulated phenotypes among fungi, typically regulated by a variety of aromatic amino acid alcohols which serve as the AIs for these systems (Hornby et al., 2004; Roca et al., 2005). The above examples support QS as a convergent evolutionary strategy employed by

unicellular microorganisms across all three domains of life to coordinate behaviors and increase fitness.

While prevalent in fungi, there are no examples of this phenomenon among other eukaryotes. Yet, most eukaryotic microorganisms face many of the same challenges as prokaryotes, suggesting QS would provide an equally effective strategy for success. The obvious challenge to the discovery process is the identification of the phenotypic switch, i.e., what behavior manifests in response to a quorum being met. Motility is one commonly regulated phenotype in prokaryotic QS, as in *Staphylococcus aureus*, which uses the phenomenon to detect high cell densities prior to reaching the carrying capacity of their environment. Strategies for dealing with nutrient availability have proven a 'good bet' over evolutionary time across multiple kingdoms. Indeed, simple population dispersion to explore new environments may have been one of the earliest pressures for QS.

One obvious limiting factor to the study of the behavioral responses of the individuals within these communities is their small average size (<10 μm). We recently developed a simple particle tracking method utilizing recorded video to observe the distribution of swimming speeds in cultures of microorganisms (Folcik et al., 2020). These videos are processed using an optimized analysis pipeline including publicly available software Fiji (ImageJ), the TrackMate plug-in for this package, and R statistical computing software. Using this automated small particle tracking method, we are able to gather significant amounts of data (>3000tracks) on culture speed, directionality of movement, and cell size to investigate population dynamics in real time.

In this study, we have utilized this tracking technique to investigate the effects of culture age on the swimming speed of the model unicellular eukaryote *Chlamydomonas reinhardtii*. This model organism has been used extensively to study flagellar motility as well as both phototaxis and chemotaxis (Fujiu et al., 2011; Huang et al., 1982; W.F.Marshall, 2009; Stavis and Hirschberg, 1973; Wakabayashi et al., 2011). Our findings reveal a previously unreported correlation between swimming speed and cell density. This response is due to the accumulation of one or more low-molecular-weight organic molecules, which can be isolated from these cultures and used to stimulate increased swimming speeds at lower density cultures. This phenomenon is conserved in the closely related *Chlamydomonas moewusii*, and the signals in both species are equally active in the other. We note the similarities in this phenomenon to prokaryotic QS circuits. Finally, we discuss the potential impact of this newly observed instance of QS on nutrient acquisition and utilization in this well-represented and ecologically important genus of photoautotrophs, as well as the broader implications to our understanding of microbial ecology.

Results

Swimming Speed Increases Over Time in cc124 Cultures

We began by comparing *C. reinhardtii* wildtype (strain cc124) motility between 24-, 48-, and 72-h cultures to observe any baseline differences that might emerge as a function of culture age (videos are available on Dryad, see Data Availability Statement for information). As shown in Figure 3.1, swimming speed in cultures of *C. reinhardtii* appeared to be positively correlated with culture age. Average swimming speeds of this wildtype culture at 24, 48, and 72 h were 15, 28, and

47 µm/sec, respectively (standard error of the mean [SEM] = +/ 6–12 µm/sec).

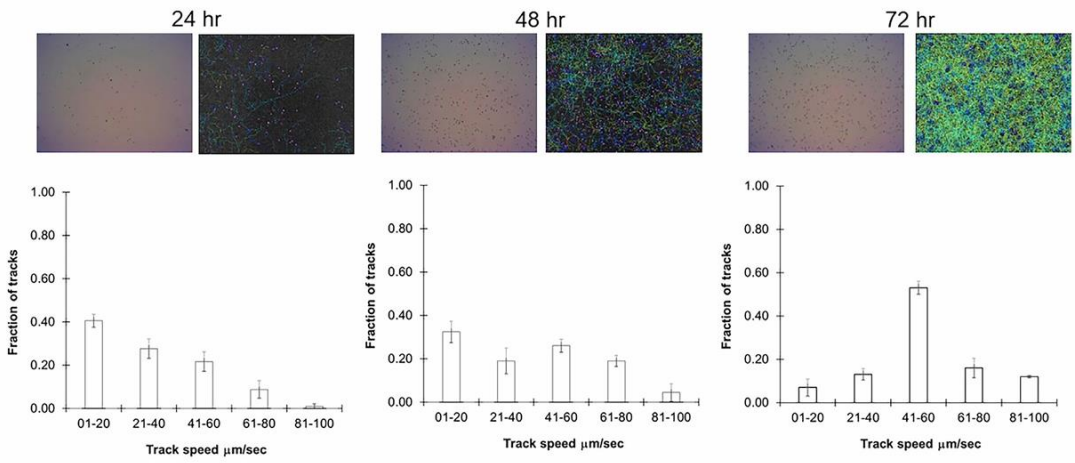

Figure 3.1 Cultures of *Chlamydomonas reinhardtii* Increase Swimming Speed as a Function of Culture Age.

Cultures were grown for the indicated time, then a fraction was isolated, and analyzed for motility. (Top) For each time point, the top left image is a single frame from a 30 s video, while the top right is an analyzed image highlighting the total number of tracks. (Bottom) Histogram of *C. reinhardtii* swimming speeds as a function of culture age. Results are the average of three videos with error bars indicating +/- SEM.

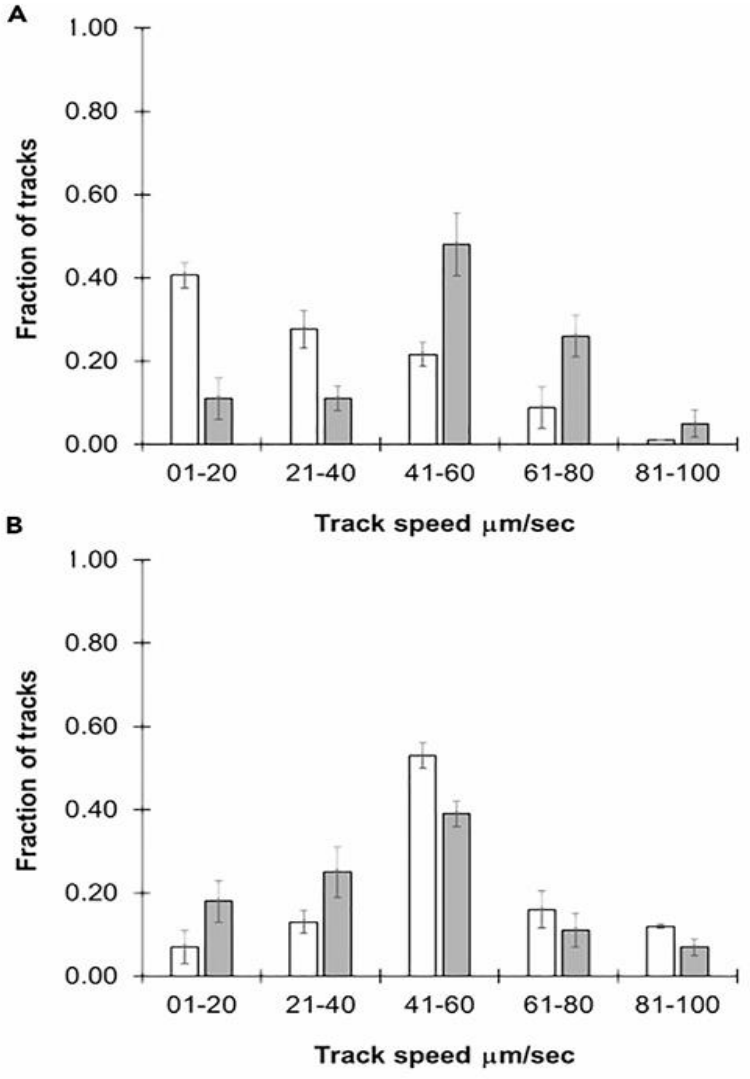

Figure 3.2 Older *Chlamydomonas reinhardtii* Media Induces Higher Swimming Speeds.

Cultures were grown for (A) 24 or (B) 72 h and then either evaluated for motility directly (white bars) or after media swap (gray bars). For the media swap, pelleted cultures of *C. reinhardtii* were suspended in the other media (24-h cells in72-h media in A and 72-h cultured cells in 24-h culture media in B). The effects on swimming speed were determined by image analysis after 6 h. Results are expressed as the mean of 3 videos with error bars indicating +/- SEM.

While the average at 72 h is slower than what has been reported in some of the literature (Marshall, 2009), it is consistent with our previous studies as well as others (Chen et al., 2017; Folcik et al., 2020). In addition to average speed, our method allows us to observe speed distributions within the population, as shown by the histograms provided in Figure 3.1. Over the 48 h of this assay, there was a significant reduction in low or no motility (≤ 20 μm/sec) cells.

Over the duration of this study, cultures increased in density from ≤ 10^5 cells/ml at 24 h to ≥ 10^7 cells/ml at 72 h. This 100-fold increase in cell density would almost certainly reduce the amount of nutrients available, potentially driving the search for new nutrient sources. Prior observations that *C. reinhardtii* is capable of chemotaxis toward nitrogen sources when this nutrient is scarce support this "direct" model based on nutrient deficiency (Byrne et al., 1992; Ermilova et al., 2007). Alternatively, increased cell-cell contact, as density increases over culture age, could trigger increased swimming. Prior studies have confirmed that *C. reinhardtii* can respond to physical stressors, supporting the viability of this "mechanical" model (Herron et al., 2019). Finally, as cultures age, a low-molecular-weight compound that increases swimming speed could be released (signal/cue model).

Cell-Cell Contact Does Not Increase Swimming Speeds

We hypothesized that a simple media swap experiment would allow us to distinguish simple mechano-sensitivity (the response to physical contact) from the "direct" and "signal/cue" models described above. As seen in Figure 3.2, 6 hours after their exposure to filter-sterilized (0.2 μm cutoff) 72-h-old media, 24-h cultures showed a significant increase in the average speed of the population (51 ± 12 μm/sec SEM). This increase was statistically indistinguishable from that for

72-h cultures (47 ± 11 μm/sec SEM, $p < 0.01$). Seventy two-hour cultures displayed a moderate reduction in their swimming speeds following exposure to 24-h culture media (42 ± 6 μm/sec SEM). These results support the "direct" or "signal/cue" models for increasing swimming speed, while arguing against the "mechanical" model, as cell density does not increase in these studies.

A Low-Molecular-Weight Compound Triggers the Increase in Swimming Speed

The previous media swap experiment is unable to distinguish between the remaining two models proposed for increased culture swimming speeds: the "direct" detection of reduced nutrients or signal/ cue-induced changes in swimming speeds. We therefore envisioned an experiment that would allow us to extract organic compounds from the culture media and apply them to cultures of different ages and nutrient content. To accomplish this, we performed an organic extraction of cell-free 24- and 72-h *C. reinhardtii* culture media with ethyl acetate.

The addition of the 72-h extracts to 24-h-old cultures showed an increase in cell swimming speed upon treatment (44 ± 7 μm/sec SEM) (Figure 3.3). Twenty-four-hour extracts had no significant effect on the swimming speeds of either 24- or 72-h cultures of *C. reinhardtii* (data not shown). Dimethyl sulfoxide (DMSO) loading controls also had no effect on motility in either 24- or 72-h cultures.

As 72-h extracts were able to increase swimming speeds in the more nutrient-rich 24-h cultures, it argues against a "direct" nutrient deficiency model to explain the increase in swimming speed. These findings are consistent with our proposed "signal/cue" model of a diffusible low-

molecular-weight compound being responsible for this effect. We refer to this unknown signal(s) or cue(s) as the *Chlamydomonas* swimming speed factor (CSSF) for the remainder of the text.

CSSF Increases Swimming Speed in a Time-Dependent Manner

Next, we evaluated the time dependence for the observed increase in swimming speeds due to CSSF exposure. Seventy-two-hour extracts were applied to 24-h *C. reinhardtii* cultures and then monitored for changes in swimming speed over a two-hour period. As shown in Figure 3.4, a population-wide shift in the swimming speed is observable after 30 min of CSSF exposure (from <20 μm/sec to 31 μm/sec). One hour after CSSF exposure, swimming speeds in 24-h cultures were indistinguishable from two-hour CSSF exposures (average: 44 vs 47 ± 7–9 μm/sec SEM). This similarity was also reflected in the distribution of swimming speeds across the population.

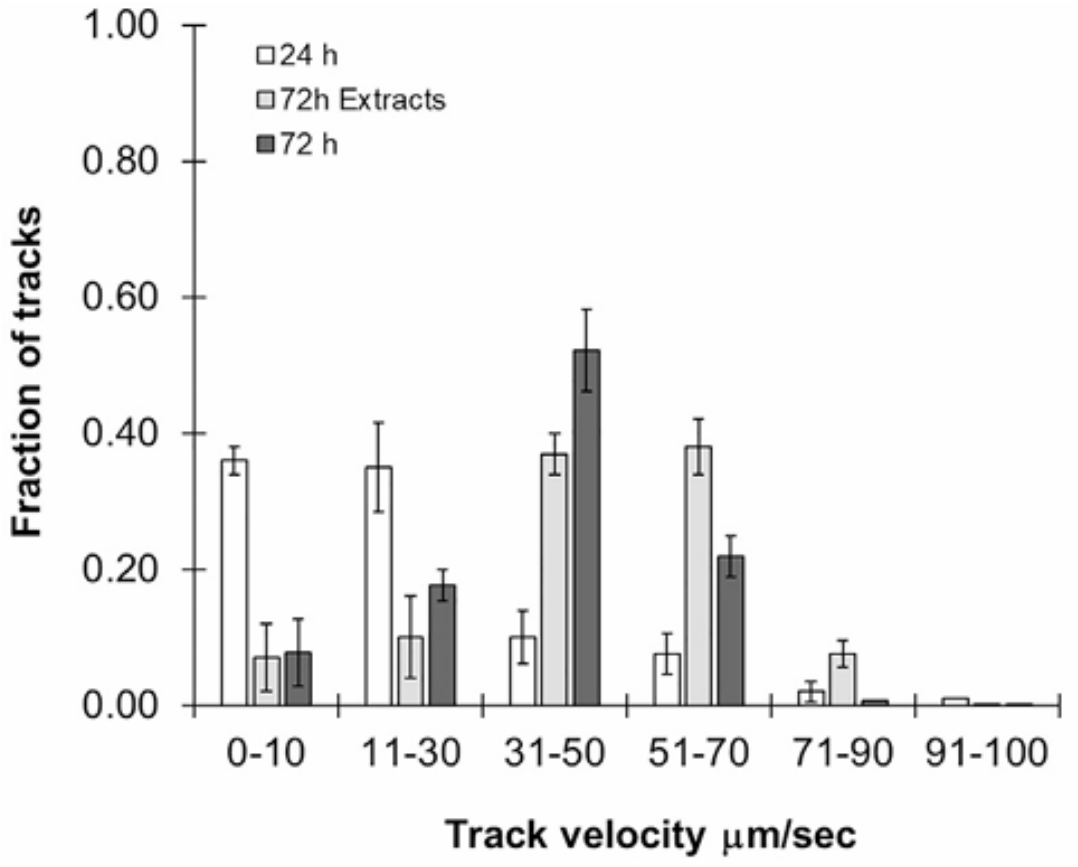

Figure 3.3 Motility in *Chlamydomonas reinhardtii* is Modulated by a Low-Molecular-Weight Signal.

Extracts of 24-h (white) and 72-h (dark gray) cultures of *C. reinhardtii* were dissolved in DMSO and added directly to 24-h (light gray) cultures of *Chlamydomonas reinhardtii* in Tris-acetate-phosphate (TAP). Samples were incubated for 2 h and then evaluated for changes in swimming speed. Results are expressed as the mean of 3 videos with error bars indicating +/- SEM.

CSSF Activity Requires Changes in Gene Expression/Protein Production

CSSF-induced increases in swimming speeds in *C. reinhardtii* may be a purely physiological response or coupled to a change in gene/protein expression. We hypothesized that cycloheximide, a fungal metabolite capable of inhibiting mRNA translation in microorganisms, could help resolve these two models. As seen in Figure 3.5, 24-hour cultures of *C. reinhardtii* co-incubated with72-h extracts and 1mM cycloheximide showed no increase in swimming speed and were indistinguishable from extract-free controls ($p = 0.55$). Seventy-two-hour *C. reinhardtii* cultures incubated with an equal concentration of cycloheximide for 2 h showed no significant reduction in swimming speed (data not shown). These findings are consistent with the production of new molecular machinery playing a significant role in the switch to increased swimming speeds rather than a simple physiological switch.

Culture Density, Not Age, Determines Swimming Speed

Our results thus far are consistent with the density, rather than age, dependent accumulation of a chemical signal or cue responsible for the observed increase in swimming speeds. If this is indeed the case, then artificially increasing cell density should mimic the effect of an older culture, i.e., by increasing swimming speeds. To evaluate this possibility, we artificially increased the cell density of 24-h cultures from $\approx 5.00 * 10^5$ to $2.00 * 10^7$ cells/ml. As shown in Figure 3.6, concentrated cultures showed a statistically significant increase in swimming speed over 30 min relative to untreated controls ($p < 0.001$). The perturbation caused by centrifugation and resuspension of these cells does cause an observable increase in swimming speed; however,

this was still significantly less than that in the concentrated samples. Taken together, these results support the hypothesis that cell density rather than age determines the switch in behavior.

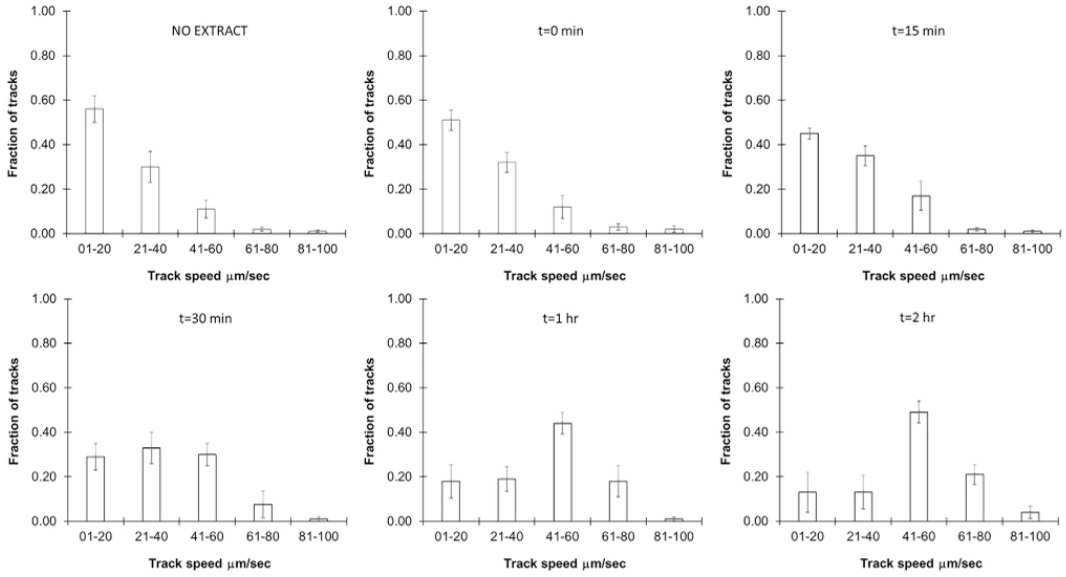

Figure 3.4 Extract Time Dependence in *C. reinhardtii.*

Twenty-four-hour cultures of *C. reinhardii* cc124 were treated with 72-h extracts and then evaluated for changes in swimming speed at the indicated time points. Results are expressed as the mean of 3 videos with error bars indicating +/- SEM.

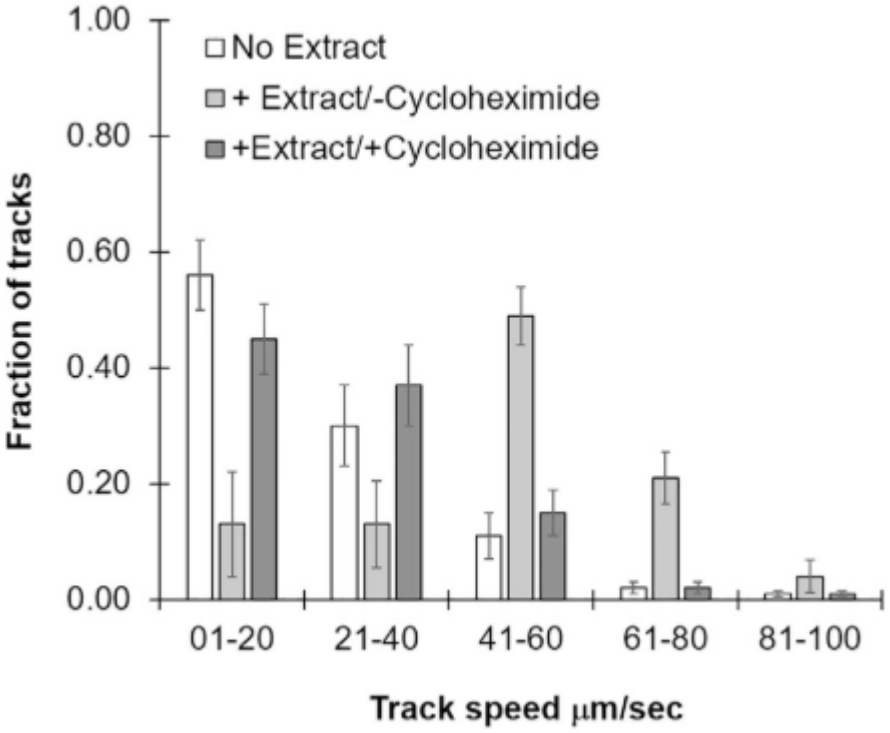

Figure 3.5 *C. reinhardtii* Response to Extract Signals Is Transcription Dependent.

Twenty-four-hour cultures of *C. reinhardtii* were evaluated for changes to swimming speed without modification (white), after a 2-h exposure to 72-h *C. reinhardtii* extract (light gray) or after a 2-h exposure to both 72-h extract and 1 mM cycloheximide (dark gray). Results are expressed as the mean of 3 videos with error bars indicating +/- SEM.

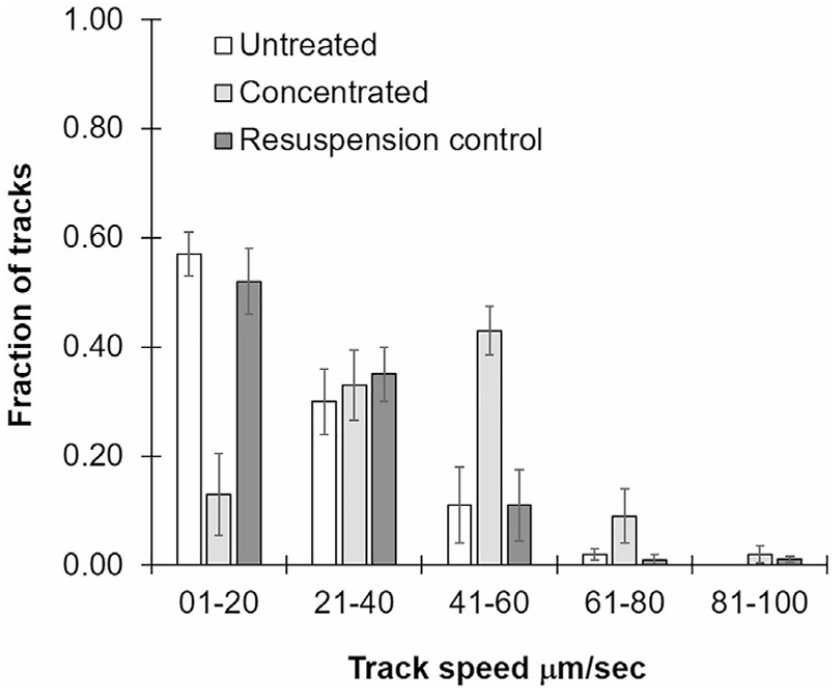

Figure 3.6 Population Density Determines Phenotypic Switch.

Twenty-four-hour cultures of *C. reinhardtii* were pelleted by centrifugation and then re-suspended in either a reduced volume of the original TAP media to increase cell density from 10^5 cells/ml to 10^7 cells/ml (light gray) or the full volume of the original TAP media (dark gray). Samples were evaluated for changes to swimming speed relative to untreated control cultures (white) after 30 min. Results are expressed as the mean of 3 videos with error bars indicating +/- SEM.

CSSF and Response Is Conserved in *Chlamydomonas spp.*

Finally, we wanted to determine if this behavior was unique to *C. reinhardtii* or could be found in other members of this genus. We ultimately selected *Chlamydomonas moewusii* (cc1419) as this strain is well characterized and readily available for further study (Watanabe and Lewis, 2017). As shown in Figure 3.7A, cultures of *C. moewusii* showed a similar trend of increased speed as a function of culture age/density. As with *C. reinhardtii*, this increase in swimming speed could be induced in 24-h cultures by exposure to extracts from 72-h culture media (Figure 7B). Furthermore, the signals or cues responsible for this behavior appear conserved between these species as 72-h extracts from *C. reinhardtii* and *C. moewusii* were able to increase swimming speed in the other species after 2 h treatments (Figure 3.7C). Taken together, these findings strongly support the conservation of a density-dependent phenomenon, not unlike QS, within this genus, although the extent of this remains to be determined.

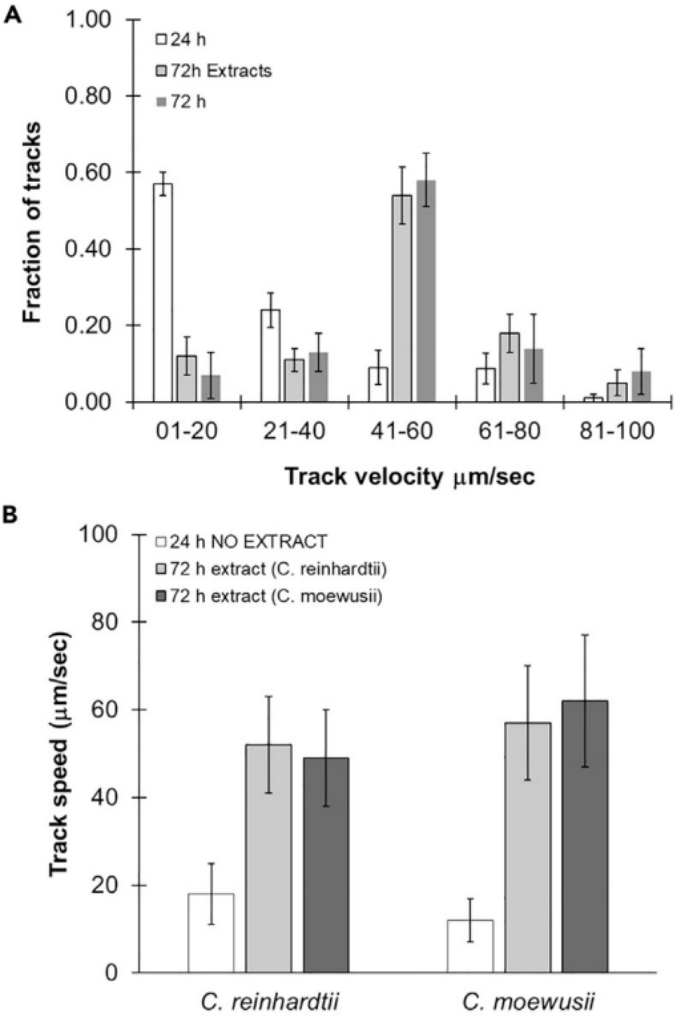

Figure 3.7 QS Is Conserved Among Members of the Genus *Chlamydomonas*

(A) Cultures of *C. moewusii* were evaluated for swimming speed at 24 (white) and 72 h (dark gray). The effects of 72-h *C. moewusii* culture extracts on swimming speeds in 24-h cultures of *C. moewusii* after two hours are shown in light gray. (B) Twenty-four-hour cultures of *C. reinhardtii* or *C. moewusii* were exposed to extracts of 72-hour cultures of either *C. reinhardtii* (light gray) or *C. moewusii* (dark gray) algae for 2 hours and then imaged for changes in swimming speed. Results are the average of three videos with error bars indicating +/- SEM.

Discussion

Investigating how microbial communities change behavior in response to external stimuli, cell density, and other factors is important to our fundamental understanding of how these populations interact with the surrounding world. Many unicellular microorganisms, including yeast and bacteria, display phenotypic switches like QS to regulate crucial behaviors such as bioluminescence, antibiotic production, biofilm formation, and many other phenotypes with significance to host-microbial associations, microbial ecology, and more (Miller and Bassler, 2001). QS has emerged as a convergent strategy among various microorganisms as a way to couple phenotypic switching to cell density (Fuller et al., 2017). However, while prevalent in fungi, there are no examples of this phenomenon among other eukaryotes. Yet, most eukaryotic microorganisms face many of the same challenges as prokaryotes, suggesting QS would provide an equally effective strategy for success. The obvious challenges to the QS discovery process are (i) what behavior changes in response to a quorum being met and (ii) the identity of the signal(s) or cue(s).

Herein, we utilized an in-house particle tracking method to monitor individual, as well as population-wide, changes in the swimming behavior of *C. reinhardtii* and determined that they were positively correlated with culture age and/or population density (Figure 3.1). Following this observation, we sought to identify the driving factor (or model) associated with this change. Swapping the media of younger and older *C. reinhardtii* cultures ruled out increased physical contact (mechanosensory) as the driver of increased swimming speeds but could not distinguish if the shift in motility was due to a decrease in nutrient availability (direct model) or due to the

accumulation of a particular molecule (Figure 3.2). Yet, organic extracts from 72-h cultures added directly to comparatively nutrient-rich 24-h cultures show an increase in swimming speeds (Figure 3.3) over a one-hour period (Figure 3.4).

These findings are consistent with the presence of a low-molecular-weight organic compound which accumulates over time as the driver for increased swimming speeds in this model photosynthetic eukaryote. We have named this molecule the CSSF as a placeholder while ongoing studies attempt to identify it. As with many phenomena in which an external factor elicits a response in biology, most especially QS, there is some question as to whether the CSSF should be defined as a signal or a cue (Diggle et al., 2007). A signal would imply a purposeful exchange between the cells which, presumably, provides some selective advantage to the group. For example, the CSSF could be a mechanism for these cells to inform each other of the need to increase swimming speed, based on the amount of CSSF as a proxy for cell density, due to pending nutrient deficiency. However, a clear benefit to the coordination of these responses remains unclear, and as a result, it is best to refer to the CSSF as a cue at present.

CSSF-induced changes are likely dependent on the synthesis of new molecular machinery, specifically protein, as inhibition of the ribosome, via cycloheximide, prevented 72-h extracts from increasing the swimming speed of 24-h cultures of *C. reinhardtii* (Figure 3.5). We further verified that this process was indeed density dependent, by artificially concentrating a 24-h culture, mimicking the density of 72-h cultures. Results suggest that an increase in cell density, and thus accumulated CSSF, is responsible for this behavior and not culture age (Figure 3.6). Taken

together, these results strongly support the observed phenomenon as a new example of QS among unicellular eukaryotes.

This QS or QS-like phenomenon does not appear to be unique to *C. reinhardtii* as cultures of the closely related species, *C. moewussi*, display a similar behavior (Figure 3.7). The use of similar QS signals (AIs) for multiple species is well documented (Palmer et al., 2011b) and appears to be the case between these two species, which are sensitive to each other's cognate CSSF. Indeed, this phenomenon is potentially broadly conserved among the chlorophycean algae given the evolutionary distance between the two species tested: *C. reinhardtii* of the Reinhardtinia phylogroup and *C. moewusii* (cc1419) of the Moewusinia phylogroup (clade Moewusii), as this strain is well characterized and readily available for further study (Watanabe and Lewis, 2017). This underscores the potential conservation of the molecular mechanisms at work in this new QS-like behavior.

The observation of a potential QS circuit conserved between two members of this genus suggests that the phenomenon of density-dependent phenotypic switching may be even more broadly distributed among unicellular eukaryotes than once thought. However, one hallmark of QS is that AI detection increases AI synthesis, as the name implies, thereby ensuring smooth and population-wide switches in behavior. As a specific molecule has yet to be identified for this process, it is unclear whether such autoinduction actually occurs. We are currently working to identify the molecule(s) responsible for this process, as well as the timing and the molecular mechanisms which regulate it. These findings will be the subject of a subsequent manuscript.

In conclusion, the potential that QS occurs in this crucial class of photoautotrophs across multiple ecosystems suggests this phenomenon is more broadly distributed than once thought. This discovery may provide novel insight into the formation and maintenance of microbial communities. It also suggests the potential, as with prokaryotic QS systems, to employ chemical biology approaches to create synthetic regulators of this phenomenon, capable of both characterizing as well as controlling these phenotypes (Njoroge and Sperandio, 2009; Palmer et al., 2011a; Studer et al., 2014). *C. reinhardtii*, a model system for the study of motility and photosynthesis, now provides a genetically tractable and well-characterized platform for the study of this new form of eukaryotic QS.

Chapter 4 Isolation and Characterization of the *Chlamydomonas* QSM

Introduction

The phenomenon known as quorum sensing (QS), which couples phenotypic switching to cell density, was originally discovered in prokaryotes where it controls a wide variety of behaviors including swarming, biofilm production, virulence factor production, and bioluminescence (Papenfort and Bassler, 2016; Welsh and Blackwell, 2016). Broadly distributed among both Gram-positive and Gram-negative prokaryotes, many of the molecular systems which direct these processes have been extensively characterized. These processes depend on the synthesis of specific signals, which are released into the environment and then perceived by dedicated receptors. Perception of these signals induces population-wide phenotypic switching. QS restricts certain behaviors to conditions at which they would be most useful (e.g., one bacterium producing biofilm is not likely to provide benefit, but a million producing them will likely be more effective).

The most well characterized of these is the LuxI/R QS system, in which the LuxI synthase produces N-acyl-L-homoserine lactones (AHLs) which diffuse into the extracellular environment and accumulate at a rate closely approximating the cell density of the species producing it. Once the signal molecule reaches a certain threshold to meet the binding moiety with the Lux receptor, it causes transcription factor activation and new gene expression. This in turn causes a phenotype across the population to switch and a new population-wide behavior emerges. Many QS signal

molecules have been reported for prokaryotes including AI-2 (a furanosyl borate diester or tetrahydroxy furan, depending upon species), cyclic peptides, comX, quinolones (PQs), and 4-hydroxy-2- alkylquinolines (HQs).

Since unicellular eukaryotes face the same or similar challenges as prokaryotes, researchers have turned to looking for QS systems in these organisms. Indeed, it was found that some fungi, mostly yeasts, do appear to have QS-like systems. For instance, the economically important species *Saccharomyces cerevisiae*, has been reported to use aromatic alcohols such as tyrosol, phenylethanol, and tryptophol, along with the sesquiterpene farnesol, to control the switch between budding and filamentous growth. Similar systems have been reported for pathogenic fungi like *Candida albicans* and *C. tropicalis.* QS systems have also been reported for *Ceratocystis ulmi,* which use 2-methyl-1-butanol, methylvaleric acid, and 4-hydroxyphenylacetic acid, *Cryptococcus neoformans* which utilize a peptide signal called qsp1, and *Histoplasma capsulatum* which use α-(1,3)-glucan.

Recently, we observed that *C. reinhardtii*, a ubiquitous photoautotroph, utilizes a QS system that causes the population to increase its average swim speed (Folcik, et al., 2020). The signal molecule, dubbed the *Chlamydomonas* swim speed factor (CSSF) has yet to be characterized. Yet the isolation and identification of this signal(s) is critical to understanding the molecular underpinnings of the QS phenomenon in this model unicellular eukaryote. Identification of this signal can also help in the search for other species in which this particular QS mechanism may be conserved. Indeed, the discovery of the AHL family of compounds facilitated the search for QS among Gram-negative bacteria. While our early efforts to isolate the QSM associated with *C.*

reinhardtii relied on traditional organic phase extractions, here we present a new method to isolate and concentrate the exudates of this microorganism via solid phase extraction (SPE). This method proved less wasteful and provided more consistent extracts for further identification and characterization of the QSM. In the present study, we have leveraged our existing phenotypic assay with rounds of high-performance liquid chromatography (HPLC), high resolution tandem mass spectrometry (LC-MS/MS) and nuclear magnetic resonance (NMR) to propose putative signal molecules as the candidate QSM for this organism.

Materials and Methods

All reagents were obtained from LabAlley, Fisher Scientific, or Sigma Aldrich, unless otherwise stated. *Chlamydomonas* strains used for testing were purchased from the *Chlamydomonas* Resource Center (www.chlamycollection.org).

Culture Growth

C. reinhardtii cc-124 was grown in 25 ml of tris-acetate-phosphate (TAP) media on a shaker at 150 rpms, under continuous red/blue lights for either 24 or 72 hours. Cultures grown for extraction were grown for 72-120 hours in 100 mL of TAP under the same conditions. Cell density was measured using a hemocytometer and formaldehyde-fixed cells.

Organic Extraction

Extracts were made from 500 mL of high cell density (HCD; $\geq 6x10^6$ cells/mL) cc-124 cultures using either organic-phase extraction methods with ethyl acetate or solid phase extraction (SPE) methods with Waters Oasis HLB 6cc SPE Cartridge System. The columns were conditioned using LCMS grade methanol and water according to manufacturer directions, then the sample was put

through the column, and the extract was collected with 2 ml of methanol. Extracts were stored in a -40 °F freezer until used.

Extract Fractions

Whole HCD cc-124 extract was fractioned into parts using a Waters dual-pump binary HPLC. The system was loaded with 500 µL of sample with a flow rate of 5 mL per minute, and run for 25 minutes, starting with 100% water with 0.01% formic acid, ramped over ten minutes to 100% methanol, held for five minutes at 100% methanol, and then ramped back to 100% water with 0.01% formic acid over another ten minutes, which was held another minute to clear the column. A total of five fractions were collected, each fraction comprising three minutes of the total run time.

Active fractions, as verified using our in-house devised activity assay (Folcik, et al., 2020) were run again on the Waters dual-pump binary HPLC to collect five more fractions. The system was loaded with 500 µL of sample with a flow rate of 5 mL per minute and run for a total of 23 minutes, starting with 100% water with 0.01% formic acid, ramping to 80/20 water/methanol over one minute, holding that ratio for three minutes, then ramping over one minute to 50/50 water/methanol, was held for three minutes and then ramped over one minute to 20/80 water/methanol which was held for one minute, then ramped to 100% methanol and held for five minutes. The system then ramped back to 100% water and 0.01% formic acid over two minutes and was held at that for five minutes. New fractions were collected every five minutes.

Extract Activity Testing

Whole Extract Testing: Whole cc-124 extracts made using the SPE method were split in half, with 1 mL of extract dried via rotovap to evaporate the methanol and resuspended in TAP and 1%

DMSO for activity testing and the other half (1 mL) remaining in methanol in the -40 °F freezer until used for further sample preparation and testing. The half resuspended in TAP and DMSO was used for activity testing as per Folcik, et al., 2020.

Cell densities of overnight cultures of *C. reinhardtii* cc-124 were confirmed by hemocytometer to be $\leq 2x\ 10^6$ cells/mL and then aliquoted by 980 µL into 2-mL microcentrifuge tubes and 20 µL of resuspended extracts were added to bring the total volume of samples to one mL. The samples were vortexed to mix and then allowed to incubate in the dark at room temperature for one hour. One mL untreated control samples were also tested in the same manner. Thirty second videos were then acquired using an Olympus CH30 binocular microscope at ×100 magnification. Cells were allowed to settle to avoid slide drift. Amscope software was used to collect videos with a frame rate of 7.5 frames/s with an AmScope MU100 fixed microscope camera. The videos were then analyzed using Fiji, as per the method in Folcik, et al., 2020. Data was compiled and average swim speeds were compared for treated and untreated samples.

Fractioned Extract Testing: Each of the five fractions from the whole extract acquired via the HPLC were split in half. Half went into the -40 °F freezer until used for further preparation and testing. The other half had the solvent evaporated using a rotovap and were resuspended in TAP with 1% DMSO. The half resuspended in TAP and DMSO was used for activity testing as above, per Folcik, et al., 2020. The videos were then analyzed using Fiji, as per the method in Folcik, et al., 2020. Data was compiled and average swim speeds were compared for treated and untreated samples. Fractions which showed increased average swimming were subjected to additional fractionation by HPLC using the second elution method (described above). Collected fractions

were subsequently analyzed for motility differences as described previously. The most active fractions from this second round of HPLC, as identified by the motility assay, were then prepared and analyzed by ^{1}H and ^{13}C NMR, as well as LC-MS/MS.

LC-MS/MS Method

Five µL of sample were loaded into a ThermoFisher Scientific Vanquish LCMS system with an Orbitrap Exploris 120. The instrument was run with a flow rate of 1.5 ml/min starting with 100% water with 0.01% formic acid, ramped over ten minutes to 100% methanol, held for five minutes at 100% methanol, and then ramped back to 100% water with 0.01% formic acid over another ten minutes, which was held another minute to clear the column. This was run for each of the second round HPLC extract samples, as well as the whole fraction 3 extract sample from the first round of HPLC.

NMR

Selected fractions were evaporated to remove excess solvent then dissolved in deuterated water (D_2O) and deuterated methanol (MeOD), respectively. ^{1}H and ^{13}C NMR scans on the samples were collected on a Bruker Avance 400 NMR system.

Signal Molecule Identification Process

Analysis of MS data was done using the Xcaliber and Freestyle applications from the ThermoFisher Scientific website (https://thermo.flexnetoperations.com/control/thmo/login). Element abundance for empirical formula calculations excludes Cl atoms, ^{32}P, and ^{32}S. Peaks from the total ion chromatogram (TIC) of fraction 3.4 were investigated and molecules with a signal-to-noise ratio (s/n) above 30 were chosen for further identification. The species with the highest s/n throughout the TIC were then identified and empirical formula data was gathered from them. The empirical formula together with the m/z were then put through the search engine, Google

(www.google.com), to find potential molecules. These species were also assigned a Simplified Molecular Input Line Entry System (SMILES) that was read using the free software, SMILES explorer (https://www.cheminfo.org/Chemistry/Cheminformatics/Smiles/index.html). This program converted the data into a structural model of the potential molecules. All potential molecules were then screened against known *Chlamydomonas reinhardtii* and other known plant metabolites.

Graphs and Statistical Analysis for Activity Testing

Graphs and analyses were generated in Excel or Graphpad Prism v10.2.3. One-way ANOVA and Tukey's multiple comparisons test were run on all data sets in Graphpad Prism to determine significant differences between variables compared to untreated LCD cultures. Outliers were removed from the data using the ROUT method.

Results

SPE method verification

The SPE method for collecting HCD cc124 extracts was verified using the in-house devised activity method. Extracts collected using this method increased the speed of LCD cc124 cultures. This activity indicates that the CSSF signal molecule is effectively collected using this new, streamlined method.

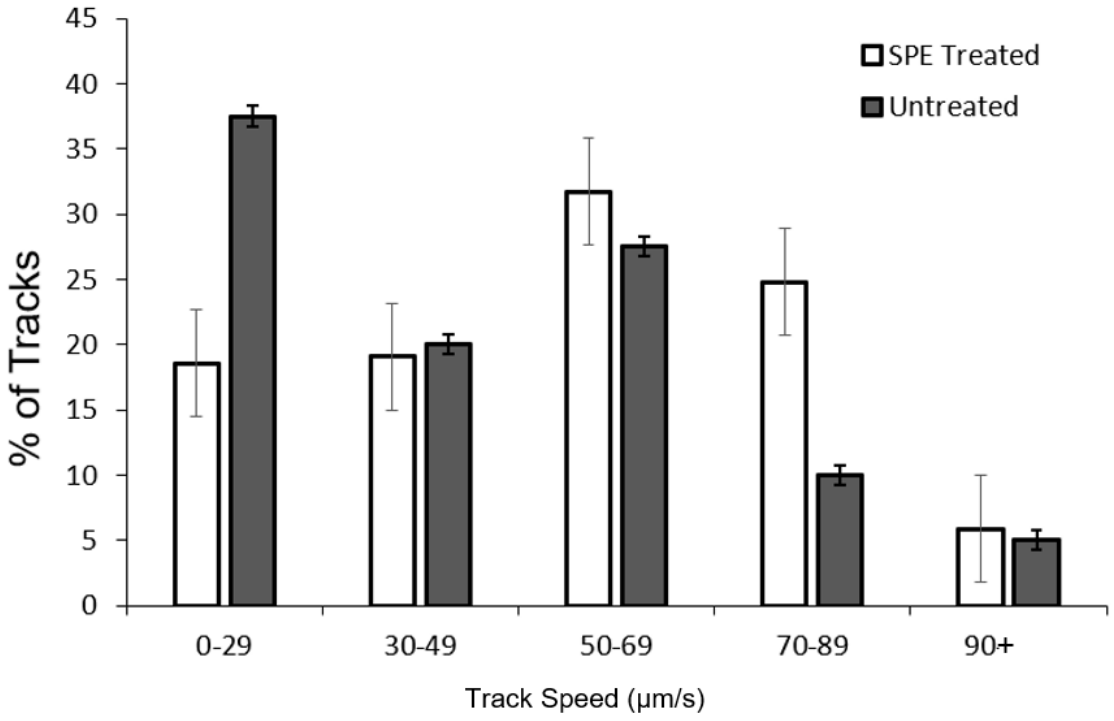

Figure 4.1 SPE extract contains CSSF

LCD cultures of cc124 were treated with HCD extract using SPE method. The treated sample (white bars) has an increase in swim speed compared to LCD controls (dark gray bar). Results are expressed as the mean of 3 videos with error bars indicating =/- SEM[(1)]. Average swim speeds are statistically different (*t*-test, $p<0.05$).

High performance liquid chromatography

The first round of HPLC UV-Vis data had a large peak at just over four minutes (fraction one), at six minutes (fraction two), and a very active region between ten and fifteen minutes (fraction three). UV-Vis spectral scan from 260 nm to 700 nm was also collected, indicated by the dark blue line. The most UV-Vis activity appears from minutes 10 to 15, which was collected in fraction three.

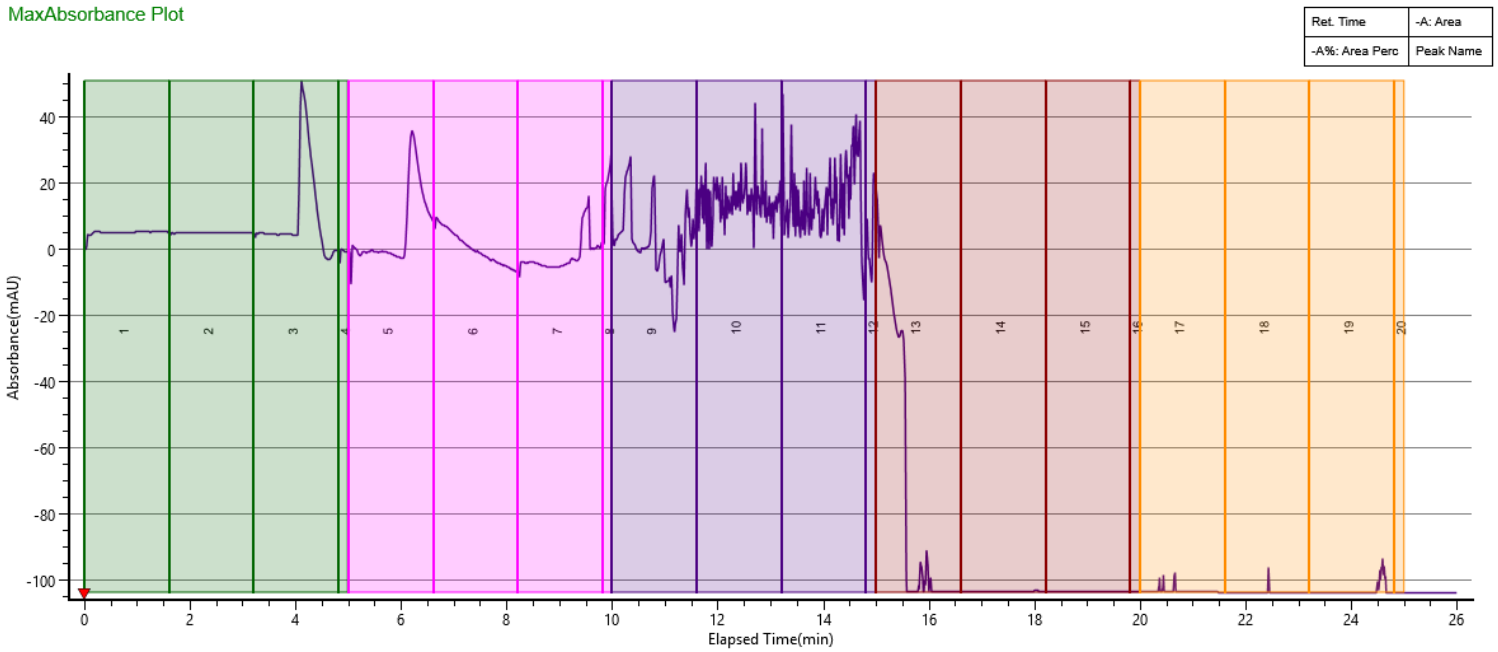

Figure 4.2 HCD cc124 whole extract is separated into testable fractions by HPLC.

Colored areas indicate fractions collected, (from left to right) where the green-shaded area is fraction one, pink is fraction two, purple is fraction three, brown is fraction four, and yellow is fraction five. Numbers in shaded areas indicate the test tube number fraction was collected into on the collection tray. UV-Vis spectral scan from 260 nm to 700 nm was also collected, indicated by the dark blue line. The most UV-Vis activity appears from minutes 10 to 15, which was collected in fraction three.

HPLC fraction analysis

Fractions of whole extract testing: The fractions of whole extract from the HPLC were tested on LCD cultures of cc124 and indicated that fraction three had the highest increase in swimming speeds. Fraction four also indicated higher activity. Fraction two, however, indicated a decrease in swimming speeds compared to both LCD controls and the whole extract. The whole extract was not statistically different from the LCD control, which showed a higher than previously reported swim speed for LCD cultures.

Fractions of fraction three testing: The fractions created from using the HPLC on fraction three from the whole extract were tested on LCD cc124 cultures. These results indicate that fraction 3.4 (the fourth fraction of fraction three from the whole extract) had the most effect on swimming speeds. All fractions tested had statistically lower swimming speeds than the HCD culture controls, but were statistically higher than the LCD culture controls, as well.

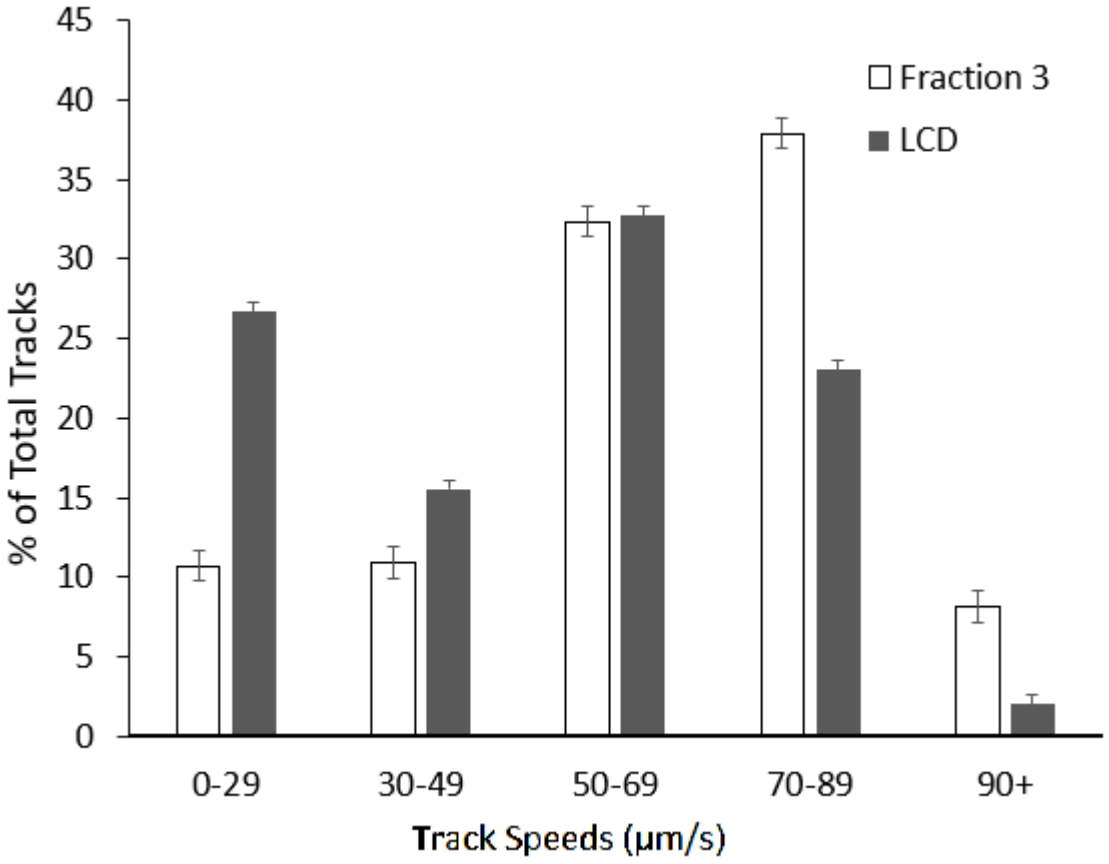

Figure 4.3 The shift in swimming speed of cc124 LCD cultures treated with fraction 3 extract compared to untreated cc124 LCD cultures.

The majority of tracks (~78%) in the treated sample (white bars, n=3) are swimming at ≥50 µm/sec compared to only ~58% of tracks swimming at the same speeds in the untreated samples (gray bars, n=9). The average swim speed of the treated sample is statistically different from the untreated control (one-way ANOVA). Error bars indicate standard error.

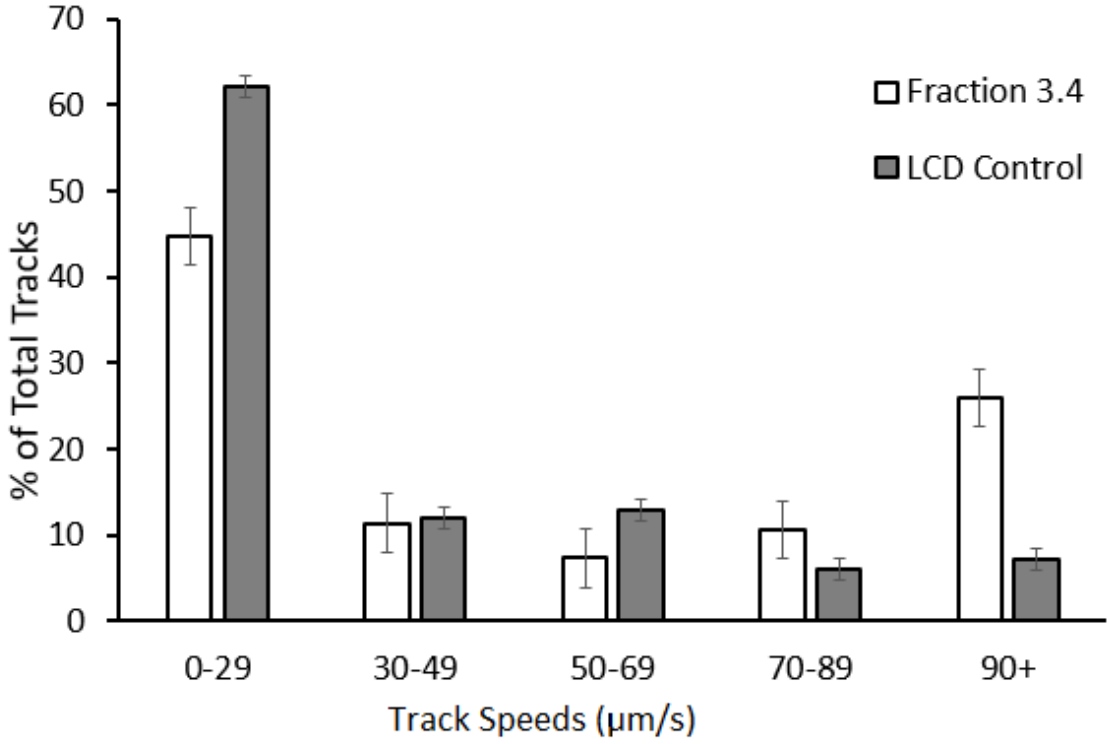

Figure 4.4 The shift in swimming speed of cc124 LCD cultures treated with fraction 3.4 extract compared to untreated cc124 LCD cultures.

26% of tracks in the treated sample (white bars, n=3) swam at speeds ≥90 µm/sec, compared to only ~7% in the untreated LCD cultures (gray bars, n=9). The average speed and statistical analysis of fraction 3.4 (the fourth fraction of the third fraction from whole HCD extract) indicates that this fraction contains more of the active molecule(s) than the other fractions and is statistically different from the LCD control. Error bars indicate standard error.

Nuclear Magnetic Resonance

^{13}C NMR: NMR was run on fraction 3.4 to help identify potential structural qualities of CSSF. However, there is a potential analyte carbon peak that is masked by the solvent peak (Fig 4.5, red circle). Deuterated methanol was used as the solvent, which should show as a septuplet in the 50 ppm range. This scan indicated that there were eight peaks instead of the seven peaks we should see. Resolving this region revealed a carbon peak at 49.9045 ppm (Fig 4.6), and another potential carbon peak at 17.2885 ppm. The peak at 61.7053 ppm indicates that it is likely attached to nitrogen, due to its shift. This scan also indicates that there are no aromatic bond regions (no peaks between 120 and 150 ppm) and no carbon-carbon double bonds (no peaks in 100 to 150 ppm) in this analyte.

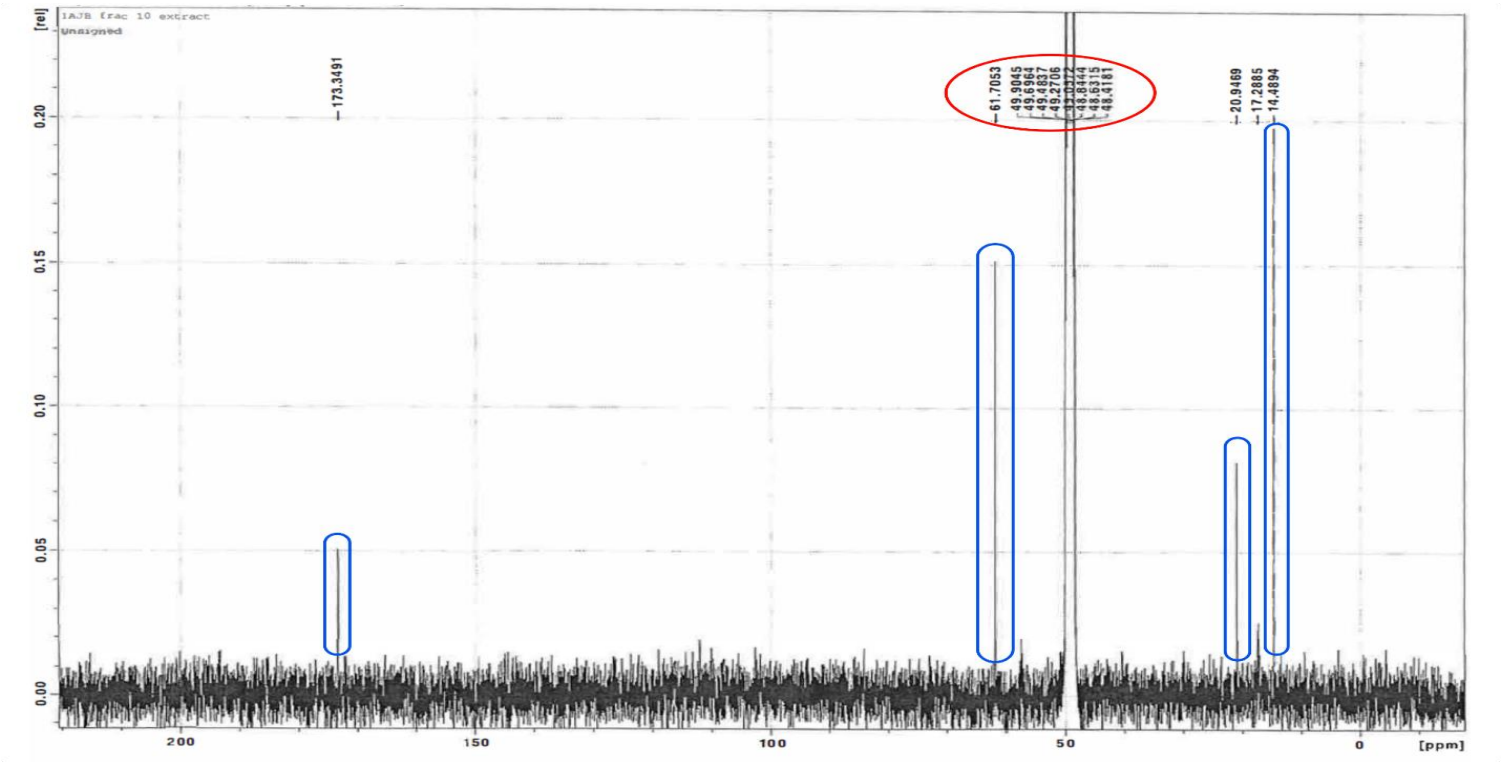

Figure 4.5 ^{13}C NMR on most active HCD cc124 extract from the second HPLC iteration.

Peaks circled in blue indicate carbons identified from the analyte. The integral circled in red indicates that a carbon peak is masked by the solvent (MeOD) peaks. In this view, carbons are indicated (peaks at 14.1894, 20.9469, 61.7053, and 173.3491 ppm). The peak at 173.3491 ppm indicates a carbonyl group. Another carbon may also be present, indicated by the peak at 17.2885 ppm. ^{13}C NMR indicates that there is one strong analyte present, and no aromatic carbons exist in the sample.

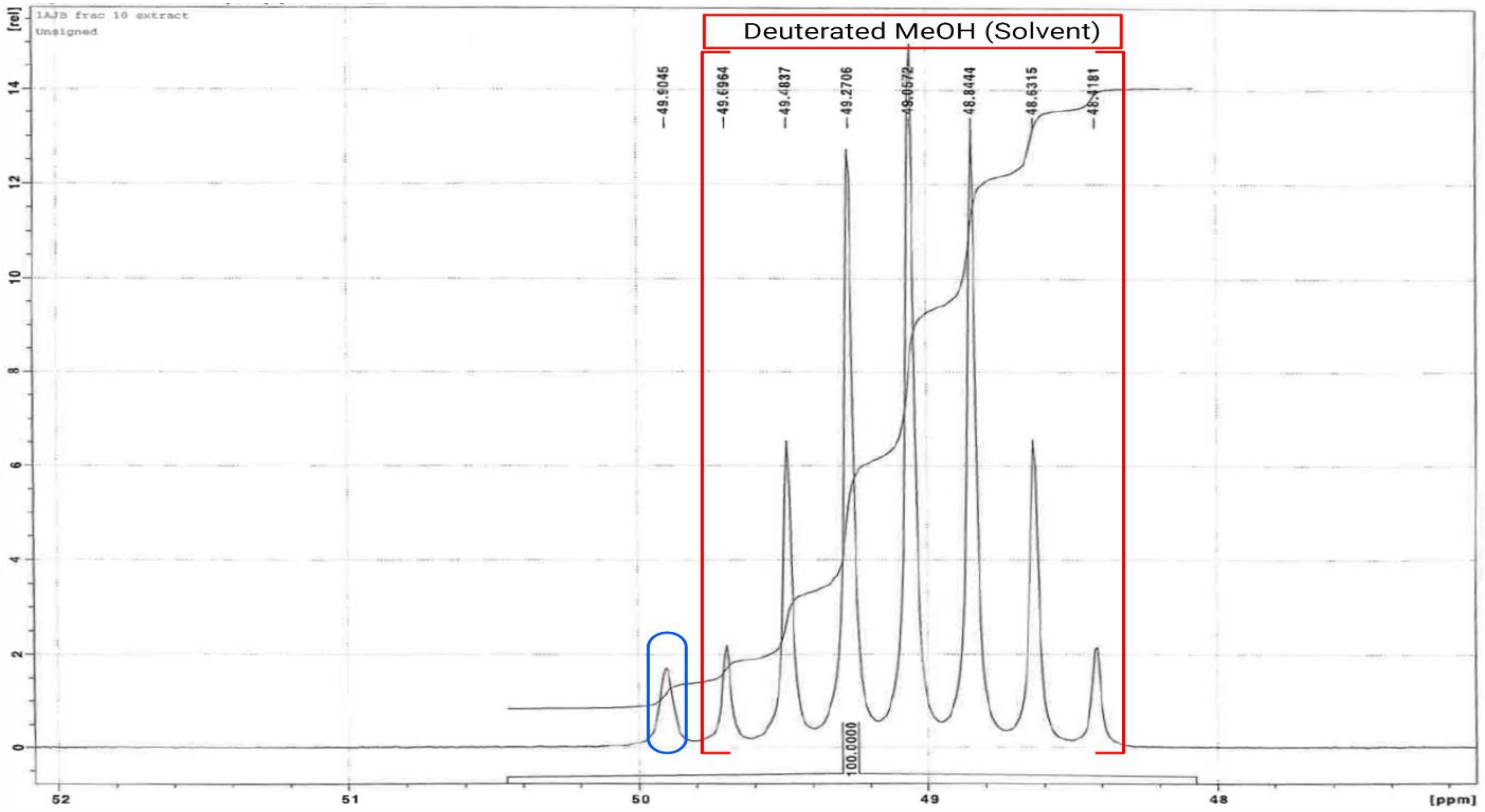

Figure 4.6 Zoomed-in view of the solvent (MeOD) peaks from 48.4181-49.9045 ppm from larger ^{13}C NMR scan.

MeOD should resolve in a septuplet, but eight peaks were indicated on the scan. Zooming-in on the peaks revealed that there is another analyte-derived carbon peak at 49.9045 ppm.

Proton NMR: Proton NMR was run on fraction 3.4 to help identify potential structural qualities of CSSF. The triplet peak at 3.5 ppm is the solvent peak (MeOD) (Fig 4.7 indicated with yellow semicircle). The large peak at 4.75 ppm is water contained within the sample (Fig 4.7 indicated with blue semicircle). The peak at 1.4 ppm indicates a likely amine or amide group, or slightly less likely alcohol (Fig 4.7, green arrow). The peak at 2.1 ppm indicates a ketone or aldehyde (Fig 4.7, light blue arrow). The peak at 4.2 is likely another amine, amide, or alcohol (Fig 4.7, red arrow). No peaks between 6.5 and 8 ppm on this spectrum indicates that there is no aromatic resonance found in this molecule.

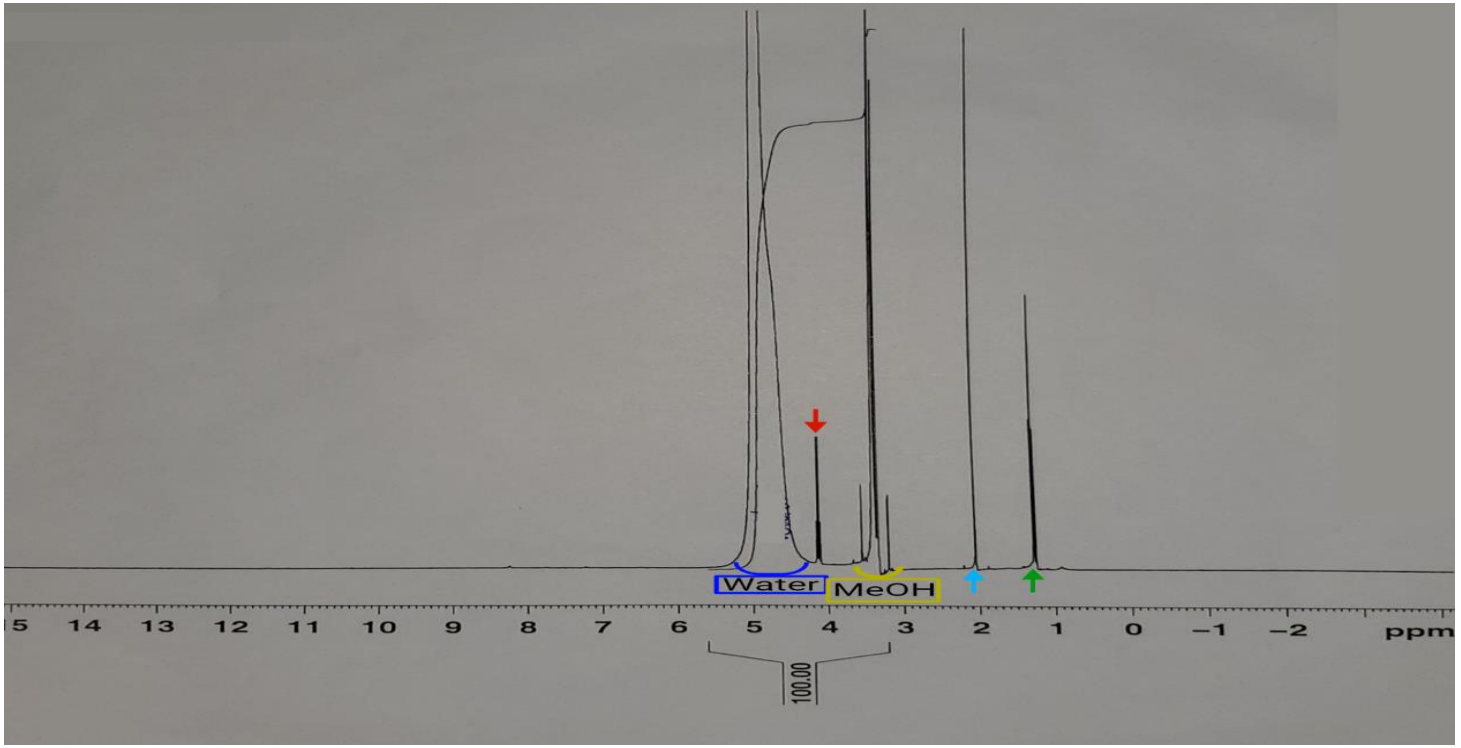

Figure 4.7 Proton NMR scan for CSSF structural analysis.

The triplet peak at 3.5 ppm is the solvent peak (MeOD) and the large peak at 4.75 ppm is water contained within the sample. The green arrow at 1.4 ppm indicates a likely amine or amide. The light blue arrow at 2.1 ppm indicates a ketone or aldehyde. The red arrow at 4.2 ppm is likely another amine, amide, or an alcohol. No peaks in the 6.5 to 8 ppm region suggests no aromatic resonance in this molecule.

Liquid chromatography tandem mass spectrometry

Data from the LC-MS/MS revealed four potential mass-to-charge (m/z) ranges for CSSF (Table 4.1). The molecule with a m/z ratio of 171.1492 was found to elute across all retention times with all ratios of the mobile phase and was the most abundant molecule of the sample. The molecule with m/z of 170.1177 was found at a retention time of 21.399 minutes and is likely the precursor molecule of the molecule found with m/z 171.1177. The molecule with m/z of 297.2789 was found at retention times between 4.0 and 20.0 minutes and the molecule with m/z of 271.2632 was found at retention times between 7.0 and 18.0 minutes. The Freestyle application yielded potential empirical formulas of $C_9H_{19}ON_2$ (m/z 171.1492), $C_9H_{16}O_2N$ (m/z 170.1177), $C_{19}H_{37}O_2$ (m/z 297.2789) and $C_{17}H_{35}O_2$ (m/z 271.2632) using statistical analysis based on the m/z ratios, elemental isotopes, and elemental abundance. The three molecules with m/z ratios of 171.1492, 271. 2632, and 297.2789 often appear together within the same peaks on the total ion chromatogram (TIC) and at very high signal-to-noise (s/n) ratios, indicating they are abundant within that sample.

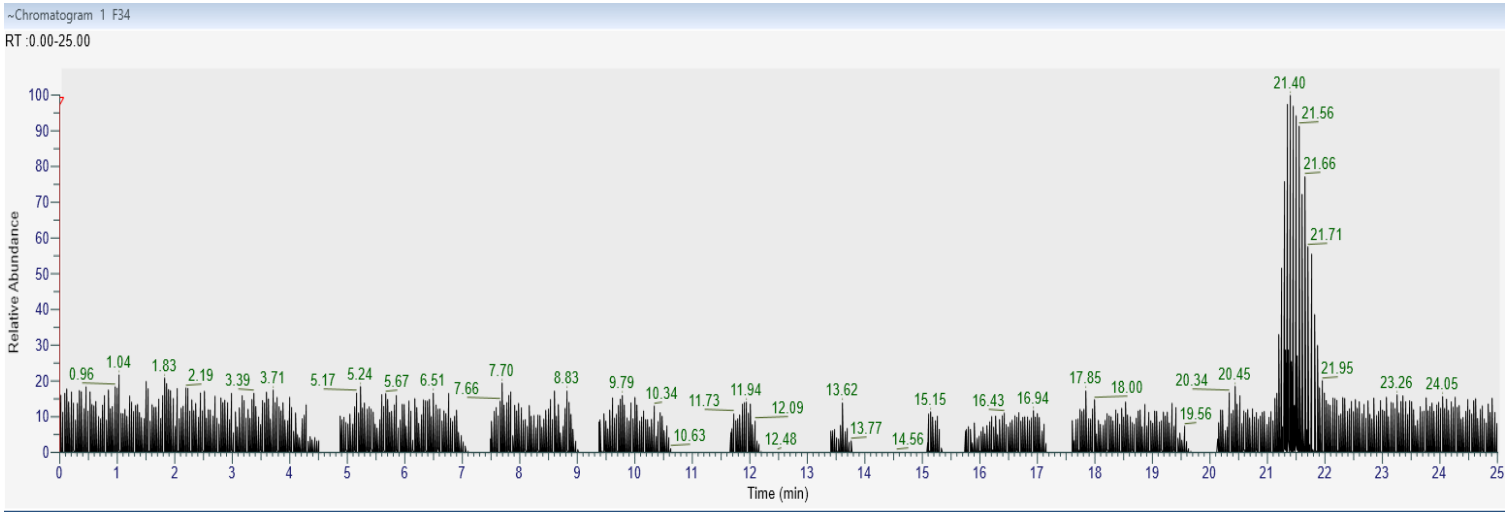

Figure 4.8 Total Ion Chromatogram for fraction 3.4.

A high max absorbance is seen in the retention time range of 21-22 minutes. Other clusters of activity are spread throughout the chromatogram.

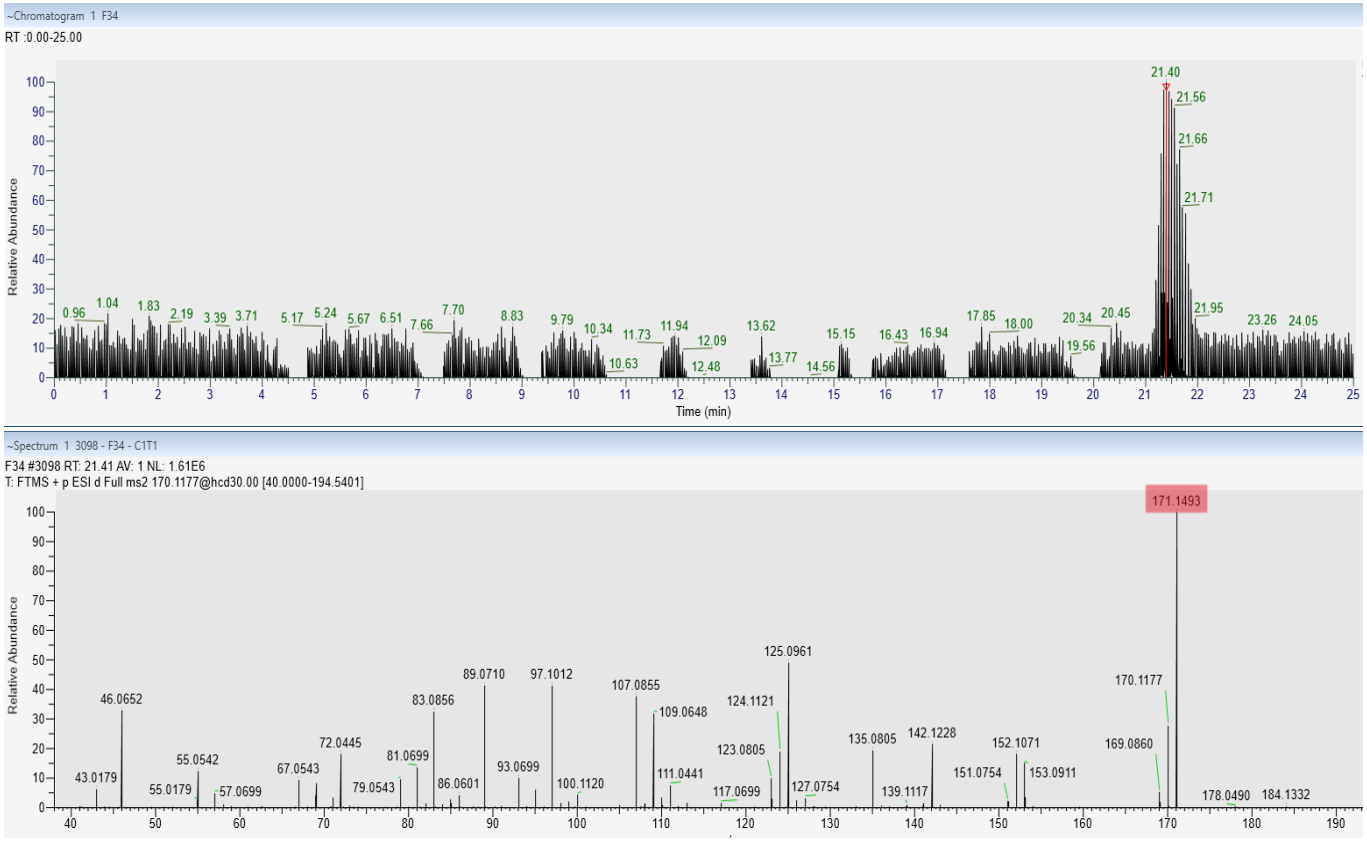

Figure 4.9 Total ion chromatogram of fraction 3.4 with the m/z spectrum at a retention time of 21.41 minutes. Highlighted in red is the m/z 171.1493, which appears in almost all RT spectra throughout this sample.

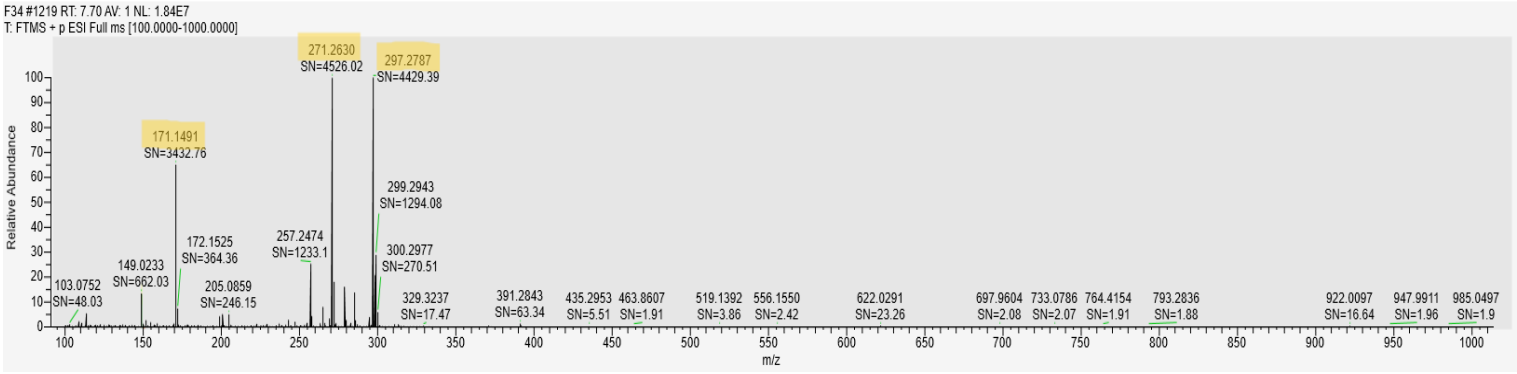

Figure 4.10 Spectrum of fraction 3.4 at retention time of 7.70 minutes.

Highlighted in yellow are the three most prevalent m/z that appear throughout the sample. They often coincide in the same peaks.

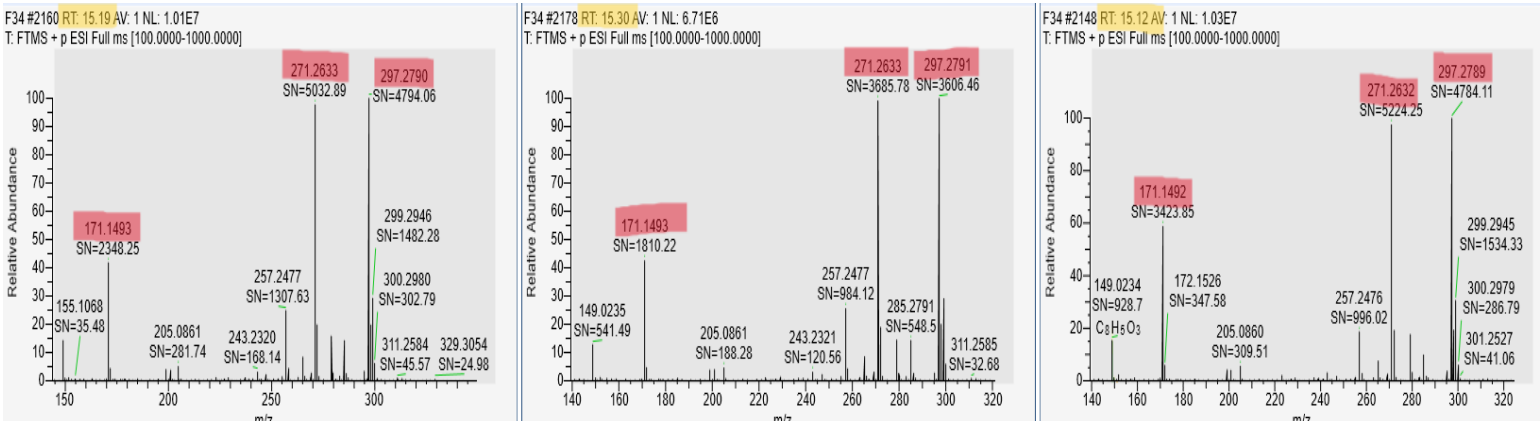

Figure 4.11M/z spectra of retention times in the 15-minute range.

The peaks with m/z of 171.1493, 271.2633, and 297.2790 are highlighted in red at retention time of 15.19 minutes (Left), 15.30 minutes (middle), and 15.12 minutes (right). These three often have the highest signal to noise ratio, indicating their prevalence within the sample.

Table 4.2 Putative CSSF empirical formulas from MS Data

Retention Time (min)	m/z (+/- 1)	Potential Empirical Formula
0.02-25.0	171.1492	$C_9H_{19}ON_2$
20.0-22.0	170.1177	$C_9H_{16}O_2N$
4.0-20.0	297.2789	$C_{19}H_{37}O_2$
7.0-18.0	271.2632	$C_{17}H_{35}O_2$

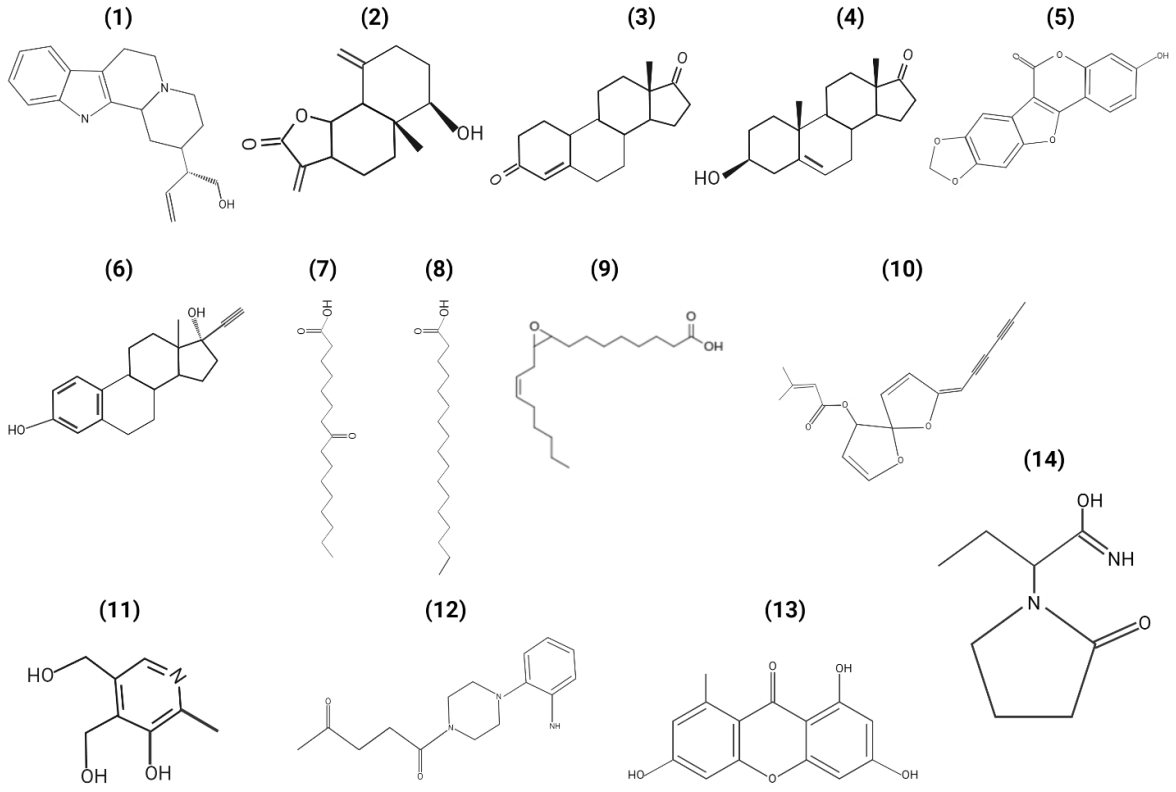

Figure 4.12 Putative structures of the QSM in *C. reinhardtii*.

Most structures were identified using a SMILES reader from the putative structures identified by LC-MS/MS (www.cheminfo.org/Chemistry/Cheminformatics/Smiles/index.html). (1) representative structure of an indole alkaloid (2) sesquiterpene lactone/eudesmanolide (3) Estrone, an oxosteroid or a phytohormone precursor (4) androgen or derivative of androgen, a phytohormone precursor (5) coumestan, such as medicagol (6) estrogen or estrogen derivative, a phytohormone precursor (7) 8-oxohexadecanoic acid (8) heptadecanoic acid (9) fatty acid such as coronaric acid (10) fatty acid ester, such a truxinic acid (11) pyridoxine (12) representative alkaloid structure (13) norlichexanthone or other xanthone (14) unknown molecule with m/z ~171.12 that has a similar structure to the antiseizure medication, Levetiracetam. Image was made using Biorender (www.biorender.com).

Discussion

QS in prokaryotes has been extensively studied since the mid-1900s. Much has been gained by identifying and understanding these pathways which have led to improvements in many industries including agriculture, biomanufacturing, and pharmaceuticals. QS in eukaryotes is a relatively new area of research, having been first characterized in fungi in the early 2000s. Finding a QS system in *C. reinhardtii*, a genetically distinct eukaryote from fungi, indicates that this strategy for coordinating group behavior is broadly distributed across all domains of life.

Regulating group behaviors allows microorganisms to overcome challenges in their environments, such as nutrient scarcity and predation. Motility is a common QS-regulated phenotype, as it allows the population to disperse prior to reaching the carrying capacity of their environment. QS in *C. reinhardtii* regulates an increase in the population's swimming speeds. Gaining a better understanding of this regulation can help our understanding of how populations of microorganisms respond to their environments, to each other in mixed populations, and to our understanding of evolutionary pressures these organisms face. Elucidating the parts of this regulation can also have impacts on the biomanufacturing, biofuels, and pharmaceutical industries. To this end, I have used chemical biology and analytical chemistry techniques to help identify the QSM(s) that regulate this behavior in *C. reinhardtii*. Through the use of HPLC, NMR, and LC-MS/MS, I have narrowed the potential QSM *Candida*tes down to fourteen putative structures (Fig 4.12). These molecules span chemical classes from fatty acids, to terpenes, to phytohormones, all of which are used in both inter- and intracellular communication in plants, fungi, and prokaryotes.

While there was no significant difference between the whole extract and the LCD cultures, the whole extract clearly contained the QSM. If it did not, we would not have been able to isolate a

fraction of the extract that effectively shifted the speeds (fig 4.3). The likely cause of this is two-fold: (i) the cultures have been recently discovered to be contaminated by fungal and/or bacterial intruders that are causing slower growth and possibly excreting chemical cues that the algae are responding to with increased swimming speed and (ii) there appears to be a signal that causes a slowing-down of swimming speeds, as was evidenced by fraction 2 of the whole extract having swimming speeds statistically lower than the LCD controls and the whole extract (data not shown). This could be evidence of a QS system similar to the one seen in *Saccharomyces cerevisiae* in which one molecule inhibits the activity while the other promotes it. This "push-and-pull" mechanism could be one reason the cultures treated with the whole extract did not swim as quickly as previously recorded.

Initial investigation and determination of fatty acid (FA) composition and biosynthesis in this organism occurred in the late 1980s (Giroud and Eichenberger, 1988; Giroud et al., 1988). The FA composition of *Chlamydomonas* has been extensively studied and reported in recent years (Zauner et al., 2012; Nguyen et al., 2013; Pflaster et al., 2014; Yang, et al, 2022; for a recent review see: Song, 2024). The FA compositions of *Chlamydomonas* share characteristics with higher plants like *Arabidopsis*, with nearly all FAs esterified to polar glycerolipids containing 16 or 18 carbons. Most FAs in this species are polyunsaturated, except for a significant amount of palmitic acid (16:0) (Li-Beisson, et al, 2015). This species has been known to alter the composition of their membrane lipids in response to environmental factors, including phosphate and nitrogen scarcity (Qari and Oves, 2024).

C. reinhardtii possesses a metabolism with shared characteristics to higher plants as well as humans (Merchant, et al, 2007; Llamas, et al, 2011). In addition, it has a large amount of class

III guanylyl and adenylyl cyclase kinases, which catalyze the synthesis of cGMP and cAMP, respectively, which are not found in plants but are found in animals (Schaap, 2005). These molecules serve as secondary messengers in a myriad of signal transduction pathways and are vital to flagellar function and regulation, which is thought to allow this organism to adapt to changes in environmental conditions (Gonzalez-Ballester, et al, 2005; Pollock, et al, 2005; Merchant, 2007).

Of the fourteen putative QSMs, thirteen have known alternative roles within *C. reinhardtii*. However, one molecule, detected at nearly all retention times in the MS data with an m/z of approximately 171.12, lacks an established role in this or any other organism. The putative structure of this unknown molecule is similar to the anti-seizure medication Levetiracetam, though it has different structural components in the side chain. This molecule also contains structural elements of CSSF identified by NMR, including nitrogen and a carbonyl group. Therefore, I propose this molecule as the QSM in *C. reinhardtii*.

The identification of any potentially unknown novel metabolite requires certain assumptions to be made during the processes of isolation, screening, and characterization. Here we will consider each of these decisions, their potential limitations, and how to proceed in the search for the CSSF. First, we have assumed that the CSSF is a specific molecule or closely related family of signals. This seemed a reasonable position given what has been previously observed in other quorum sensing systems such as AHLs which are insensitive to the quorum sensing signals of other systems. We also are making this assignment based on the hypothesis that the functional groups which we observed by NMR of the 3.4 fraction corresponds to the active compound. While this may be the case, because this fraction is derived from two rounds of separation and screening, the biologically relevant compound (i.e. the CSSF) may actually occur in these samples at a much

lower concentration. Finally, the assignment itself is based on putative chemical formulas generated by the mass-to-charge ratio which is subject to interpretation.

Yet, the potential of this method to identify putative targets signals must not be overlooked. The proposed signal molecule should be purchased and/or synthesized for testing as a possible target molecule. Improved resolution of the signal may be possible by third and/or fourth rounds of extract separation coupled to activity screening. This is particularly important as even Fraction 3.4 may contain over 100 analytes derived from the exudate of *C. reinhardtii*. Lastly, it is possible that tandem mass spectrometry data (MS/MS) could provide improved structural characterization through the analysis of fragmentation patterns. Ultimately, we have taken an important step forward in the process of identifying the CSSF.

Chapter 5 Discussion and Future Directions

Discussion

The discovery of quorum sensing (QS) in *Chlamydomonas reinhardtii* has significant implications for microbial ecology and evolution. This organism is a ubiquitous photoautotroph and can be found in both freshwater and soil. *C. reinhardtii* can therefore provide common goods, such as carbon sources, to other organisms in their environment as well as producing molecular oxygen, making it an ecologically important microorganism. Understanding the molecular underpinnings of communication is crucial for better understanding how these organisms inform and coordinate behaviors. These discoveries can help shape our understanding of the microbiosphere, how microorganisms integrate multiple stimuli and respond to the environment and other organisms around them. Having a better understanding of these systems may also provide us with insight how complex microbial associations occur within the rhizosphere, as well as the evolutionary pressures that cause these systems to emerge as convergent strategies across microorganisms.

Uncovering QS in non-fungal eukaryotes provides additional evidence that systems regulating group behaviors, aiding in population persistence, are a convergent strategy across all domains of life. *Chlamydomonas reinhardtii* is a good candidate species for these investigations as it is a model organism for motility, has a large library of variant wildtypes and mutants, and has previously displayed the capacity to evolve group behaviors. Through experimentation with this species, I attempted to answer four questions:

- Question 1: How do we measure and characterize the swimming speeds of microorganisms? (Chapter 2)
- Question 2: How do we know what behavior to look for in a microorganism when investigating QS? (Chapter 3)
- Question 3: Does *C. reinhardtii* quorum sense? (Chapter 3)
- Question 4: What is the identity of the QSM in *C. reinhardtii*? (Chapter 4)

To help answer these questions, I have developed a computer-assisted tracking method, as previous tracking methods were insufficient for making population-wide assertions on swimming speeds, because they relied on <30 tracks to reflect motility in a population that is often in excess of 10^5 cells/ml. This new process facilitated our ability to record global swimming data on a large subset of tracks within this population (Fig 2.1). This made characterizing swimming speeds for *C. reinhardtii* and its motility mutants possible and allowed us to assess this organism's response to varying environmental conditions, such as nutrient scarcity (Fig 2.3 & 2.4). Shifts in the population's speeds could be observed, tracked, and compared using histograms and average speed metrics and is the primary focus of Chapter 2.

Using this new cell tracking method, it was observed that older (72 hr) *C. reinhardtii* cultures had a higher average speed than younger (24 hr) cultures (Fig 3.1). This higher average speed was correlated to a shift in the number of cells moving at higher speeds. To investigate the cause of this shift in speeds, several experiments were conducted, including media swaps and organic extractions (Fig 3.2 & 3.3). The result of these tests verified that a chemical signal was the cause of this behavior, and that it could be extracted from older cell cultures. I was also able to

verify that this behavior could be artificially induced by manually increasing the cell density of younger cultures (24 hr; ~$5x10^5$ cells/ml) to the density found in the older (72 hr; ~$2x10^7$ cells/ml) cultures (Fig 3.6). The results of these experiments allowed me to make the assertion that the increase in swimming speeds was due to a QS-regulated pathway in *C. reinhardtii* and is the primary focus of Chapter 3.

It is important to identify molecular components of QS systems to better understand how these organisms adapt group behaviors in response to environmental changes. To this end, I attempted to identify the signaling molecule used by *C. reinhardtii* to increase the population's swimming speeds. In order to accomplish this goal, I developed a new method that is quicker and easier by extracting the chemical signal using solid phase extraction (SPE) (Fig 4.1). This allowed for the rapid accumulation of extracts containing the chemical signal for use in analytical processing techniques for identification of the extract components.

Coupling HPLC and the developed motility assay, I was able to identify portions of the extract that contained the signal molecule(s) (Fig 4.3). The use of HPLC allowed me to reduce the number of molecules within the extract sample to reduce the amount of noise within the sample. Once an active fraction of extract was identified via the motility assay, a subsequent round of HPLC was used to improve separation for the purposes of signal identification. This second round of extract fractions was tested, and the QS-active fraction was then concentrated and submitted to LC-MS/MS to identify putative molecules for further testing, and NMR (^{13}C and ^{1}H) was run to identify potential structural architecture of the signal molecule (Fig 4.4, 4.5, 4.7 and 4.8-11). A list of fourteen potential molecules, mostly consisting of fatty acids, sterols, and phytohormones, have

been identified for further testing using these methods (Table 4.1 & Fig 4.12) and is the focus of Chapter 4.

C. reinhardtii has been known to alter their membrane lipid composition in response to various environmental factors and NMR scans of the QSM-containing fraction indicate that the active molecule likely contains one or more nitrogen as well as at least one oxygen. Therefore, it is unlikely that these long-chain fatty acids are the signal source themselves but could be an additional result of this QS-mediated pathway. Excreting lipids into their environment or altering the lipid components of their membrane could potentially lower their surface tension and allow them to swim more quickly. The LC-MS/MS data indicated that the potential QS molecule contains nitrogen.

It should be noted that there is a structural difference in lipids derived from fatty acids and those derived from other biosynthetic sources, such as sterols. Fatty acid lipids have a glycerol backbone, sometimes accompanied by a phosphate group, and one to three chains of carbon-hydrogen tails of various lengths, oxidations, and saturation, whereas sterols have a ring structure motif. Sterols and sterol-derived molecules serve many functions within cells, including as signal and regulation molecules (Salimova, et al., 1999; Findakly, 2021). Sterols are well characterized by NMR techniques and signatures for the molecules are not observed in the active fraction arguing against this class of compounds as the active QSM (Wilson, et al., 1996).

Sphingolipids and glycerophospholipids can also contain nitrogen and are ubiquitous across organisms. Sphingolipids are essential components of the plasma membrane and are vital for numerous biological processes, including transmission of various intracellular signals, cell polarization, differentiation, and migration (Zhu, et al, 2023). However, these molecules fulfill

numerous roles within the cell and as such their prevalence could be unrelated to the QS behavior in *C. reinhardtii*.

Out of the fourteen putative QSMs, thirteen have alternative roles they can fill within *C. reinhardtii*. However, the one molecule found at nearly all retention times in the MS data, with the m/z ~171.12 has no established role within this organism. Indeed, it has no established role in any organism. The putative structure of this currently unknown molecule is similar to that of an anti-seizure medication, Levetiracetam, but the side chain has different structural components. This molecule also carries the structural components identified using NMR, containing nitrogen and a carbonyl group. It is for these reasons that I am proposing this molecule as the QSM in *C. reinhardtii*.

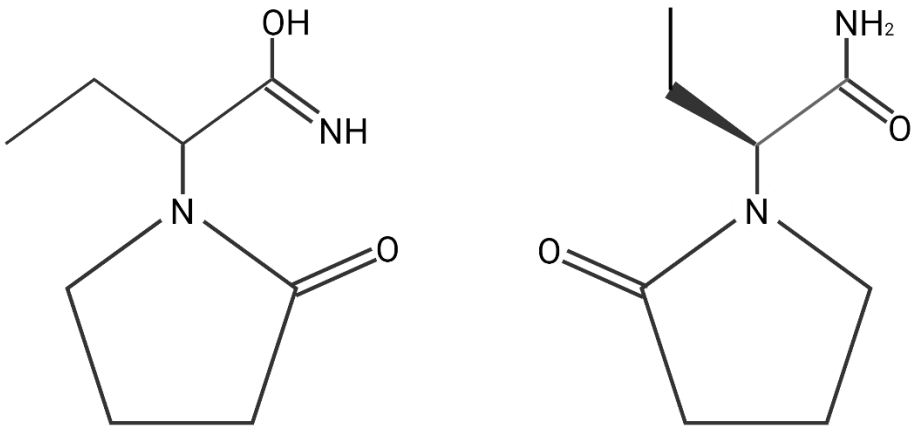

Unknown Molecule
with m/z ~171.12

Levetiracetam

Figure 5.1 Comparison of QSM molecule structure to that of the antiseizure medication, Levetiracetam.

The substituent structures are different between these two molecules, as the unknown QSM has a ketimine group and a hydroxide where Levetiracetam has a ketone and amine.

Our ability to measure swimming speeds in *C. reinhardtii* and its mutants, along with the closely related *C. moewusii* supports the usefulness of these methods for understanding QS in this genus, which includes over 300 species. Although my focus is on this model unicellular eukaryote, the approaches described in this dissertation are easily transferable to other genera. Identifying a QS-regulated system in *C. reinhardtii* and *C. moewusii* strongly supports the hypothesis that QS is more broadly distributed across microorganisms than originally thought and expands the potential for discovering QS in other unicellular eukaryotic species. This discovery and future ones offer new insights into microbial ecology, evolution, modes of pathogenesis, and other aspects of microbial behavior.

Future Directions

Motility is an essential function to most microorganisms, as it allows them to find resources, avoid harmful environments (such as predation, abiotic and biotic stressors), and effectively interact within hosts. In *C. reinhardtii*, the ability to relocate allows these organisms to optimize their ability to photosynthesize and gather other resources (e.g., photo- and chemotaxis). While *C. reinhardtii* can utilize environmental carbon sources, photosynthesis provides additional energy through carbon uptake and serves as an alternative carbon source when environmental carbon is limited. Without the ability to move, they would be reliant on the replenishment of carbon sources in their settled environment, as *C. reinhardtii* are not able to float in water. That environment could be deep under water and with little to no light, which would cause them to have a diminished capacity to generate energy. Therefore, motility is a crucial aspect of fitness in this species.

This work is the first non-fungal QS system identified in unicellular eukaryotes, but further work into this system is essential to further our understanding of microbial communication. The clear next step in this line of research is to test the identified putative molecules for the QS-related phenotype. This would allow for the identification of the signal molecule, or class of molecules, and lead to further structure-activity testing such as seen in Palmer and associates' work (2011a & 2011b) and in Lee and associates' work (2020). Probing these systems in this way allows for the ability to use QSM analogs to manipulate these systems for more beneficial outcomes.

Another clear next step is testing other *C. reinhardtii* wildtype lines for the prevalence of this QS system within the species. Many prokaryotic species have species variants that do not possess the QS pathway, so-called "social cheaters," but still reap the benefits of the social behavior. It would be interesting to see if this phenomenon of "social cheating" also occurs among eukaryotes. Another step in this same line of questioning would be to test if other closely related species of *Chlamdamonas* also possess this, or other QS-regulated pathways.

Once the chemical signal is identified, it would be pertinent to also identify the metabolic pathway or synthase involved in producing the QSM, as well as the cognate receptor for it. Finding these molecular components will allow for further manipulation of the system for beneficial outcomes. Identifying these molecular parts will also allow for screening to identify the genetic components involved and will allow for finding similar genetic systems in other species. This would potentially increase the pool of identified QS systems in unicellular eukaryotes.

References

Albuquerque, P., and Casadevall, A. (2012). Quorum sensing in fungi–a review. Med. Mycol. 50, 337–345.

Alem M., Oteef M.D.Y., Flowers T.H., Douglas L.J. (2006). Production of Tyrosol by Candida albicans Biofilms and Its Role in Quorum Sensing and Biofilm Development. Eukaryotic Cell. 5(10). https://doi.org/10.1128/ec.00219-06

Alfred SE, Surendra A, Le C, Lin K, Mok A, Wallace IM, Proctor M, Urbanus ML, Giaever G, Nislow C. (2012). A phenotypic screening platform to identify small molecule modulators of *Chlamydomonas* reinhardtii growth, motility and photosynthesis. Genome Biology. 13(R105). https://doi.org/10.1186/gb-2012-13-11-r105

Almaraz-Delgado AL, Flores-Uribe J, Pérez-España VH, Salgado-Manjarrez E, Badillo-Corona JA. (2014). Production of therapeutic proteins in the chloroplast of *Chlamydomonas* reinhardtii. AMB Express. 4(57). https://doi.org/10.1186/s13568-014-0057-4

Avbelj, M., Zupan, J., Kranjc, L., & Raspor, P. (2015). Quorum-sensing kinetics in *Saccharomyces cerevisiae*: a symphony of ARO genes and aromatic alcohols. Journal of agricultural and food chemistry, 63(38), 8544-8550. https://doi.org/10.1021/acs.jafc.5b03400

Barsel, S.-E., Wexler, D. E., Lefebvre, P. A., Fernindez, E. (1988). Genetic analysis of long-flagella mutants of *Chlamydomonas* reinhurdtii. Genetics 118, 637–648.

Berrocal, A., Navarrete, J., Oviedo, C. and Nickerson, K. (2012), Quorum sensing activity in Ophiostoma ulmi: effects of fusel oils and branched chain amino acids on yeast-mycelial dimorphism. Journal of Applied Microbiology, 113(1), 126–134. https://doi.org/10.1111/j.1365-2672.2012.05317.x

Bloodgood, R. A., Salomonsky, N. L. (1989). Use of a novel *Chlamydomonas* mutant to demonstrate that flagellar glycoprotein movements are necessary for the expression of gliding motility. Cell Motil. Cytoskeleton 13 (1), 1–8. doi: 10.1002/cm.970130102

Blount, Z. D., Barrick, J. E., Davidson, C. J., & Lenski, R. E. (2012). Genomic analysis of a key innovation in an experimental Escherichia coli population. Nature, 489(7417), 513–518. https://doi.org/10.1038/nature11514

Bowers, J.H., and Parke, J.L. (1993). Colonization of pea (Pisum sativum L.) taproots by Pseudomonas fluorescens: effect of soil temperature and bacterial motility. Soil Biol. Biochem. 25, 1693–1701.

Byrne, T.E., Wells, M.R., and Johnson, C.H. (1992). Circadian rhythms of chemotaxis to ammonium and of methylammonium uptake in *Chlamydomonas*. Plant Physiol. 98, 879–886. https://doi.org/10.1104/pp.98.3.879

Chen, H., & Fink, G. R. (2006). Feedback control of morphogenesis in fungi by aromatic alcohols. Genes & development, 20(9), 1150-1161. https://doi.org/10.1101/gad.1411806

Chen, H, Fujita, M, Feng, Q, & Fink, GR (2004). Tyrosol is a quorum-sensing molecule in *Candida albicans*. 101(14). https://doi.org/10.1073/pnas.0401416101

Chen X, Schauder S, Potier N, Van Dorsselaer A, Pelczer I, Bassler BL, Hughson FM. (2002). Structural identification of a bacterial quorum-sensing signal containing boron. Nature, 415(6871), 545-549. https://doi.org/10.1038/415545a

Chen, M.-T., & Weiss, R. (2005). Artificial cell-cell communication in yeast *Saccharomyces cerevisiae* using signaling elements from Arabidopsis thaliana. Nature Biotechnology, 23(12), 1551–1555. https://doi.org/10.1038/nbt1162

Chen, X., Zeng, L., Wu, Y., Gao, Y., and Zhao, Y. (2017). Swimming characteristics of gyrotactic microorganisms in low-Reynolds-number flow: *Chlamydomonas* reinhardtii. Energy Ecol. Environ. 2, 289–295.

Diem, K., Magaret, A., Klock, A., Jin, L., Zhu, J., Corey, L. J. (2015). Image analysis for accurately counting CD4+ and CD8+ T cells in human tissue. Virol. Methods 222, 117–121. doi: 10.1016/j.jviromet.2015.06.004

Diggle, S.P., Gardner, A., West, S.A., and Griffin, A.S. (2007). Evolutionary theory of bacterial quorum sensing: when is a signal not a signal? Philos. Trans. R. Soc. B Biol. Sci. 362, 1241–1249.

Engel BD, Ishikawa H, Feldman JL, Wilson CW, Chuang P-T, Snedecor J, Williams J, Sun Z, Marshall WF. (2011). A cell-based screen for inhibitors of flagella-driven motility in

Chlamydomonas reveals a novel modulator of ciliary length and retrograde actin flow. Cytoskeleton (Hoboken, N.J.), 68(3), 188–203. https://doi.org/10.1002/cm.20504

Engel, B. D., Ishikawa, H., Wemmer, K. A., Geimer, S., Wakabayashi, K. I., Hirono, M., et al. (2012). The role of retrograde intraflagellar transport in flagellar assembly, maintenance, and function. J. Cell Biol. doi: 10.1083/jcb.201206068

Ermilova, E.V., Nikitin, M.M., and Ferna´ndez, E. (2007). Chemotaxis to ammonium/ methylammonium in *Chlamydomonas* reinhardtii: the role of transport systems for ammonium/methylammonium. Planta 226, 1323 1332.

Espino-Díaz, M., Sepúlveda, D. R., González-Aguilar, G., & Olivas, G. I. (2016). Biochemistry of Apple Aroma: A Review. Food technology and biotechnology, 54(4), 375–397. https://doi.org/10.17113/ftb.54.04.16.4248

Flowers, J. M., Hazzouri, K. M., Pham, G. M., Rosas, U., Bahmani, T., Khraiwesh, B., Nelson, D. R., Jijakli, K., Abdrabu, R., Harris, E. H., Lefebvre, P. A., Hom, E. F. Y., Salehi-Ashtiani, K., & Purugganan, M. D. (2015). Whole-Genome Resequencing Reveals Extensive Natural Variation in the Model Green Alga *Chlamydomonas* reinhardtii. The Plant Cell, 27(9), 2353–2369. https://doi.org/10.1105/tpc.15.00492

Folcik, A.M., Haire, T., Cutshaw, K., Riddle, M., Shola, C., Nassani, S., Rice, P., Richardson, B., Shah, P., Nazamoddini-Kachouie, N., and Palmer, A. (2020). Computer-assisted tracking of *Chlamydomonas* species. Front. Plant Sci. 10, 1616.

Fujiu, K., Nakayama, Y., Iida, H., Sokabe, M., and Yoshimura,K. (2011). Mechanoreception in motile flagella of *Chlamydomonas*. Nat. Cell Biol. 13, 630–632.

Fuller, A., Young, P., Pierce, D., Kitson-Finuff, J., Jain, P., Schneider, K., Lazar, S.,Taran, O., Palmer, A., and Lynn, D.G. (2017). Redox-mediated quorum sensing in plants. PLoS One 12, e0182655.

Gabaldón, T. (2021). Origin and Early Evolution of the Eukaryotic Cell. Annual Review of Microbiology, 75(Volume 75, 2021), 631–647. https://doi.org/10.1146/annurev-micro-090817-062213

Giroud and Eichenberger, 1988; Giroud, C. and Eichenberger, W. (1988). Fatty-acids of *Chlamydomonas* reinhardtii– structure, positional distribution and biosynthesis. Biol. Chem. H-S, 369,18–19.

Giroud et al., 1988: Giroud, C., Gerber, A. and Eichenberger, W. (1988). Lipids of *Chlamydomonas* reinhardtii– analysis of molecular-species and intracellular site(s) of biosynthesis. Plant Cell Physiol. 29, 587–595.

González-Ballester, David, et al. (2005) Functional genomics of the regulation of the nitrate assimilation pathway in *Chlamydomonas*. Plant Physiology, vol. 137, no. 2. pp. 522–533, https://doi.org/10.1104/pp.104.050914.

Haire, T. C., Bell, C., Cutshaw, K., Swiger, B., Winkelmann, K., Palmer, A. G. (2018). Robust microplate-based methods for culturing and in vivo phenotypic screening of *Chlamydomonas* reinhardtii. Front. Plant Sci. 9. doi: 10.3389/fpls.2018.00235

Hara, Y. (2020). Specialization of nuclear membrane in eukaryotes. Journal of Cell Science, 133(12), jcs241869. https://doi.org/10.1242/jcs.241869

Harris EH. (2001). *Chlamydomonas* as a Model Organism. Annual review of plant physiology and plant molecular biology, 52, 363–406. https://doi.org/10.1146/annurev.arplant.52.1.363

Harris, E. H., Witman, G., Stern, D. eds. (2013). "Motility and Behavior," in The *Chlamydomonas* Sourcebook: A Comprehensive Guide to Biology and Laboratory Use (Academic Press), 89–117.

Herron, M.D., Borin, J.M., Boswell, J.C., Walker, J., Chen, I.C.K., Knox, C.A., Boyd, M., Rosenzweig, F., and Ratcliff, W.C. (2019). De novo origins of multicellularity in response to predation. Sci. Rep. 9, 2328

Hibbing, M.E., Fuqua, C., Parsek, M.R., and Peterson, S.B. (2010). Bacterial competition: surviving and thriving in the microbial jungle. Nat. Rev. Microbiol. 8, 15–25.

Homer, C. M., Summers, D. K., Goranov, A. I., Clarke, S. C., Wiesner, D. L., Diedrich, J. K., Moresco, J. J., Toffaletti, D., Upadhya, R., Caradonna, I., Petnic, S., Pessino, V., Cuomo, C. A., Lodge, J. K., Perfect, J., Yates, J. R., Nielsen, K., Craik, C. S., & Madhani, H. D. (2016). Intracellular Action of a Secreted Peptide Required for Fungal Virulence. Cell Host & Microbe, 19(6), 849–864. https://doi.org/10.1016/j.chom.2016.05.001

Hornby, J.M., Jacobitz-Kizzier, S.M., McNeel, D.J., Jensen, E.C., Treves, D.S., and Nickerson, K.W. (2004). Inoculum size effect in dimorphic fungi: extracellular control of yeast-mycelium dimorphism in Ceratocystis ulmi. Appl. Environ. Microbiol. 70, 1356–1359. Huang, B., Piperno, G., Ramanis, Z., Luck, D. J. J. (1981). Radial spokes of *Chlamydomonas* flagella: genetic analysis of assembly and function. J. Cell Biol. 88 (1).

Huang, B., Ramanis, Z., Dutcher, S. K., Luck, D. J. L. (1982b). Suppressor mutations in *Chlamydomonas* reveal a regulatory mechanism for flagellar function. Cell 29 (3), 745–753. doi: 10.1016/0092-8674(82)90436-6

Huang, B., Ramanis, Z., and Luck, D.J.L. (1982). Suppressor mutations in *Chlamydomonas* reveal a regulatory mechanism for flagellar function. Cell 28, 115–124.

Huang, B., Ramanis, Z., and Luck, D. J. L. (1982a). Uniflagellar mutants of *Chlamydomonas*: evidence for the role of basal bodies in transmission of positional information. Cell 29, 745–753.

Jagtap, S., Bedekar, A., & Rao, C. (2020). Quorum Sensing in Yeast. In Quorum Sensing: Microbial Rules of Life (Vol. 1374, pp. 235–250). https://doi.org/10.1021/bk-2020-1374.ch013

Jang, H., & Ehrenreich, I. M. (2012). Genome-Wide Characterization of Genetic Variation in the Unicellular, Green Alga *Chlamydomonas* reinhardtii. PLOS ONE, 7(7), e41307. https://doi.org/10.1371/journal.pone.0041307

Jones, C. S., & Mayfield, S. P. (2012). Algae biofuels: versatility for the future of bioenergy. Current opinion in biotechnology, 23(3), 346–351. https://doi.org/10.1016/j.copbio.2011.10.013

Kalaidzidis, Y. J. (2009). Multiple objects tracking in fluorescence microscopy. J. Math. Biol. 58 (1–2), 57–80. doi: 10.1007/s00285-008-0180-4

Kamiya, R., Kurimoto, E., Muto, E. J. (1991). Two types of *Chlamydomonas* flagellar mutants missing different components of inner-arm dynein. Cell Biol. 112 (3). doi: 10.1083/jcb.112.3.441

Kamiya, R. J. (1988). Mutations at twelve independent loci result in absence of outer dynein arms in Chylamydomonas reinhardtii. Cell Biol. 107 (6 Pt 1), 2253–2258. doi: 10.1083/jcb.107.6.2253

Kavanaugh, J. S., Gakhar, L., & Horswill, A. R. (2011). The structure of LsrB from Yersinia pestis complexed with autoinducer-2. Acta Crystallographica Section F: Structural Biology and Crystallization Communications, 67(Pt 12), 1501–1505. https://doi.org/10.1107/S1744309111042953

Kong, H., Akakin, H. C., Sarma, S. E. (2013). A generalized laplacian of gaussian filter for blob detection and its applications. IEEE Trans. Cybern. 43 (6), 1719–1733. doi: 10.1109/TSMCB.2012.2228639

Kovács, R., & Majoros, L. (2020). Fungal Quorum-Sensing Molecules: A Review of Their Antifungal Effect against *Candida* Biofilms. Journal of Fungi, 6(3), Article 3. https://doi.org/10.3390/jof6030099

Kuchka, M. R., Jarvik, J. W. J. (1982). Analysis of flagellar size control using a mutant of *Chlamydomonas* reinhardtii with a variable number of flagella. J. Cell Biol. 92 (1). doi: 10.1083/jcb.92.1.170

Kuchka, M. R., Jarvik, J. W. (1987). Short-Flagella Mutants of *Chlamydomonas* reinhardtii. Genetics 115 (4).

Kügler, S., Sebghati, T. S., Eissenberg, L. G., & Goldman, W. E. (2000). Phenotypic variation and intracellular parasitism by Histoplasma capsulatum. Proceedings of the National Academy of Sciences, 97(16), 8794–8798. https://doi.org/10.1073/pnas.97.16.8794

Lee, H., Chang, Y. C., Nardone, G., & Kwon-Chung, K. J. (2007). TUP1 disruption in Cryptococcus neoformans uncovers a peptide-mediated density-dependent growth phenomenon that mimics quorum sensing. Molecular microbiology, 64(3), 591–601. https://doi.org/10.1111/j.1365-2958.2007.05666.x

Lee, J.-H., Kim, Y.-G., Khadke, S. K., & Lee, J. (2021). Antibiofilm and antifungal activities of medium-chain fatty acids against *Candida albicans* via mimicking of the quorum-sensing molecule farnesol. Microbial Biotechnology, 14(4), 1353–1366. https://doi.org/10.1111/1751-7915.13710

Leal Taixé, L., Heydt, M., Rosenhahn, A., Rosenhahn, B. (2009). Automatic tracking of swimming microorganisms in 4D digital in-line holography data. 2009 Workshop on Motion and Video Computing, WMVC ’09. doi: 10.1109/WMVC.2009.5399244

Llamas, Ángel, et al. (2011). Molybdenum metabolism in the alga *Chlamydomonas* stands at the crossroad of those in Arabidopsis and humans. Metallomics, vol. 3, no. 6, 27. pp. 578–590, https://doi.org/10.1039/c1mt00032b.

Li, L., Pan, Y., Zhang, S., Yang, T., Li, Z., Wang, B., Sun, H., Zhang, M., & Li, X. (2023). Quorum sensing: cell-to-cell communication in *Saccharomyces cerevisiae*. Frontiers in microbiology, 14, 1250151. https://doi.org/10.3389/fmicb.2023.1250151

Li-Beisson,Yonghua, Fred Beisson, Wayne Riekhof. Metabolism of acyl-lipids in *Chlamydomonas* reinhardtii. Plant Journal, 82 (3), 504-522. (2015). https://doi.org/10.1111/tpj.12787.

Liu, C. L., Xue, K., Yang, Y., Liu, X., Li, Y., Lee, T. S., Bai, Z., & Tan, T. (2022). Metabolic engineering strategies for sesquiterpene production in microorganism. Critical reviews in biotechnology, 42(1), 73–92. https://doi.org/10.1080/07388551.2021.1924112

Lu, Y., Su, C., Unoje, O., & Liu, H. (2014). Quorum sensing controls hyphal initiation in *Candida albicans* through Ubr1-mediated protein degradation. Proceedings of the National Academy of Sciences of the United States of America, 111(5), 1975–1980. https://doi.org/10.1073/pnas.1318690111

Luck, D., Piperno, G., Ramanis, Z., Huang, B. (1977). Flagellar mutants of *Chlamydomonas*: Studies of radial spoke- defective strains by dikaryon and revertant analysis. Cell Motil. Cytoskeleton 74 (8), 3456–3460. doi: 10.1073/pnas.74.8.3456

Lupp, C., Urbanowski, M., Greenberg, E. P., & Ruby, E. G. (2003). The Vibrio fischeri quorum-sensing systems ain and lux sequentially induce luminescence gene expression and are important for persistence in the squid host. Molecular microbiology, 50(1), 319–331. https://doi.org/10.1046/j.1365-2958.2003.t01-1-03585.x

Marshall, W.F. (2009). Quantitative high throughput assays for flagella-based motility in *Chlamydomonas* using plate-well image analysis and transmission correlation spectroscopy. J. Biomol. Screen. 14, 133–141.

Mehmood, A., Liu, G., Wang, X., Meng, G., Wang, C., & Liu, Y. (2019). Fungal Quorum-Sensing Molecules and Inhibitors with Potential Antifungal Activity: A Review. Molecules, 24(10), Article 10. https://doi.org/10.3390/molecules2410195

Miller, M.B., and Bassler, B.L. (2001). Quorum sensing in bacteria. Annu. Rev. Microbiol. 12, 165–199. Montgomery, K., Charlesworth, J.C., LeBard, R., Visscher, P.T., and Burns, B.P. (2013). Quorum sensing in extreme environments. Life (Basel, Switzerland) 3, 131–148.

Merchant, Sabeeha S., et al. (2007). The *Chlamydomonas* genome reveals the evolution of key animal and plant functions. Science, vol. 318, no. 5848 pp. 245–250, https://doi.org/10.1126/science.1143609.

Miller, S. T., Xavier, K. B., Campagna, S. R., Taga, M. E., Semmelhack, M. F., Bassler, B. L., & Hughson, F. M. (2004). Salmonella typhimurium recognizes a chemically distinct form of the bacterial quorum-sensing signal AI-2. Molecular cell, 15(5), 677–687. https://doi.org/10.1016/j.molcel.2004.07.020

Miranda, V., Torcato, I. M., Xavier, K. B., & Ventura, M. R. (2019). Synthesis of d-desthiobiotin-AI-2 as a novel chemical probe for autoinducer-2 quorum sensing receptors. Bioorganic chemistry, 92, 103200. https://doi.org/10.1016/j.bioorg.2019.103200

Miyashiro, T., & Ruby, E. G. (2012). Shedding light on bioluminescence regulation in Vibrio fischeri. Molecular microbiology, 84(5), 795–806. https://doi.org/10.1111/j.1365-2958.2012.08065.x

Monds, R., & O'Toole, G. (2014). Metabolites as Intercellular Signals for Regulation of Community-Level Traits. In Chemical Communication among Bacteria (pp. 105–129). https://doi.org/10.1128/9781555815578.ch8

Najmi, S. M., & Schneider, D. A. (2021). Quorum sensing regulates rRNA synthesis in *Saccharomyces cerevisiae*. Gene, 776, 145442. https://doi.org/10.1016/j.gene.2021.145442

Neiditch, M. B., Federle, M. J., Pompeani, A. J., Kelly, R. C., Swem, D. L., Jeffrey, P. D., Bassler, B. L., & Hughson, F. M. (2006). Ligand-induced asymmetry in histidine sensor kinase complex regulates quorum sensing. Cell, 126(6), 1095–1108. https://doi.org/10.1016/j.cell.2006.07.032

Neiditch, M. B., Federle, M. J., Miller, S. T., Bassler, B. L., & Hughson, F. M. (2005). Regulation of LuxPQ receptor activity by the quorum-sensing signal autoinducer-2. Molecular cell, 18(5), 507–518. https://doi.org/10.1016/j.molcel.2005.04.020

Nguyen, H.M., Cuine, S., Beyly-Adriano, A., Legeret, B., Billon, E., Auroy, P., Beisson, F., Peltier, G. and Li-Beisson, Y. (2013) The green microalga *Chlamydomonas* reinhardtii has a single x-3 fatty acid desaturase that localizes to the chloroplast and impacts both plastidic and extraplastidic membrane lipids. Plant Physiol. 163, 914–928.

Njoroge, J., and Sperandio, V. (2009). Jamming bacterial communication :new approaches for the treatment of infectious diseases. EMBO Mol. Med. 1, 201–210.

Oncel, S. (2013). Microalgae for a macroenergy world. Renewable and Sustainable Energy Reviews, 26, 241–264. https://doi.org/10.1016/j.rser.2013.05.059

Padder, S. A., Prasad, R., & Shah, A. H. (2018). Quorum sensing: A less known mode of communication among fungi. Microbiological research, 210, 51–58. https://doi.org/10.1016/j.micres.2018.03.007

Palmer, A.G., Ali, M., Yang, S., Parchami, N., Bento, T., Mazzella, A., Oni,M., Riley, M.C., Schneider, K. & Massa, N. (2016). Kin recognition is a nutrient-dependent inducible phenomenon. Plant Signaling & Behavior, 11:9, https://doi.org/10.1080/15592324.2016.1224045

Palmer, A. G., Senechal, A. C., Mukherjee, A., Ané, J. M., & Blackwell, H. E. (2014). Plant responses to bacterial N-acyl L-homoserine lactones are dependent on enzymatic degradation to L-homoserine. ACS chemical biology, 9(8), 1834–1845. https://doi.org/10.1021/cb500191a

Palmer, A.G., Streng, E., and Blackwell, H.E. (2011a). Attenuation of virulence in pathogenic bacteria using synthetic quorum-sensing modulators under native conditions on plant hosts. ACS Chem. Biol. 6, 1348–1356.

Palmer, A.G., Streng, E., Jewell, K.A., and Blackwell, H.E. (2011b). Quorum sensing in bacterial species that use degenerate autoinducers can be tuned by using structurally identical non-native ligands. Chembiochem 12, 138–147.

Papenfort, K., and Bassler, B.L. (2016). Quorum sensing signal-response systems in Gram negative bacteria. Nat. Rev. Microbiol. 14, 576–588.

Parapouli, M., Vasileiadis, A., Afendra, A.-S., & Hatziloukas, E. (2020). *Saccharomyces cerevisiae* and its industrial applications. AIMS Microbiology, 6(1), 1–31. https://doi.org/10.3934/microbiol.2020001

Peralta-Yahya, P. P., Zhang, F., del Cardayre, S. B., & Keasling, J. D. (2012). Microbial engineering for the production of advanced biofuels. Nature, 488(7411), 320–328. https://doi.org/10.1038/nature11478

Pereira, C. S., McAuley, J. R., Taga, M. E., Xavier, K. B., & Miller, S. T. (2008). Sinorhizobium meliloti, a bacterium lacking the autoinducer-2 (AI-2) synthase, responds to AI-2 supplied by other bacteria. Molecular microbiology, 70(5), 1223–1235. https://doi.org/10.1111/j.1365-2958.2008.06477.x

Pereira, C. S., de Regt, A. K., Brito, P. H., Miller, S. T., & Xavier, K. B. (2009). Identification of functional LsrB-like autoinducer-2 receptors. Journal of bacteriology, 191(22), 6975–6987. https://doi.org/10.1128/JB.00976-09

Pereira, C. S., Thompson, J. A., & Xavier, K. B. (2013). AI-2-mediated signalling in bacteria. FEMS microbiology reviews, 37(2), 156–181. https://doi.org/10.1111/j.1574-6976.2012.00345.x

Pflaster, E.L., Schwabe, M.J., Becker, J., Wilkinson, M.S., Parmer, A., Clemente, T.E., Cahoon, E.B. and Riekhof, W.R. (2014). A high-throughput fatty acid profiling screen reveals novel

variations in fatty acid biosynthesis in *Chlamydomonas* reinhardtii and related algae. Eukaryot. Cell, 13, 1431–1438. https://doi.org/10.1128/ec.00128-14

Pollock, Steve V., et al. (2005) Insights into the acclimation of *Chlamydomonas* reinhardtii to sulfur deprivation." Photosynthesis Research, vol. 86, no. 3, 15. pp. 475–489, https://doi.org/10.1007/s11120-005-4048-9.

Pröschold, T., Harris, E. H., Coleman, A. W. (2005). Portrait of a species: *Chlamydomonas* reinhardtii. Genetics 170, 1601–10. doi: 10.1534/genetics.105.044503

Qari, H.A., Oves, M. (2020). Fatty acid synthesis by *Chlamydomonas* reinhardtii in phosphorus limitation. J Bioenerg Biomembr 52, 27–38 https://doi.org/10.1007/s10863-019-09813-8

R Development Core Team. (2016). R Found. Stat. Comput. Vienna Austria, 0, doi: 10.1038/sj.hdy.6800737

Racey, T. J., Hallett, R., Nickel, B. (1981). A quasi-elastic light scattering and cinematographic investigation of motile *Chlamydomonas* reinhardtii. Biophys. J. 35 (3), 557–571. doi: 10.1016/S0006-3495(81)84812-6

Rappleye, C. A., Eissenberg, L. G., & Goldman, W. E. (2007). *Histoplasma capsulatum* α-(1,3)-glucan blocks innate immune recognition by the β-glucan receptor. Proceedings of the National Academy of Sciences of the United States of America, 104(4), 1366–1370. https://doi.org/10.1073/pnas.0609848104

Rasala, B. A., & Mayfield, S. P. (2015). Photosynthetic biomanufacturing in green algae; production of recombinant proteins for industrial, nutritional, and medical uses. Photosynthesis research, 123(3), 227–239. https://doi.org/10.1007/s11120-014-9994-7

Rezzonico, F., & Duffy, B. (2008). Lack of genomic evidence of AI-2 receptors suggests a non-quorum sensing role for luxS in most bacteria. BMC microbiology, 8, 154. https://doi.org/10.1186/1471-2180-8-154

Roca, M.G., Arlt, J., Jeffree, C.E., and Read, N.D. (2005). Cell biology of conidial anastomosis tubes in Neurospora crassa. Eukaryot. Cell 4, 911–919.

Rodrigues, C. F., & Černáková, L. (2020). Farnesol and Tyrosol: Secondary Metabolites with a Crucial quorum-sensing Role in *Candida* Biofilm Development. Genes, 11(4), 444. https://doi.org/10.3390/genes11040444

Schaap P. (2005) Guanylyl cyclases across the tree of life. Front Biosci. 10:1485-98. https://doi.org/10.2741/1633.

Schindelin, J., Arganda-Carreras, I., Frise, E., Kaynig, V., Longair, M., Pietzsch, T., et al. (2012). Fiji: an open-source platform for biological-image analysis. Nat. Meth. 9 (7), 676–682. doi: 10.1038/nmeth.2019

Schneider, C. A., Rasband, W. S., Eliceiri, K. W. (2012). NIH Image to ImageJ: 25 years of image analysis. Nat. Methods 9, 671–675. doi: 10.1038/nmeth.2089

Scranton, M. A., Ostrand, J. T., Fields, F. J., & Mayfield, S. P. (2015). *Chlamydomonas* as a model for biofuels and bio-products production. The Plant journal: for cell and molecular biology, 82(3), 523–531. https://doi.org/10.1111/tpj.12780

Sebaa, S., Boucherit-Otmani, Z., & Courtois, P. (2019). Effects of tyrosol and farnesol on *Candida albicans* biofilm. Molecular Medicine Reports, 19, 3201-3209. https://doi.org/10.3892/mmr.2019.9981

Segal, R. A., Huang, B., Ramanis, Z., Luck, D. J. J. (1984). Mutant strains of *Chlamydomonas* reinhardtii that move backwards only. Cell Biol. 98 (6), 2026–2034. doi: 10.1083/jcb.98.6.2026

Stavis, R.L., and Hirschberg, R. (1973). Phototaxis in *Chlamydomonas* reinhardtii. J. Cell Biol. 59, 367–377.

Stewart, P.S., and Franklin, M.J. (2008). Physiological heterogeneity in biofilms. Nat. Rev. Microbiol. 6, 199–210.

Studer, S.V., Schwartzman, J.A., Ho, J.S., Geske, G.D., Blackwell, H.E., and Ruby, E.G. (2014). Non native acylated homoserine lactones reveal that LuxIR quorum sensing promotes symbiont stability. Environ. Microbiol. 16, 2623–2634.

Song, Yanhui, et al. (2024). Engineering fatty acid biosynthesis in microalgae: Recent progress and Perspectives. Marine Drugs, 22(5), 216 https://doi.org/10.3390/md22050216.

Syvitski, R. T., Tian, X. L., Sampara, K., Salman, A., Lee, S. F., Jakeman, D. L., & Li, Y. H. (2007). Structure-activity analysis of quorum-sensing signaling peptides from Streptococcus mutans. Journal of bacteriology, 189(4), 1441–1450. https://doi.org/10.1128/JB.00832-06

Tamsir, A., Tabor, J.J., and Voigt, C.A. (2011). Robust multicellular computing using genetically encoded NOR gates and chemical "wires". Nature 469, 212–215.

Tan, S. Z., & Prather, K. L. (2017). Dynamic pathway regulation: recent advances and methods of construction. Current opinion in chemical biology, 41, 28–35. https://doi.org/10.1016/j.cbpa.2017.10.004

Tans-Kersten, J., Huang, H., and Allen, C. (2001). Ralstonia solanacearum needs motility for invasive virulence on tomato. J. Bacteriol. 183, 3597–3605.

Tejada-Jimenez, Manuel, et al. (2023). *Chlamydomonas* reinhardtii—a reference microorganism for eukaryotic molybdenum metabolism. Microorganisms, vol. 11, no. 7, p. 1671, https://doi.org/10.3390/microorganisms11071671.

Tian, X., Ding, H., Ke, W., & Wang, L. (2021). Quorum Sensing in Fungal Species. Annual review of microbiology, 75, 449–469. https://doi.org/10.1146/annurev-micro-060321-045510

Tian, X., He, G. J., Hu, P., Chen, L., Tao, C., Cui, Y. L., Shen, L., Ke, W., Xu, H., Zhao, Y., Xu, Q., Bai, F., Wu, B., Yang, E., Lin, X., & Wang, L. (2018). Cryptococcus neoformans sexual reproduction is controlled by a quorum sensing peptide. Nature microbiology, 3(6), 698–707. https://doi.org/10.1038/s41564-018-0160-4

Tinevez, J.-Y., Perry, N., Schindelin, J., Hoopes, G. M., Reynolds, G. D., Laplantine, E., et al. (2017). TrackMate: an open and extensible platform for single-particle tracking. Methods 115, 80–90. doi: 10.1016/j.ymeth.2016.09.016

Torcato, I. M., Kasal, M. R., Brito, P. H., Miller, S. T., & Xavier, K. B. (2019). Identification of novel autoinducer-2 receptors in Clostridia reveals plasticity in the binding site of the LsrB receptor family. The Journal of biological chemistry, 294(12), 4450–4463. https://doi.org/10.1074/jbc.RA118.006938

Vellai, T., & Vida, G. (1999). The origin of eukaryotes: The difference between prokaryotic and eukaryotic cells. Proceedings of the Royal Society of London. Series B: Biological Sciences, 266(1428), 1571–1577. https://doi.org/10.1098/rspb.1999.0817

Verbeke, F., De Craemer, S., Debunne, N., Janssens, Y., Wynendaele, E., Van de Wiele, C., & De Spiegeleer, B. (2017). Peptides as Quorum Sensing Molecules: Measurement Techniques and Obtained Levels In vitro and In vivo. Frontiers in neuroscience, 11, 183. https://doi.org/10.3389/fnins.2017.00183

Vila, T., Kong, E. F., Ibrahim, A., Piepenbrink, K., Shetty, A. C., McCracken, C., Bruno, V., & Jabra-Rizk, M. A. (2019). *Candida albicans* quorum-sensing molecule farnesol modulates staphyloxanthin production and activates the thiol-based oxidative-stress response in Staphylococcus aureus. Virulence, 10(1), 625–642. https://doi.org/10.1080/21505594.2019.1635418

Wakabayashi, K.I., Misawa, Y., Mochiji, S., and Kamiya, R. (2011). Reduction-oxidation poise regulates the sign of phototaxis in *Chlamydomonas* reinhardtii. Proc. Natl. Acad. Sci. U. S. A 108, 11280–11284.

Watanabe, S., and Lewis, L.A. (2017). Phylogenetic interpretation of light and electron microscopic features of selected members of the phylogroup Moewusinia (Chlorophyceae), with new generic taxonomy. Phycologia 56, 329–353.

Welsh, M.A., and Blackwell, H.E. (2016). Chemical probes of quorum sensing: from compound development to biological discovery. FEMS Microbiol. Rev. 40, 774–794.

Whiteley, M., Diggle, S. P., & Greenberg, E. P. (2017). Progress in and promise of bacterial quorum sensing research. Nature, 551(7680), 313–320. https://doi.org/10.1038/nature24624

Winters, M., Arneborg, N., Appels, R., & Howell, K. (2019). Can community-based signalling behaviour in *Saccharomyces cerevisiae* be called quorum sensing? A critical review of the literature. FEMS Yeast Research, 19(5). https://doi.org/10.1093/femsyr/foz046

Wuster, A. & Babu, M. (2009). Transcriptional control of the quorum sensing response in yeast. Molecular BioSystems, 6(1), 134–141. https://doi.org/10.1039/B913579K

Xavier, K. B., & Bassler, B. L. (2005). Interference with AI-2-mediated bacterial cell-cell communication. Nature, 437(7059), 750–753. https://doi.org/10.1038/nature03960

Xie, L., and Wu, X.L. (2014). Bacterial motility patterns reveal importance of exploitation over exploration in marine microhabitats. Part I: Theory. Biophys. J. 107, 1712–1720.

Yang, Miao, et al. (2022). Differences in glycerolipid response of *Chlamydomonas* reinhardtii Starchless mutant to high light and nitrogen deprivation stress under three carbon supply regimes. Frontiers in Plant Science, 13(860966), https://doi.org/10.3389/fpls.2022.860966.

Zauner et al., 2012; Zauner, S., Jochum, W., Bigorowski, T. and Benning, C. (2012). A cytochrome b(5)-containing plastid-located fatty acid desaturase from *Chlamydomonas* reinhardtii. Eukaryot. Cell, 11, 856–863. doi: 10.1128/ec.00079-12

Ziegler, E. W., Brown, A. B., Nesnas, N., & Palmer, A. G. (2019). Abiotic Hydrolysis Kinetics of N-Acyl-L-homoserine Lactones: Natural Silencing of Bacterial Quorum Sensing Signals. European Journal of Organic Chemistry, 2019(17), 2850–2856. https://doi.org/10.1002/ejoc.201900322

Appendix

Chapter 2

Supplementary Material

The Supplementary Material for this article can be found online at:

https://frontiersin.figshare.com/collections/Computer-Assisted_Tracking_of_*Chlamydomonas*_Species/4827747

Chapter 3

Data and Code Availability

No specific code was developed for this work. Macros associated with ImageJ are not required but are available upon request. All data sets from this publication are available upon request. Videos are available on Dryad: https://doi.org/10.5061/dryad.w6m905qnj.

Supplementary Material

Supplemental Information can be found online at https://doi.org/10.1016/j.isci.2020.101714.